

*Port of Tauranga Dredging Reconsenting*

# Assessment of Effects on Turbidity and Morphodynamics

July 2026

Dr Willem de Lange
[redacted]

# Table of Contents


1.0 Introduction ..... 7

2.0 Geology, geomorphology and hydrodynamics of Te Awanui ..... 9

3.0 Sediment extraction impacts ..... 25

4.0 Sediment disposal impacts ..... 44

5.0 Post-dredging impacts ..... 52

5.1 Neutral to El Niño conditions ..... 82

5.2 La Niña conditions ..... 82

5.3 Episodic storm events ..... 82

5.4 Implications for dredging ..... 83

6.0 Summary ..... 84

7.0 Appendices ..... 88


# List of Tables


Table 1 – Summary of the calibration and validation statistics (Sutherland et al, 2004; Winter 2007) for the SCHISM/WMM coupled models. Model skill is a non-dimensional measure of accuracy of a model prediction versus a baseline prediction, with 1 being the maximum skill score and 0 the lowest. Bias is a measure of the central tendency of the model predictions compared to observations, with 0 being a reliable prediction, positive values represent over-predictions (too high) and negative values representing under-predictions (too low). The Mean Absolute Error (MAE) is the most robust measure of the differences between predictions and observations, while the Root Mean Square Error (RMSE) is the most commonly used. Only 1 set of wave observations (A Beacon) were available for calibration period 1, and 1 set of current observations (Entrance ADCP) were available for calibration period 2 and the validation period. ..... 15

Table 2 – Summary of the average proportions in each size class for the sediment textural data plotted in Figures 7-9. Note that due to rounding errors, the proportions may not exactly sum to 100% ..... 21

Table 3– Summary univariate statistics for the turbidity and total suspended solids observations reported by the Bay of Plenty Regional Council for their estuarine and tidal sites within Te Awanui. ..... 31

Table 4 – Median statistics of turbidity data recorded by Port of Tauranga ANALITE sensors from January 2013 until October 2016. Periods analysed are all dataset (ALL, n~106), excluding dredging periods M1, M2 and CP (NO, n~106), maintenance dredging period 1 (M1, n~104), maintenance dredging period 2 (M2, n~104) and capital dredging period (CP, n~104). TSS is estimated for gey and white sediment plumes used the ANALITE calibration equations given in the text. From Table A.2 in Coppede Cussioli (2018). .. 31

Table 5 – THSD dredging scenarios simulated. The sites correspond to Figure 17. From Table 2.2, Montaño (2024). ..... 34

Table 6 – Summary of plume source contributions as a proportion of the production rate..... 36


# List of Figures


Figure 1 – Location of the main features of the harbour, port infrastructure and offshore dredge spoil disposal sites for the Port of Tauranga (Port of Tauranga Ltd). ..... 7

Figure 2 - Major tectonic features of the Central Volcanic Zone (CVZ) and offshore Bay of Plenty. Contour lines represent the depth to top of the descending Pacific plate underlying the North Island. (Figure 1 from Stagpoole et al, 2021). ..... 9

Figure 3 – Hill shaded residual gravity anomalies, with caldera and sedimentary basins marked. (Figure 7 from Stagpoole et al, 2021). ..... 10
Figure 4 – Simplified geological map of the Tauranga Volcanic Centre highlighting the structures and young pyroclastic deposits. The boxes identify groups of volcanic domes with comparable geochemical characteristics (Figure 2 from Pittari et al, 2021 ). ..... 11
Figure 5 – Conceptual model of the main sediment transport pathways in Te Awanui, based on sediment connectivity analysis. The arrows indicate the range of sediment grainsizes (colour) transported between the different estuary regions, and the relative strength of the connections (arrow size). Note that the different arrow ends may show transport of different sizes. Six divergent and convergent sub-basins are also highlighted (blue icons). Transport of coarse sediments (>300 µm) is mainly confined to the deep tidal channels, whereas sub-basins and upper estuary regions are characterised by transport of mainly finer sediment fractions (<200 µm). (Figure 4.8 from de Ruiter, 2022). ..... 13
Figure 6 – Comparison of wave conditions during an El Niño and a La Niña winter storm. Note that the La Niña colour scale is 0-6 m, while the El Niño colour scale is 0-4 m. From Figures 5.20 and 5.21 of Watson and Berthot (2024a). ..... 16
Figure 7 – Some of the larger items encountered by the trailer suction dredge during the 1991/92 Capital Dredging Programme: top left – shells cemented in estuarine mud (Eemian?); top right – shells cemented in coarse sand (beach rock); middle row (right side is an enlargement of the left) – wood, pumice, peat, iron cemented sands (ferricrete or iron pan) and rhyolite cobbles; and bottom – tree stumps. ..... 18
Figure 8 – Comparison of the average grain size distributions for hopper sediments during Maintenance and Capital dredging for all samples analysed from 2010 to 2024. The size classes are indicated: VCS = Very Coarse Sand; CS = Coarse Sand; MS = Medium Sand; FS = Fine Sand; VFS = Very Fine Sand; CZ = Coarse Silt; MZ = Medium Silt; FZ = Fine Silt; VFZ = Very Fine Silt; and C = Clay. ..... 19
Figure 9 – Comparison of the 95% (±2 standard deviation) envelopes of grain size distributions for hopper sediments during Maintenance (top) and Capital (bottom) dredging for all samples analysed from 2010 to 2024. The size classes are as summarised in the caption for Figure 7. ..... 20
Figure 10 – Comparison of the average grain size distributions for subsurface sediments obtained by vibracores before the 2015/2016 Capital Dredging Programme (de Lange et al, 2014). The textural data have been aggregated into 1 m thick slices below the sea floor that existed in 2013/14. The size classes indicated are defined in the caption for Figure 6. ..... 21
Figure 11 – Average monthly rates of infill since the last major capital dredging programme in 2015-2016 based on 1 m resolution gridded MBES surveys for the outer (left) and inner (right) channels (pers. Comm., Greg Cox, Port of Tauranga Hydrographer). The colour bar scale represents the thickness of infill sediment between the previous maintenance dredging and the pre-dredging survey (9 months later) in metres. ..... 22
Figure 12 – Scatter plot of the maximum draft and LOA for 1547 individual vessels that berthed at the Port of Tauranga between 2021-2025. The density curves above and at right indicate the frequency of vessels with the correspond LOA and draft respectively. ..... 24
Figure 13 – Trailing suction hopper dredge operating on a flood tide at the junction of the Maunganui Roads and Stella Passage during the 1991/92 Capital dredging Programme. There were very low levels of background turbidity at the time. ..... 25
Figure 14 – Release of sediment arising from dredging by (top) a trailing suction hopper dredge (TSHD) and contributions to the suspended sediment (Figure 9 from Mills & Kemps, 2016), and (bottom) a backhoe dredge (BHD (Figure 6 from Becker et al, 2015). ..... 27
Figure 15 – Release of sediment arising from dredging by (top) a trailing suction hopper dredge (TSHD) and contributions to the suspended sediment (Figure 9 from Mills & Kemps, 2016), and (bottom) a backhoe dredge (BHD (Figure 6 from Becker et al, 2015). ..... 27
Figure 16 – Schematic diagram of the sources of turbid plumes for a trailing suction dredge, where the overflow consists of two components: a concentrated discharge from a pipe at the stern of the dredge, and some discharge over the sides of the hopper. Propellor wash is not specifically shown. The zones A, B, and C correspond to the zones in Figure 15 that shows the plume behaviour with time/distance from source. ..... 28
Figure 17 – A persistent turbid plume resulting from dredging a weathered ignimbrite in the Stella Passage during the 1991/92 Capital Dredging Programme. There are two vessels in the harbour entrance: (left) the THSD heading to the disposal site; and (right) a barge moored over Tanea Shelf to extract boulders for relocation to form a new reef closer to Pilot Bay. ..... 29

Figure 18 – Turbid plume consisting mostly of clays derived from weathered tephra and discharged after heavy rain by the Wairoa River, and the Waikareao Estuary catchment. ..... 30
Figure 19 – Conceptual summary of the EWMA approach applied to averages of 6-hour long data windows. (Figure 3, Port of Melbourne Corporation, 2008). ..... 33
Figure 20 – Schematic diagram of the sources of turbid plumes for a trailing suction dredge, where the overflow consists of two components: a concentrated discharge from a pipe at the stern of the dredge, and some discharge over the sides of the hopper. Propellor wash is not specifically shown. The zones A, B, and C correspond to the zones in Figure 11 that shows the plume behaviour with time/distance from source. ..... 34
Figure 21 – Locations for dredging simulations for the large TSHD (L1-L6) and the BHD. Figure 2-1, Montaño (2024). The colours indicate the thickness of sediment proposed to be removed by capital dredging (expressed as a depth difference after dredging). ..... 35
Figure 22 – Predicted tides for the Tauranga Harbour Entrance for February 2025 from the NIWA tide forecaster. ..... 37
Figure 23 – Modelled sediment plumes (mean TSS in $mgl^{-1}$) for a large TSHD (left column) operating with no overflow during flood tide and overflow during ebb tide, and a BHD (right column), excavating sediment from the southern Stella Passage. The surface plume represents the surface 2 m of the flow, and the seafloor plume represents the deepest 2 m. The point of release is marked by a star, and surrounding circles represent a 200 m (solid line) and a 600 m (dashed line) circumference to identify the mixing zone. Concentrations <5 $mgl^{-1}$ are masked. (Figures 3.11 and 3.16 from Montaño, 2024). ..... 38
Figure 24 – Sites used to assess the hourly total suspended sediment concentrations due to dredging at the BHD and TSHD sites in Figure 17 (Figure 2-5, Montaño, 2024). ..... 39
Figure 25 – Time series of hourly total suspended sediment concentrations on Te Paritaha (Figure 20) due to a large TSHD operating at the locations in Figure 17 during La Niña summer conditions. The vertical scale is logarithmic from 0.1 to 75 $mgl^{-1}$, so bars reaching the top of the graph represents an exceedance. The bottom panel is the tidal elevation in Stella Passage. (Figure 3-6 from Montaño, 2024) ..... 40
Figure 26 – Dispersion of sediment discharged by a large TSHD (Mean TSS over 2 months) for locations L4, L5 and L2). TSS values < 5 $mg.l^{-1}$ are masked so do not appear. From Figures 5.4, 5.5 and 5.2 of Montaño (2024). ..... 42
Figure 27 - Annual average flushing time for the Tauranga Basin of Te Awanui. Figure 3.7 from Stewart (2019). ..... 43
Figure 28 – Schematic diagrams of the behaviour of turbid plumes after disposal from a hopper. The labels 1 & 2 in the bottom figure correspond to convective descent and dynamic collapse; i refers to stripping at a pycnocline; and ii refers to the near-bed radial density current formed by dynamic collapse. ..... 44
Figure 29 – Section of Figure 1 showing the main areas involving dredging extraction and disposal for the Port of Tauranga. ..... 46
Figure 30 – (Left) location of vibracores, surficial sediment samples, and seismic survey lines collected by Blackler (2024), and (Right) isopach map of dredged sediment thickness in 0.5 m increments. (Figures 2.1C and 2.4D from Blackler, 2024) ..... 49
Figure 31 – Mean surficial sediment grain size (A) and loss on ignition (LOI), which provides an estimate of organic content. (Figure 2.7 from Blackler, 2024) ..... 50
Figure 32 – 90$^{th}$ percentile of total suspended sediment concentration following the emptying of a large TSHD hopper at the centre of the combined D and H1 disposal sites (white rectangle). Plots show the surface and near bed plumes for La Niña summer and winter conditions. . Concentrations <5 $mgl^{-1}$ are masked. (Figure 3-15 from Montaño, 2024) ..... 51
Figure 33 – Predicted and measured annual-average sedimentation rates for fine (upper) and coarse (lower) terrestrial sediment. (Figures 4-5 and 4-6 from Green, 2010). ..... 53
Figure 34 – Example of a tidal stream hodograph that illustrates the direction and magnitude of tidal currents at each stage of a tidal cycle (Figure 10.6 from Simon, 2013[1]) ..... 56
Figure 35– Example of the shoaling transformations of the tidal wave as it travels into the Gironde Estuary, France (Figure 1.8 from Simon, 2013). ..... 56
Figure 36 – SCHISM/WMM time series output locations for assessing changes potentially linked to capital dredging (Figure 1-2 from Watson and Berthot, 2025). ..... 58

[1] Simon B, 2013. Coastal tides. Institut océanographique éd, Monaco. 411 p.

Figure 37 – Time series of 10-minute current speeds and reference water level at the station sites, over 2 days of a spring tide under La Niña winter conditions for the 4 historical and future bathymetric conditions (Figure 4-3 from Watson and Berthot, 2025). ..... 59
Figure 38 – Time series of hourly current speeds and reference water level at the map output sites, over 2 days of a spring tide under La Niña winter conditions for the 4 historical and future bathymetric conditions (Figure 4-4 from Watson and Berthot, 2025). Refer Figure 28 for locations. ..... 60
Figure 39 – Sketch of the morphological elements of a tidal inlet based upon a photo from an inlet near Sheep Island, North Carolina. The lower part of the figure shows a cross-section along the inlet. The Tauranga tidal inlet is simplified by the presence of Mauao, which prevents eastward migration of the inlet. ..... 62
Figure 40 – Bathymetry of the Lower Western Channel and Te Paritaha in 2011, 2017, 2021 and 2024. Figures provided by Greg Cox for Port of Tauranga Ltd. (Figure 6, de Lange, 2024) ..... 63
Figure 41 – (Left) Stacked plots of transect cross-sections of the Lower Western Channel and Te Paritaha from 2011-2024; and (Right) corresponding time series of channel cross-sectional areas for the transects. The transects are marked in Figure 39 on the plots for 2011 and 2024..... 64
Figure 42 – Contour map of Te Paritaha (Centre Bank) showing the locations of batter slope profiles (1-5) and pipi survey locations (A-C). ..... 65
Figure 43 – Sections of chart NZ5412 showing the junction of the Cutter Channel, Maunganui Roads and Pilot Bay channel in 2015 and 2019..... 66
Figure 44 – Transects 2, 3 and 5 (Figure 41) before (2011-2015) and after (2017-2022) the 2016-17 Capital Dredging Programme showing the changes to the batter slopes along the margin of Te Paritaha. ..... 67
Figure 45 – Transects used to assess shoreline movement from CoastSat analysis of shoreline positions from satellite images by Berthot et al 2024). ..... 68
Figure 46 – Time series of raw and tidally corrected shoreline positions relative to the long-term mean shoreline position for the transects in Figure 35. Capital dredging occurred during 2015-16. (Figure 4-7, Berthot et al, 2024) ..... 69
Figure 47 – Migration of selected depth contours at Panepane, Matakana Island, between 2007, before capital dredging, and 2021, after capital dredging. Left-hand image is a plan view with the shaded areas representing the maximum excursions for each depth contour, while the right-hand images are time-series of excursion distances for the transects XS1-5. Figures and data provided by Greg Cox, GJC Consulting. ..... 70
Figure 48 – Contours showing the initial 2011 shoreline (black) and the modelled shorelines after simulated a year of waves in ShorelineS for pre-dredge 2015 (blue), post-dredge 2016 (green), pre-dredge 2023 (yellow) and post originally proposed 2026 capital dredging (red) wave scenarios. The red dashed line is the 2012 survey for reference. Black circles indicate location of wave parameters extracted from the SCHISM/WMM model (Figure 4-16, Berthot et al, 2024)..... 71
Figure 49 - Aerial photographs for 1943 and 1969, and Google Earth images for June 2018, January 2022, February 2025 of the entrance to Tauranga Harbour showing changes to Panepane; and a Google Earth image for November 2023 for the shoreline adjacent to the western side of the ebb tidal delta. Open white arrows mark the positions of the marginal flood channel on the seaward side of the spit, and the yellow arrow on the June 2018 mars and arcuate embayment associated with swash bar focussing wave energy. ..... 73
Figure 50- Summary time series of statistics for the flood (positive) and ebb (negative) speeds recorded by the Port of Tauranga ADCP. Before 2006, the ADCP was bottom mounted within the channel. From 2006 to 2025, a rotating series of ADCPs were buoy mounted at No.2 Tanea on the eastern side of the channel. ..... 75
Figure 51 - A time series of water elevations recorded by the GeoNet station TAUT near Salisbury Wharf, Mt Maunganui, showing the changes in mean water level due to the inverse barometric effect (IBE - black line), and the timing of the flooding in the Wairoa River and the 29 July 2025 Kamchatka Tsunami (see text for further explanation). ..... 75
Figure 52 - North and East current vectors for No.2 Tanea Buoy during the period 29 July to 4 August 2025: blue = ADCP measured; black = predicted; and red = residual. Vertical blue and red dashed lines mark the onset of flooding in the Wairoa River, and PTWC predicted Kamchatka Tsunami arrival time respectively. ..... 76
Figure 53 - Annual significant wave height and wave approach direction distributions based on all available data for the Pukehina wave buoy. To make it easier to visualise the direction values have been adjusted by adding 360° to recorded directions less than 180°. ..... 77

Figure 54- Monthly Troup Southern Oscillation Index for January 1970 to August 2025. Values above 0.7 (red dashed line) correspond to La Niña conditions; below -0.7 (blue dashed line) correspond to El Niño conditions; and between 0.7 and -0.7 correspond to neutral conditions. The calendar years with periods of erosion for the ebb tidal delta and Panepane Point shoreline are shown. SOI data from Australian Bureau of Meteorology. ..... 78
Figure 55 - Time series of 3-month running average Niño3.4 index between 1950 and 2024. The blue dashed line corresponds to an index of -1 (1 standard deviation), and the blue shaded areas are super-long La Niña events. (Figure 1, Wang et al, 2024). ..... 79
Figure 56 - Conceptual model for tidal inlet bypassing in the vicinity of a headland in response to changing rates of wave-induced longshore transport (LST). Figure 11 from Pullig et al (2025). ..... 80
Figure 57 – Schematic diagrams of the sediment transport patterns and associated areas of erosion and deposition associated with different ENSO patterns. ..... 81

I have read and agree to comply with the Code of Conduct for Expert Witnesses as set out in the Environment Court Consolidated Practice Note 2023 where it is relevant to this report, acknowledging that this is a technical report rather than expert evidence.

# 1.0 Introduction

The Port of Tauranga Ltd proposal involves both ongoing maintenance dredging of all the channels and berthing areas used by vessels transiting to and from the Port (Figure 1) to maintain design depths and the following capital dredging:

- deepening the approach to berth 1
- deepening an area of the Passing Lane to smooth the entrance corner
- Deepening of the existing Sitting Basins

The Port is intending to use a Trailing Suction Hopper Dredging (TSHD) for most of the capital dredging, while a Back-Hoe Dredge (BHD) will be used for dredging work in tight or difficult to reach areas.

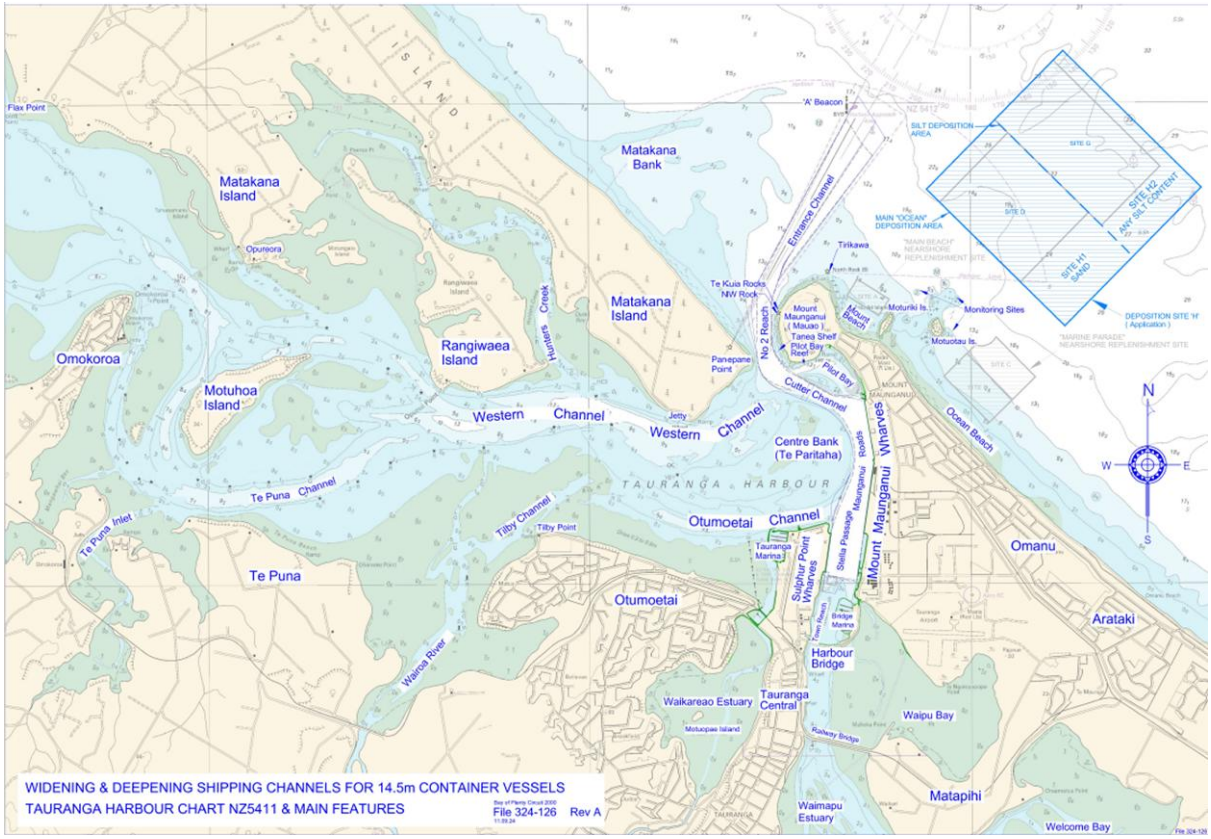



*Figure 1 – Location of the main features of the harbour, port infrastructure and offshore dredge spoil disposal sites for the Port of Tauranga (Port of Tauranga Ltd).*

Maintenance dredging has been ongoing at the Port since the 1970s. The current resource consents for maintenance dredging were also issued in 2013 and expire in December of 2027. The Port proposes to conduct maintenance dredging as and where needed in all of the channels and turning areas that are used by vessels accessing and leaving the Port. It is expected that maintenance dredging will likely continue to be undertaken in much the same way as it is currently done using a TSHD.

This report considers the impact of the proposed capital and maintenance dredging on seafloor topography and morphology as a result of excavation, turbidity generation, and sediment deposition. Typical dredging activities may result in adverse impacts during three phases (EPA, 2016[2]): during the excavation of the seabed; during the disposal of the extracted sediment (which includes reclamation utilising the sediment); and during the post-dredging or recovery period.

During the excavation phase, the main potential impacts are excavation of benthic biota, and the release of potential contaminants into the water column including suspended sediment (turbidity) and dissolved or absorbed materials such as heavy metals, hydrocarbons and pesticides.

During the disposal phase, the main potential impacts are burial of benthic biota, and the release of potential contaminants into the water column including suspended sediment (turbidity) and dissolved or absorbed materials such as heavy metals, hydrocarbons and pesticides.

Both excavation and disposal phase impacts are transient, although there may be a cumulative effect such as the bioaccumulation and biomagnification of heavy metals resulting from contaminants released from sediment during dredging. The characteristics of the impacts for both phases are predominantly determined by the texture (size distribution) of sediment being dredged, the level of contamination contained within the dredged sediments, and the dredging technology and methodology used.

During the post-dredging or recovery phase, the main potential impacts are: changes to the tidal circulation and sediment transport within and outside the harbour; changes to the behaviour of depth-dependent phenomena, such as waves and storm surges; changed patterns of erosion and accretion; and dispersal of sediment from the disposal site. Changes to tidal circulation primarily may occur within the harbour, but can affect the ebb-tidal delta, and manifest as changes to the shape of the tidal elevation curve (affecting tidal range, the timing of high and low tide, the duration of flood and ebb tidal flows, and tidal flushing). The post-dredging changes may be permanent, or persist for years before returning to pre-dredging conditions.

The impacts during the post-dredging phase are predominantly determined by the changes made to the morphology (mostly the tidal channels), and the subsequent morphodynamics response, which involves an interactive system of changing currents and morphology. Usually, areas subject to dredging are naturally changing in response to processes such as weather events and variations in sediment supply. Depending on the scale of the changes produced by dredging, it can be difficult to identify the extent of adverse effects due to dredging. The scale of the dredging can be managed by staging the dredging process, and allowing time for recovery between stages.

This report considers the characteristics of the sediment to be dredged, and the potential impacts during the excavation and disposal phases for different dredging methodologies focusing on turbidity. The report also examines the potential impacts for the post-dredging phase, including changes to the tidal circulation and morphology, and the implications for Te Awanui.

[2] EPA, 2016. Technical guidance: Environmental impact assessment of marine dredging proposals, Environmental Protection Agency, Western Australia: 23 pp.

## 2.0 Geology, geomorphology and hydrodynamics of Te Awanui

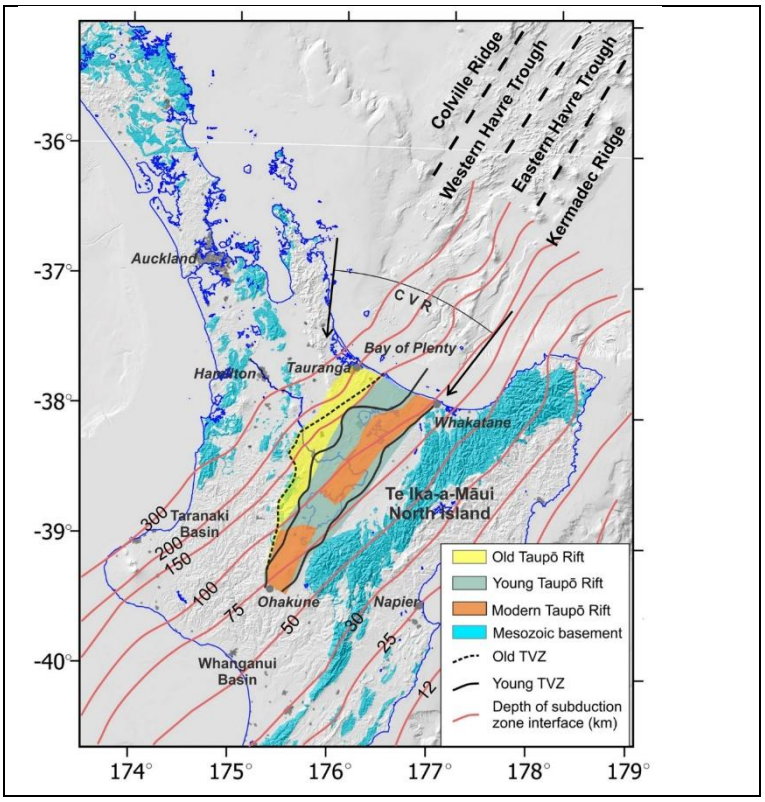



*Figure 2 - Major tectonic features of the Central Volcanic Zone (CVZ) and offshore Bay of Plenty. Contour lines represent the depth to top of the descending Pacific plate underlying the North Island. (Figure 1 from Stagpoole et al, 2021[3]).*

Te Awanui (Tauranga Harbour) is a geologically young feature in the Bay of Plenty, having formed within the last 7,500-8,500 years in response to sea level rise since the last ice age. It occupies two basins: the Katikati Basin in the northwest; and the Tauranga Basin in the southeast. These basins are located on the western margin of the Central Volcanic Zone (CVZ - Figure 2). The Katikati Basin is inferred to occupy a caldera within the Coromandel Volcanic Zone, based on regional gravity anomaly data (Figure 3); while the Tauranga Basin mostly occupies a rift formed during the initial development of the Taupo Volcanic Zone (TVZ) based on regional gravity anomalies and geological data (Figure 4).

[3] Stagpoole, V., Miller C, Caratori Tontini F, Brakenrig T, & Macdonald N, 2021. A two-million-year history of rifting and caldera volcanism imprinted in new gravity anomaly compilation of the Taupō Volcanic Zone, New Zealand. New Zealand Journal of Geology and Geophysics 64(2-3): 358-371.

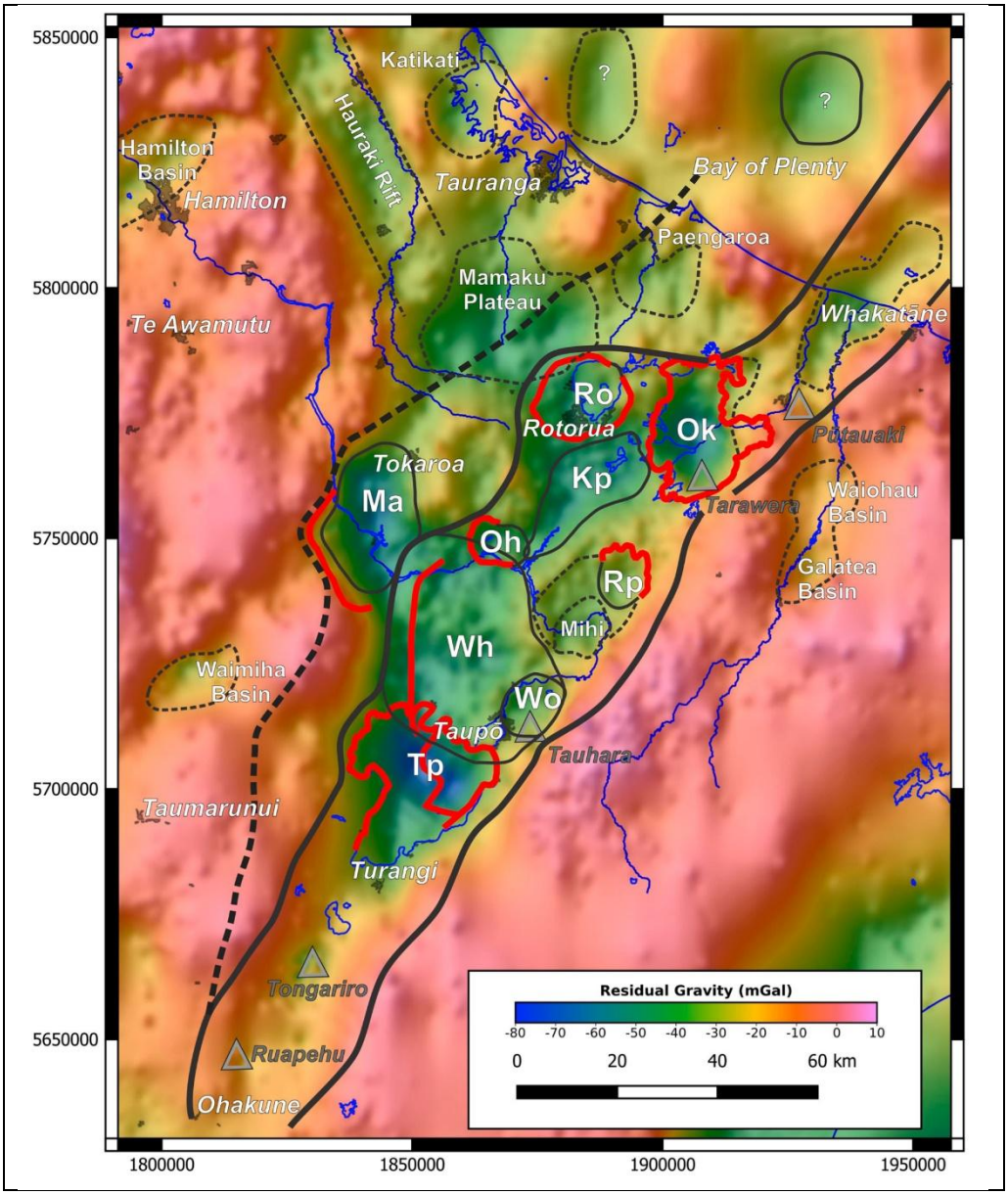



*Figure 3 – Hill shaded residual gravity anomalies, with caldera and sedimentary basins marked. (Figure 7 from Stagpoole et al, 2021).*

These basins are separated by a shallow interfluve between Matahui Point and Matakana Point that is only submerged around high tide, which represents the region between the underlying caldera and rift. While the rift system appears to still be undergoing subsidence associated with active faults (i.e. faults that have moved at least once in the last 125,000 years), the interfluves are rising. The Papamoa Hills are also rising based on continuous GPS (cGPS) data collected by GeoNet. There do not appear to be any active faults in the Katikati Basin, although there is evidence from gravity anomaly data (Figure 3) for a significant displacement by the inferred Tuapiro Fault (Figure 4 – top left). It is considered that the distribution of warm to hot springs around Te Awanui is controlled by faults associated with the underlying caldera and rift system (Braithwaite and Christie, 1996)[4].

[4] Brathwaite RL, Christie AB. 1996. Geology of the Waihi area: part sheets T13 and U13 [map]. Lower Hutt (NZ): Institute of Geological & Nuclear Sciences. 1 folded map + 64 p., scale 1:50,000. (Institute of Geological & Nuclear Sciences geological map; 21)

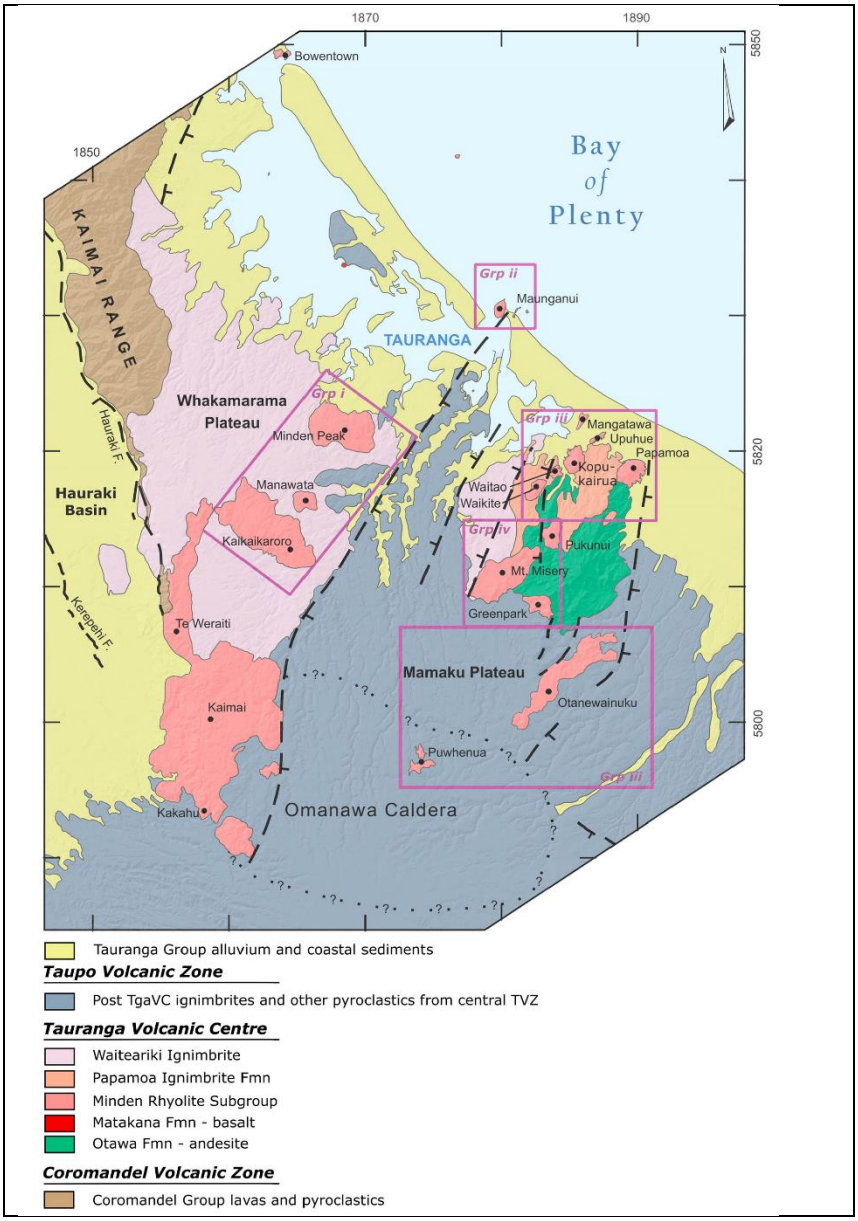



*Figure 4 – Simplified geological map of the Tauranga Volcanic Centre highlighting the structures and young pyroclastic deposits. The boxes identify groups of volcanic domes with comparable geochemical characteristics (Figure 2 from Pittari et al, 2021[5] ).*

The sediment within the harbour is predominantly sourced from erosion of young volcanic deposits formed by eruptions in the Tauranga Volcanic Centre, primarily by fluvial transport (braided rivers) during glacial conditions when sea level was 100-120 m lower than at present (MacPherson *et al*, 2017)[6]. The fluvial deposits have been overlain by a marine deposit of variable thickness formed by reworked volcaniclastic sediment that has been transported into the harbour from offshore. Some sediment is also supplied by fluvial transport from the surrounding catchments, and from erosion of volcanic deposits around the shoreline. The sediment source within the port area is predominantly marine and associated with the ebb and flood tidal delta system (MacPherson *et al*, 2017).

[5] Pittari, A., Prentice, M. L., McLeod, O. E., Yousef Zadeh, E., Kamp, P. J. J., Danišík, M., & Vincent, K. A. (2021). Inception of the modern North Island (New Zealand) volcanic setting: spatio-temporal patterns of volcanism between 3.0 and 0.9 Ma. New Zealand Journal of Geology and Geophysics, 64(2-3), 250-272.

[6] MacPherson D, Fox BRS & de Lange WP, 2017: Holocene evolution of the southern Tauranga Harbour, *New Zealand Journal of Geology and Geophysics* 60: 392-409.

The development of Te Awanui/Tauranga Harbour since sea level reached about the present level some 7000 years ago, has followed the classic evolution from a juvenile to mature estuary. However, that the progression is quite slow compared to many other New Zealand estuaries due to a limited supply of sediment and rising relative sea level in the Tauranga Basin caused by subsidence. This means that there is a strong tidal influence (with minimal freshwater effects), and sufficiently deep water at high tide to allow moderate wave action.

Siltation within Te Awanui tidal channels may occur in response to sediment supplied from one, or both, of two sources: marine sediment transported into Te Awanui by waves and tidal currents; and terrestrial sediment from freshwater catchments and shoreline erosion, reworked and transported by waves and tidal currents within the harbour. The boundary between marine-dominated and terrestrial-dominated sediment is not static: it varies with the changing magnitude of tidal flows over spring-neap cycles, magnitude of freshwater inflows, and the influence of storms through storm surges and floods. In the long-term, as the harbour matures, the boundary moves seaward as the harbour naturally infills with sediment.

NIWA undertook a sediment study for Te Awanui focusing on the Tauranga Basin between 2007 and 2010 (Parshotam et al, 2008[7]). This study developed models to:

- Assess relative contributions of various sediments within catchments surrounding Te Awanui;
- Assess the characteristics of significant sediment sources; and
- Investigate the fate (dispersal and deposition) of catchment sediments within Te Awanui.

The NIWA sediment study included the development for the Tauranga Basin of Te Awanui of a hydrodynamic and sediment transport study (Pritchard *et al*, 2009[8]) and a sedimentation model linking sources and sinks (Green, 2010[9]). To provide calibration data for the sediment transport and sedimentation models, NIWA undertook a literature review and sampling programme utilising short cores to determine sediment characteristics and sedimentation rates (Hancock *et al*, 2009[10]).

Apart from the tidal delta system at the Tauranga harbour entrance, the sediment sources for the Tauranga Basin of Te Awanui were found to be from terrestrial catchments. The NIWA study did not consider sediment contributions from shoreline erosion or coastal landslides, which can be locally significant for areas within Te Awanui (*viz*. Healy *et al,* 2010[11];Garae, 2015[12]; OPUS, 2015[13]; Podrumac, 2016[14]; and Tonkin and Taylor Ltd, 2018[15]).

---

[7] Parshotam A, Hume T, Elliott S, Green M, & Wadhwa, 2008. Tauranga Harbour Sediment Study: Specifications of Scenarios. NIWA Client Report: HAM2008-117, August 2008.

[8] Pritchard M, Gorman R, & Hume T, 2009a. Tauranga Harbour Sediment Study: Hydrodynamic and Sediment Transport Modelling. NIWA Client Report: HAM2009-032, February 2009.

[9] Green MO, 2010. Tauranga Harbour Sediment Study: Predictions of Harbour Sedimentation under Future Scenarios. Report to Environment Bay of Plenty, NIWA Client Report HAM2009-078, May 2010

[10] Hancock N, Hume T, & Swales A, 2009. Tauranga Harbour Sediment Study: Harbour bed sediments. NIWA Client Report: HAM2008-123, March 2009.

[11] Healy TR, Scarfe B, & Schimmel A, 2010. *Eastern Tauranga Harbour historical erosion assessment: Aerial photograph GIS.* Report by Coastal Marine Group, Department of Earth Sciences, The University of Waikato, Hamilton, New Zealand

[12] Garae CP. 2015. *Estimating patterns and rates of coastal cliff retreat around Tauranga Harbour.* MSc Thesis, The University of Waikato, Hamilton, New Zealand

[13] OPUS, 2015. *High level coastal erosion study: Coastal erosion risk, cost benefit analyses and site proritisation*. Tauranga Inner Harbour Contract 14-1011. 48 pp

[14] Podrumac A, 2016. *Holocene evolution of the Upper Western Channel within Tauranga Harbour*. MSc Thesis, The University of Waikato, Hamilton.

[15] Tonkin and Taylor Ltd, 2018. *Tauranga Harbour coastal hazards study: Coastal erosion hazard assessment*. Report prepared for Bay of Plenty Regional Council. 41 pp.




*Figure 5 – Conceptual model of the main sediment transport pathways in Te Awanui, based on sediment connectivity analysis. The arrows indicate the range of sediment grainsizes (colour) transported between the different estuary regions, and the relative strength of the connections (arrow size). Note that the different arrow ends may show transport of different sizes. Six divergent and convergent sub-basins are also highlighted (blue icons). Transport of coarse sediments (>300 µm) is mainly confined to the deep tidal channels, whereas sub-basins and upper estuary regions are characterised by transport of mainly finer sediment fractions (<200 µm). (Figure 4.8 from de Ruiter, 2022).*

de Ruiter (2022[16]) utilised a numerical model of Te Awanui to undertake a sediment connectivity analysis to identify the main sediment pathways, sources and sinks for the entire harbour. The results were used to develop the conceptual model in Figure 5. The shallow interfluve between the two main basins only allows exchange of water and sediment at high tide. The movement is primarily driven by currents created by wind stress (typically at velocity <3% of the wind velocity) and sediment transport only involves locally-sourced sediment (Figure 5). Overall, transport of coarse and medium sand (>300 µm, <1.75 phi) is predominantly confined to tidal channels and the flood tidal delta, and finer sediment is moved in shallower areas (de Ruiter et al, 2026)[17].

[16] de Ruiter PJ, 2022. Hypsometric and geometric controls on hydrodynamics, tidal asymmetry, and sediment connectivity in shallow estuarine systems. PhD Thesis, The University of Waikato, Hamilton, NZ. 116 p.

[17] de Ruiter, PJ, Mullarney, JC, Bryan, KR, & Winter, C, 2026. Relationships between sediment connectivity and hypsometry in an intertidal microtidal estuary. Geomorphology, 110241.

The NIWA and de Ruiter studies show that fine sediment accumulation is restricted to the harbour margins, particularly in areas of locally high sediment supply, and/or very low wave activity (de Ruiter, 2022). Elsewhere, there is sufficient turbulence to result in the export of fine sediment from Te Awanui.

Watson and Berthot (2024a[18]) undertook numerical modelling of waves and currents for Te Awanui and the Western Bay of Plenty. Their modelling examined the effects of seasonality (Summer versus Winter) and climate variability associated with the El Niño-Southern Oscillation (ENSO) focusing on the El Niño and La Niña extremes. Modelling was performed with a coupled hydrodynamic model (Semi-implicit Cross-scale Hydroscience Integrated System Model – SCHISM) and a Wind Wave Model (WWM version III). The models utilised an unstructured grid that:

- Accounts for potentially strong wave-current interactions, such as occur over the ebb tidal delta (Ramli, 2016[19]).
- Allows for a higher resolution grid in areas of complex bathymetry and/or rapid changes in wave and current conditions, such as the tidal inlet.
- Allow for real-time forecasting of dredge plume dispersion during dredging operations if required.

The SCHISM model was calibrated and validated using all available measurements of bathymetry, tidal currents, water levels, and freshwater inflows for the period 2014 to 2023. The WMM-III model was calibrated with offshore wave measurements from the BOPRC directional wave recorder offshore from Bowentown, the Port of Tauranga Ltd non-directional wave recorder at A Beacon, and hindcast wave data from the SWAN wave model used for operational wave forecasting around New Zealand. The coupled SCHISM/WMM models were calibrated over to periods: 4th September to 3rd October 2015; and 3rd December 2022 to 1st January 2023. Validation was undertaken for the period 2nd April to 1st May 2023.

As is usually the case, the calibration and validation scores for water levels are excellent, while those for currents and waves are lower (Table 1). This is partly due to the current and wave predictions being dependent on the water level so any uncertainties in water level increase the uncertainty for current and wave predictions. For the Te Awanui modelling, the grid resolution and available calibration data decreased with distance from the Port of Tauranga, which increases the uncertainties.

The MAE values in Table 1 are the most useful for indicating the minimum magnitude of change that can be predicted by the coupled models. Watson & Berthot (2024a) provide individual statistics for all sites with comparisons between predictions and observations used for calibration and validation. Their calibration and validation procedure used water level and current observations within Te Awanui, and wave observations for the offshore region in the Western Bay of Plenty. This was a consequence of the available observations, but does capture the main drivers of water and sediment movement for both Te Awanui and the offshore area, except for the ebb tidal delta (Matakana Banks) where tidal currents can be locally dominant. However, for the purposes of this assessment additional information for the

[18] Watson H, & Berthot A, 2024a. Hydrodynamic and wave modelling, Report prepared for Port of Tauranga, MetOcean Solutions, December 2024. 112 p.

[19] Ramli AY, 2016. *The Impact of Dredging on the Stability of Matakana Banks Ebb-Tidal Delta*. PhD Thesis, University of Waikato, Hamilton, New Zealand.

ebb tidal delta is available from the PhD studies of Ramli (2016) and Spiers (2013[20]), and from Montaño et al (2023[21]).

*Table 1 – Summary of the calibration and validation statistics (Sutherland et al, 2004[22]; Winter 2007[23]) for the SCHISM/WMM coupled models. Model skill is a non-dimensional measure of accuracy of a model prediction versus a baseline prediction, with 1 being the maximum skill score and 0 the lowest. Bias is a measure of the central tendency of the model predictions compared to observations, with 0 being a reliable prediction, positive values represent over-predictions (too high) and negative values representing under-predictions (too low). The Mean Absolute Error (MAE) is the most robust measure of the differences between predictions and observations, while the Root Mean Square Error (RMSE) is the most commonly used. Only 1 set of wave observations (A Beacon) were available for calibration period 1, and 1 set of current observations (Entrance ADCP) were available for calibration period 2 and the validation period.*

| Parameter | Model skill | Bias | MAE | RMSE |
|---|---|---|---|---|
| Calibration period 1 | | | | |
| Water level | 0.98 - 1.00 | -0.03 – 0.08 m | 0.04 - 0.12 m | 0.05 – 0.15 m |
| Currents | 0.83 - 0.97 | -0.05 – 0.02 $m.s^{-1}$ | 0.06-0.10 $m.s^{-1}$ | 0.06-0.13 $m.s^{-1}$ |
| Waves | 0.83 | 0.10 m | 0.18 m | 0.22 m |
| Calibration period 2 | | | | |
| Water level | 0.99 - 1.00 | 0.02 - 0.06 m | 0.05 - 0.09 m | 0.06 - 0.11 m |
| Currents | 0.97 | -0.6 $m.s^{-1}$ | 0.15 $m.s^{-1}$ | 0.19 $m.s^{-1}$ |
| Waves | 0.96 – 0.97 | -0.15 – 0.02 m | 0.19 m | 0.27 – 0.29 m |
| Validation period | | | | |
| Water level | 0.99 – 1.00 | -0.07 - -0.03 m | 0.05 - 0.10 m | 0.07 – 0.12 |
| Currents | 0.97 | -0.09 $m.s^{-1}$ | 0.14 $m.s^{-1}$ | 0.18 $m.s^{-1}$ |
| Waves | 0.97 | -0.03 – 0.14 m | 0.15 – 0.18 m | 0.19 - 0.23 m |

The tidal flow behaviour reported by Watson and Berthot (2024a) is consistent with all the previous models, apart for areas where the bathymetry has changed since the earlier studies: primarily in the channels enlarged during the last capital dredging campaign in 2015/16. These changes were assessed by Watson and Berthot (2025[24]), which will be discussed below in Section 5 under post-dredging impacts.

Watson and Berthot (2024a) also simulated the seasonal effects and the impacts of ENSO climate variability, which was not systematically addressed in previous studies. They defined four 62-day periods corresponding to historical ENSO extremes:

- El Niño summer: 3rd January 2016 – 5th March 2016
- La Niña summer, 3rd January 2012 – 5th March 2012
- El Niño winter, 3rd July 2016 – 3rd September 2016
- La Niña winter, 3rd July 2011 – 3rd September 2011

All the simulations were run using the 2023 bathymetry, so any differences would reflect seasonal and climate variability changes in forcing of water levels, currents and waves.

[20] Spiers K, 2013. *Investigation of access channel sedimentation processes and the impact of capital dredging on harbour circulation patterns.* PhD Thesis, The University of Waikato, Hamilton, New Zealand.
[21] Montaño M., Suanda SH, & de Souza JMAC, 2023. Modelled coastal circulation and Lagrangian statistics from a large coastal embayment: The case of Bay of Plenty, Aotearoa New Zealand. Estuarine, Coastal and Shelf Science, 281, 108212.
[22] Sutherland J, Peet AH, & Soulsby RL, 2004. Evaluating the performance of morphological models. Coastal Engineering, 51(8), 917-939.
[23] Winter C, 2007. On the evaluation of sediment transport models in tidal environments. Sedimentary Geology, 202(3), 562-571.
[24] Watson H, & Berthot A, 2025. Tauranga Harbour historical configurations modelling, Report prepared for Port of Tauranga, MetOcean Solutions, January 2025. 82 p.

The model results indicate little change to surface and depth-averaged current velocities within Te Awanui and at the offshore disposal sites H1 and H2 (refer Figure 29 below) in response to both seasonality and climate variability, although there are some differences at the upper tail of the velocity distribution (98$^{th}$ percentile and maximum). There is no consistent overall pattern to the differences in the upper tail and are random fluctuations within the accuracy of the model as defined by the MAE values in Table 1.

The residual currents plotted in Figures 5-14 to 5-17 of Watson and Berthot (2024a) do not show any obvious differences within Te Awanui due to seasonal or ENSO impacts. However, there are differences evident outside the tidal inlet, with increased residual circulation around Moturiki and Motuotau Islands during El Niño conditions, and strengthening of flood flow along the foreshore of Matakana Island during La Niña conditions.

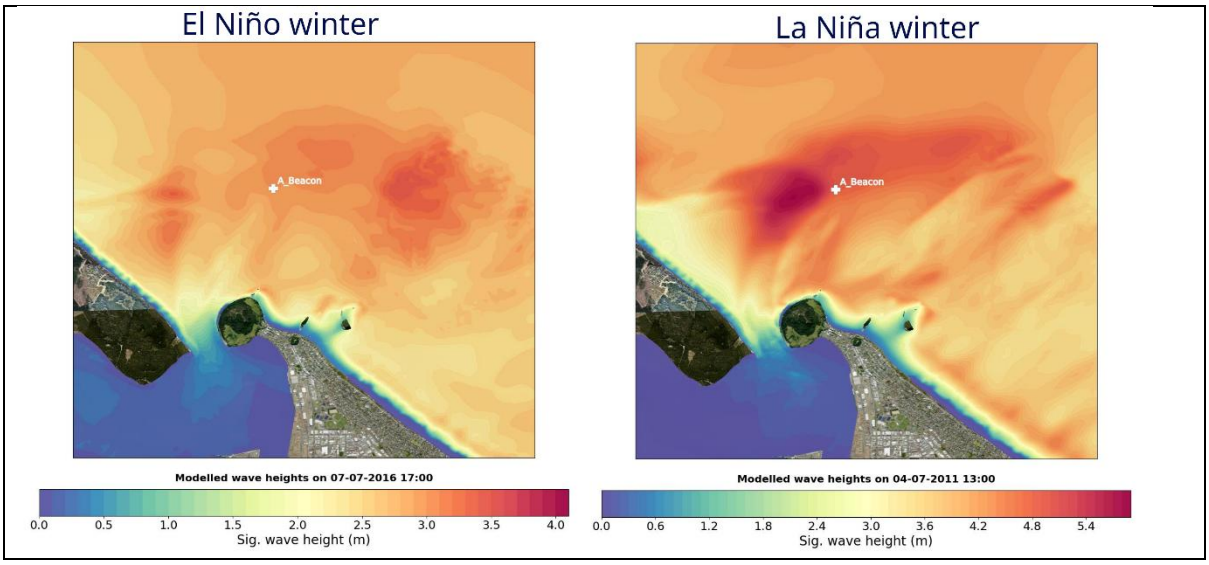



*Figure 6 – Comparison of wave conditions during an El Niño and a La Niña winter storm. Note that the La Niña colour scale is 0-6 m, while the El Niño colour scale is 0-4 m. From Figures 5.20 and 5.21 of Watson and Berthot (2024a).*

The predicted significant wave heights also show no variations with season or climate variability within Te Awanui. However, while average wave conditions are similar between El Niño and La Niña extremes of ENSO, the upper tail values increasingly deviate for the 80$^{th}$ percentile to maximum statistics. The model results indicated that for the offshore area including H1 and H2, extreme waves are larger for La Niña conditions, particularly during the winter (Figure 6).

The implications of the offshore changes to waves and currents due to ENSO will be discussed further in Section 5.

The calibrated and validated coupled SCHISM/WMM model was used as input into other models to predict the impacts of proposed dredging. These models will be discussed in the following sections.

The underlying geology is a major control on the characteristics of the sediment being dredged, and hence, the potential impacts of the process. For the port area, the underlying geology consists of reworked and primary volcaniclastic sediments (pyroclastic materials predominantly), and lava domes. Historically, the port has not needed to excavate channels through solid lava flows, but has had to remove coarse deposits of material resulting from mass movement of slope material from the flanks of lava domes (Tanea Shelf and isolated cobbles in sediments close to the entrance).

Most of the sediment previously dredged is sand-sized with low proportions of fines (silt and clay). Generally, sediment encountered during maintenance dredging differs from sediment involved in capital dredging:

- Maintenance dredging – recently deposited sediment associated with siltation in channels, may have a higher fines or coarse content depending on current velocities, more organic material, and contain contaminants.
- Capital dredging – old sediment, which may have a higher fines content and reduced biogenic content due to weathering and post-depositional alteration, and normally doesn't contain contaminants.

Within Te Awanui, the presence of biogenic material such as shells is a useful indicator of the age of sediment and the depositional environment (marine or terrestrial). During previous capital dredging programmes, biogenic material has included cemented sediments containing shells (beach rock), lumps of peat, and wood fragments to large portions of trees (Figure 7).

The materials shown in Figure 7 are not normally considered to cause any environmental impacts, but may disrupt the dredging process. Generally, excluding direct burial, impacts are predominantly associated with fine sediments (silt and clay) as discussed in the next section. Hence, it is important to have good information on the distribution of sediment textures for the volume being dredged. Resource consent conditions for existing dredging and disposal require monitoring of sediment texture in the dredge hopper, and Environmental Impact Assessments for Capital Dredging Programmes since the late 1980s have included analysis of the sediment textures for the material to be dredged.





*Figure 7 – Some of the larger items encountered by the trailer suction dredge during the 1991/92 Capital Dredging Programme: top left – shells cemented in estuarine mud (Eemian?); top right – shells cemented in coarse sand (beach rock); middle row (right side is an enlargement of the left) – wood, pumice, peat, iron cemented sands (ferricrete or iron pan) and rhyolite cobbles; and bottom – tree stumps.*

However, there has been very little analysis of sediment involved in Maintenance Dredging Campaigns, apart from some work looking at the southern area of Stella Passage when applying for consent to dispose of sediment at H1 and H2 sites (Michels and Healy, 1999)[25].

Comparing the dredge hopper sediment texture during Maintenance and Capital dredging (Figure 8 & Figure 9) provides some evidence about the differences of the two sediment sources for the port area.

The overall grain size distributions are very similar, which is consistent with most of the sediment being derived from the same original sources (the pyroclastic deposits of the Tauranga Volcanic Centre). However, there are some differences:

- Maintenance dredging sediment (primarily close to the tidal delta systems – Entrance Channel, Cutter Channel, northern Maunganui Roads), contains more coarse sand material. This includes biogenic sediment such as shell fragments, which are dissolved and lost from older, deeper sediments.
- Maintenance dredging sediment has a higher silt content than Capital sediment, which is associated with stormwater discharge and flood discharges from catchments around the harbour. Some of the silt represents heavy minerals (e.g. Titanomagnetite) that form placer deposits as lower density materials are preferentially transported away.
- Capital dredging sediment has a higher clay content resulting from weathering during glacial conditions and some hydrothermal alteration associated with hot springs (*residual* or *primary* clays). During the transport of sediment from source to the area of deposition, clays tend to be lost as they remain in suspension (contributing to the export of sediment from the harbour as demonstrated by de Ruiter, 2022). Therefore, sediment transported into the channels tends to have lost the original clay fraction.
- Capital dredging sediment tends to be better sorted (narrower and higher peak) due to lower quantities of coarse sand and medium to very fine silt.

[25] Michels, K. H., & Healy, T. R. (1999). Evaluation of an inner shelf site off Tauranga Harbour, New Zealand, for disposal of muddy-sandy dredged sediments. Journal of Coastal Research, 15(3), 830-838.

- Surficial sediments are reworked by tidal currents, and waves in shallower areas. This tends to remove coarse to medium sand and concentrate fine sand. This results in a double peak in the medium to fine sand region of the sediment size distributions.

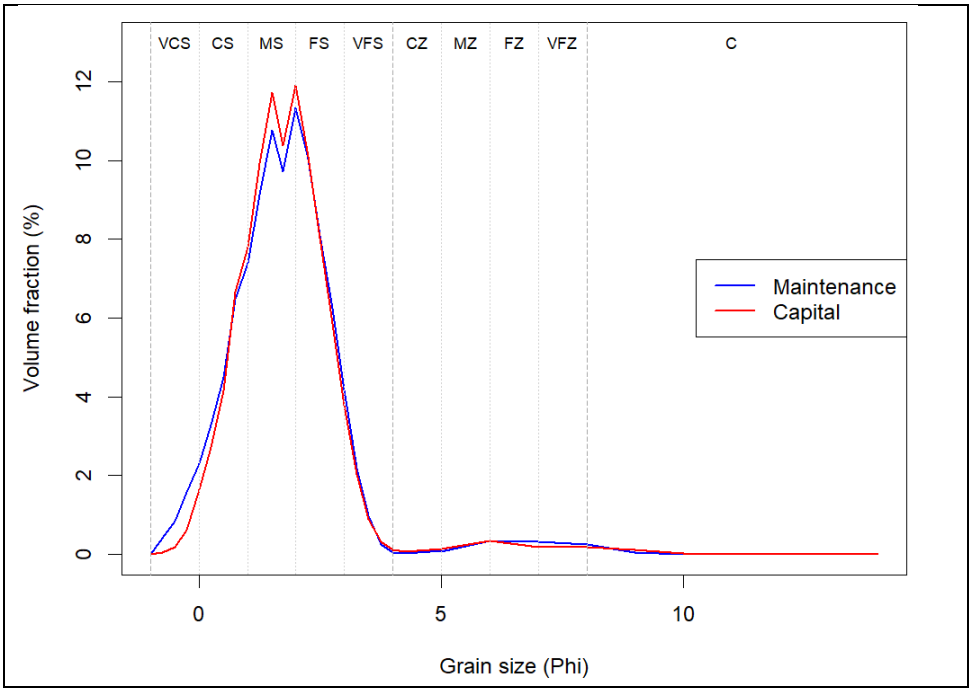



*Figure 8 – Comparison of the average grain size distributions for hopper sediments during Maintenance and Capital dredging for all samples analysed from 2010 to 2024. The size classes are indicated: VCS = Very Coarse Sand; CS = Coarse Sand; MS = Medium Sand; FS = Fine Sand; VFS = Very Fine Sand; CZ = Coarse Silt; MZ = Medium Silt; FZ = Fine Silt; VFZ = Very Fine Silt; and C = Clay.*

Figure 9 shows more clearly the difference in size distributions associated with the concentration of higher density heavy minerals in the fine sand fraction of the Maintenance dredging sediment. The concentration of heavy minerals was noted in the subsurface sediments present in a small ebb-tide delta at the mouth of the tidal channel from Waipu Bay at Whareroa Point (Moon and de Lange, 2019)[26].One difficulty with interpreting the source sediment differences from the hopper sediments, is that the dredging process will modify the original sediment texture. In particular, sediment from different locations is mixed together, and finer sediment will preferentially be removed from the hopper during any overflow discharge (contributing to turbidity).

Further, the University of Waikato upgraded their laser-sizer system in 2013, and then replaced it in 2015. This means that the Maintenance dredging samples were measured over a different range of sizes:

- 2010-2013 – measured from 1000 µm (0 phi, coarse sand) to 63 µm (4 phi, very fine sand)
- 2013-2015 – measured from 1000 µm (0 phi, coarse sand) to 0.98 µm (10 phi, clay)
- 2015-present - measured from 2000 µm (-1 phi, coarse sand) to 0.06 µm (14 phi, clay). The laser-sizer can measure up to 3000 µm (granules), but grains coarser than 2000 µm are removed before analysis by sieving to avoid blockages in the system.

[26] Moon, VG, & de Lange, WP. Characteristics of sub-surface sediments in southern Stella Passage, Tauranga Harbour. Environmental Research Institute Report 133, University of Waikato, Hamilton. 62 pp.

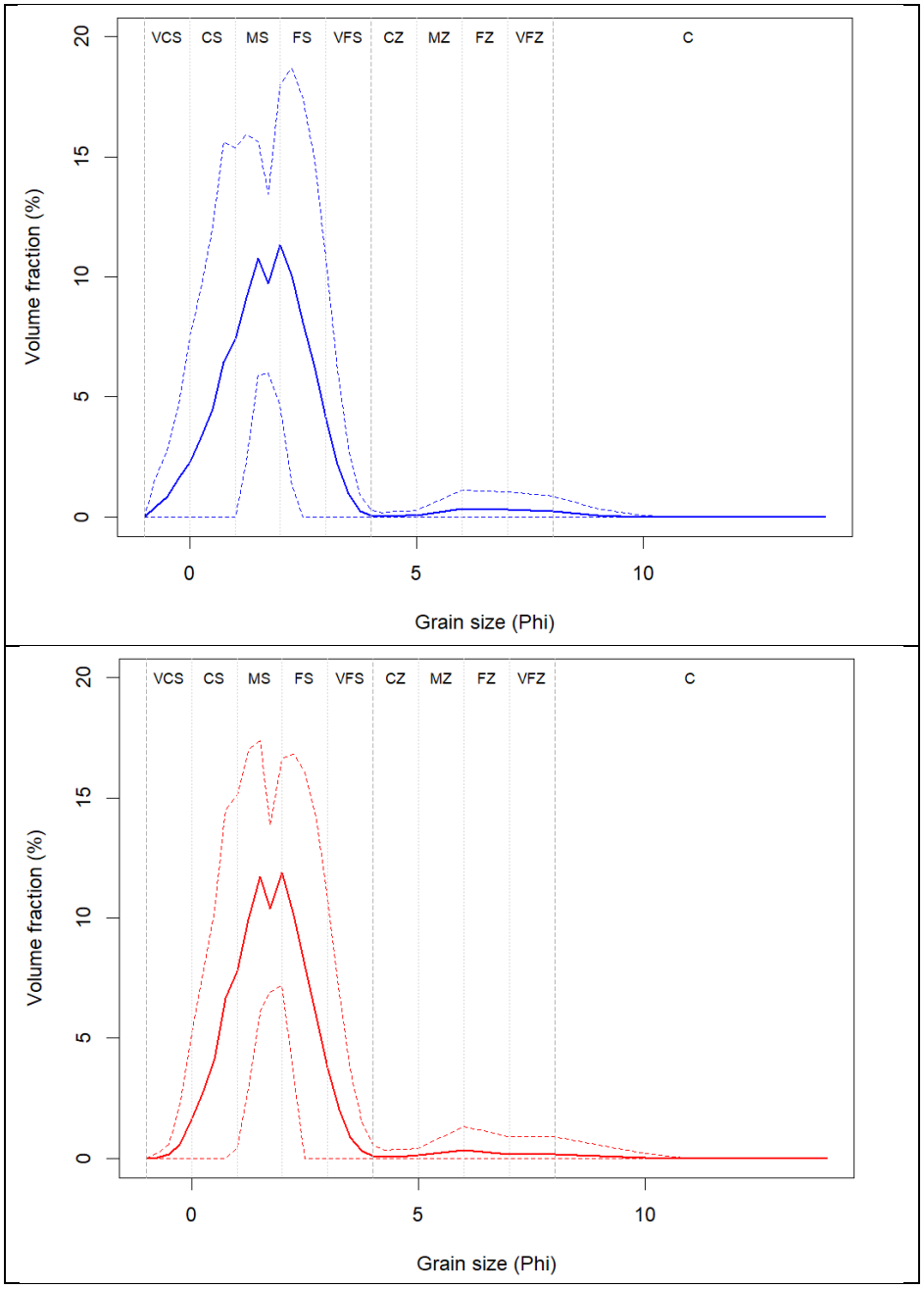



*Figure 9 – Comparison of the 95% (±2 standard deviation) envelopes of grain size distributions for hopper sediments during Maintenance (top) and Capital (bottom) dredging for all samples analysed from 2010 to 2024. The size classes are as summarised in the caption for Figure 7.*

Before the 2015/16 Capital Dredging Programme and the Stella Passage Development proposal, the subsurface sediments in the channels were investigated using a shallow seismic survey to identify structures, CPT probing to determine the geotechnical characteristics and 3-5 m vibracores to obtain core samples for description and textural analysis. The Stella Passage samples were from an area not previously dredged, and assuming that the development proceeds the material sampled will be largely removed. The deeper parts of the pre-2015/16 cores were not removed during the dredging programme, and so those data give some insight into the material to be dredged if there is further channel or sitting basin deepening.

Figure 10 shows the average size distribution for successive 1 m thick layers below the surface based on all the available data. The reports and publications produced from the core data provide a more

detailed site-specific analysis if required (e.g. de Lange et al, 2014[27]; MacPherson et al, 2017). The size distribution within the sand fraction follows the same pattern as the hopper sediments in Figure 7 (bottom), including the enhancement of the fine sand component in the upper layer. However, there is a significant change in the finer size classes (mostly within the silt fraction).

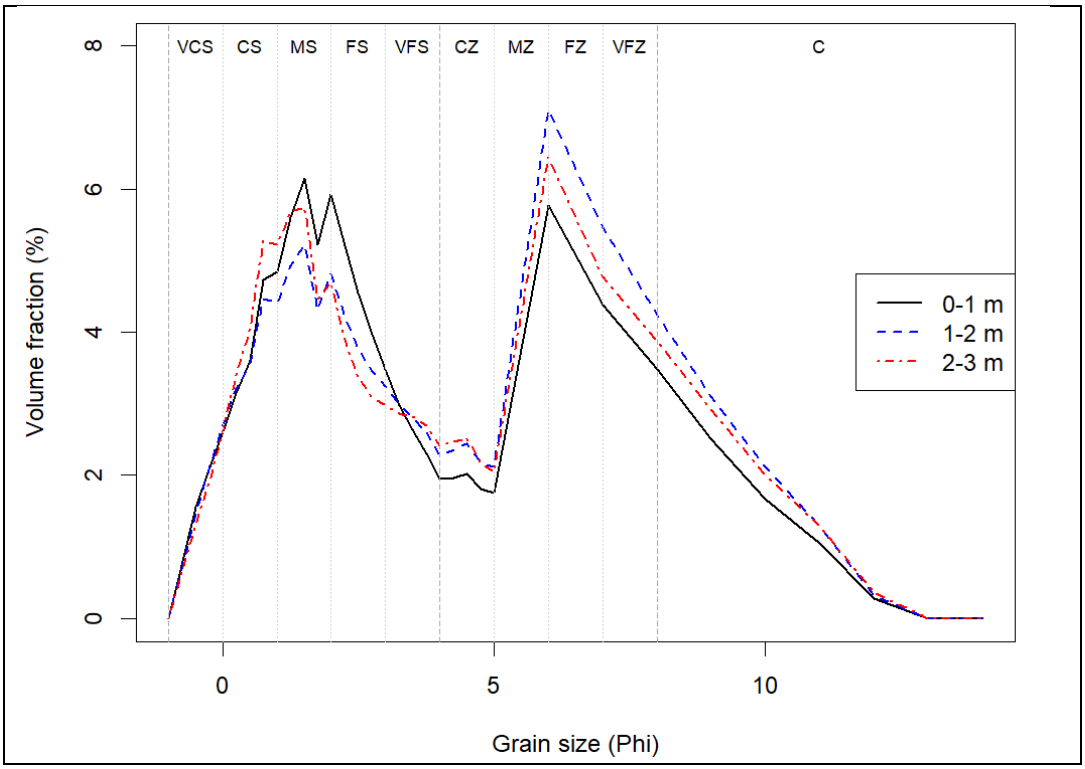



*Figure 10 – Comparison of the average grain size distributions for subsurface sediments obtained by vibracores before the 2015/2016 Capital Dredging Programme (de Lange et al, 2014). The textural data have been aggregated into 1 m thick slices below the sea floor that existed in 2013/14. The size classes indicated are defined in the caption for Figure 6.*

Table 2 summarises the average proportions within the main size classes for all of the subsurface sediments, the 3 layers in Figure 10, and the dredge hopper samples summarised in Figure 9. It is clear that during the dredging process, there has been a reduction in the fines content of the sediment being sampled. While this may be partly due to the way sediment is deposited in the dredge hopper, some of the loss is associated with the turbid plumes produced during dredging. These will be discussed in the next section.

*Table 2 – Summary of the average proportions in each size class for the sediment textural data plotted in Figures 7-9. Note that due to rounding errors, the proportions may not exactly sum to 100%*

| | Subsurface | | | | Dredge hopper | |
|---|---|---|---|---|---|---|
| | All | 1 m layer | 2 m layer | 3 m layer | Capital | Maintenance |
| Sand | 70.4 | 73.3 | 67.3 | 69.1 | 98.8 | 98.9 |
| Fines | 29.6 | 26.7 | 32.7 | 30.9 | 1.2 | 1.1 |
| Silt | 25.6 | 23.1 | 28.2 | 26.7 | 1.1 | 1.1 |
| Clay | 6.2 | 5.5 | 6.8 | 6.6 | 0.1 | 0.1 |

[27] de Lange, WP, Moon, VG, & Fox, BRS, 2014. Distribution of silty sediments in the shallow subsurface of the shipping channels of Tauranga Harbour. Environmental Research Institute Report 43, University of Waikato, Hamilton. 78 pp.

Maintenance dredging is required to ensure that there is sufficient depth and width within the shipping channels to ensure safe passage by vessels using the Port of Tauranga facilities. The Port routinely surveys the channels to monitor changes to the channel dimensions, typically 9 months after maintenance dredging is completed. The data obtained is used to determine the locations requiring maintenance dredging, and the volumes that need to be extracted. These data can also be used to determine the rates of accumulation (Figure 11).

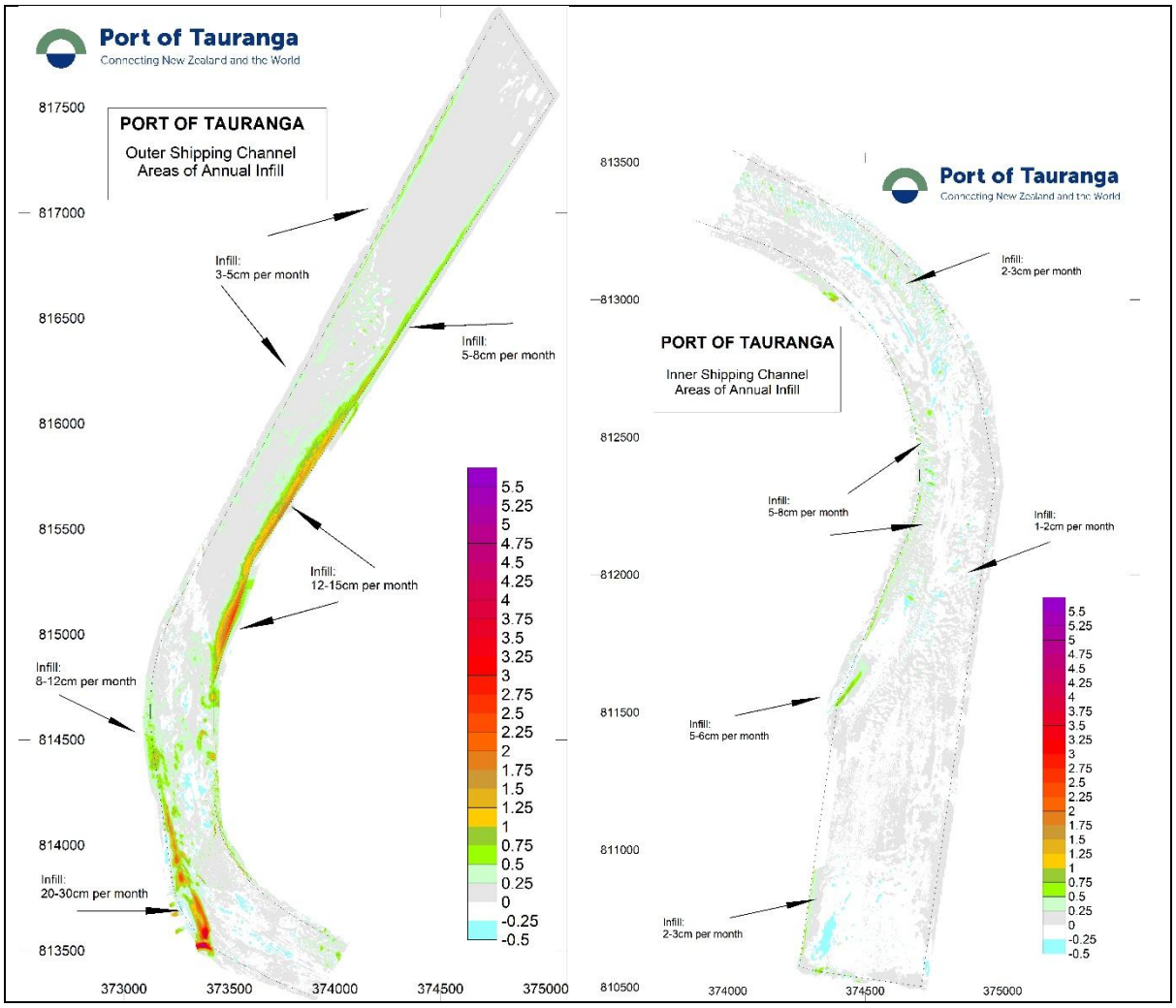



*Figure 11 – Average monthly rates of infill since the last major capital dredging programme in 2015-2016 based on 1 m resolution gridded MBES surveys for the outer (left) and inner (right) channels (pers. Comm., Greg Cox, Port of Tauranga Hydrographer). The colour bar scale represents the thickness of infill sediment between the previous maintenance dredging and the pre-dredging survey (9 months later) in metres.*

Since the completion of the last capital dredging, the infill has been concentrated in the areas arrowed in Figure 11, with the highest rates of infill occurring in the outer channels (0.03-0.30 m per month compared to 0.01 to 0.08 m per month for the inner channels). For the outer channels the highest rates occur along the eastern margin of the Entrance Channel along the northwest shoreline of Mauao, and the western margin of No.2 Reach linking the Entrance Channel with the Cutter Channel. These areas are accumulating different types of sediment reflecting their source regions:

- Sediment accumulating in the Entrance Channel contains a higher proportion of fine sand that is transported by flood tide eddies from Te Paritaha (flood tidal delta) within the harbour (Spiers, 2013).

- Sediment accumulating in No.2 Reach contains a higher proportion of coarse sand that is transported from the Matakana Banks (ebb tidal delta) by flood currents (de Lange, 2025)[28].

For the inner channels, the highest rates occur along the eastern margin of Te Paritaha in areas where predominantly medium sand transported along the ebb shield is entering the Maunganui Roads.

The rates of infill vary from year to year, but tend to be similar in areas dominated by tidal transport. However, areas affected with weather-related processes such as rainfall resulting in increased terrestrial sediment inputs, or increased wave action increasing marine sediment inputs can show larger interannual to interdecadal changes. This is particularly the case for No.2 Reach, where the volume of infill significantly increased in the 15 months following Cyclone Gabrielle in 2023 (de Lange, 2025).

With respect to vessel navigation, the narrowing of the channel at bends is more critical than shallowing of the channel. Assessment of the requirements for larger vessels by the Australian Maritime College (AMC) prior to the 2015-2016 Capital dredging programme (AMC, 2012[29]; AMC 2013[30]) identified that the transitions from the Entrance Channel (No.1 Reach) into the Cutter Channel, and then into the Maunganui Roads required changes to the orientation of No.2 Reach and widening of the Cutter Channel (Section 3.1 in Healy et al, 2009[31]). The specific changes identified for up to 347 m LOA vessels included:

- Realignment of No.2 Reach 29° to reduce the acute turns inside the harbour, and shifting more of more of the overall turn into naturally occurring deep water outside the harbour;
- Widening the Channel at Tanea Shelf by 32 m;
- Widening Cutter Channel by a maximum of 90 m on the south-western side and another 25 m on the north-eastern side, increasing the width by 115 m at that point to 285 m. This was the major increase in the total area of the shipping channels. The Cutter Channel Leads were also be realigned to ease the corners at both ends of the Channel; and
- Easing the corner between the Cutter Channel and Maunganui Roads slightly by widening by 50 m at the intersection.

The highest rates of infill shown in Figure 11 affect all these areas apart from the Tanea Shelf, and progressively restrict the maximum length of vessel that can access the port.

The minimum design depth for the dredged channels is for the inner channels at 14.5 m below lowest astronomical tide (chart datum). The water level may drop below this elevation in response to wind stress and/or increases in atmospheric pressure, or the presence of infragravity and fair-infragravity waves (meteotsunamis or rissaga) (Goring, 2009[32]). Meteotsunami have been identified as the cause

[28] de Lange, WP, 2025. Recent sediment accumulation at junction of Entrance Channel (No.2 Reach) and western Cutter Channel. Report to the Port of Tauranga Ltd, September 2025. 87 p

[29] AMC, 2012. Port of Tauranga Simulation Study from 23 March 2012 to 23 March 2012, Summary of Simulation. Project No. 12/S/09, AMC Search Ltd.

[30] AMC, 2013. Port of Tauranga Simulation Study from 20 May 2013 to 23 May 2013, Summary of Simulation. Project No. 13/S/2, AMC Search Ltd.

[31] Healy TR, Thompson G, Grace RV, & Spiers K (2009). Assessment of Environmental Effects for Port of Tauranga channel deepening and widening. Report prepared for the Port of Tauranga Ltd. University of Waikato, the Port of Tauranga Ltd, & Marine Biological Consultants, Tauranga, New Zealand 220p.

[32] Goring, D. G. (2009). Meteotsunami resulting from the propagation of synoptic-scale weather systems. Physics and Chemistry of the Earth, Parts A/B/C, 34(17), 1009-1015.

of vessel groundings at several New Zealand ports due to water elevation changes of up to 1 m: including Marsden Point, Lyttelton, and Bluff (Goring, 2005[33]).

The effective draft of vessels may also increase due to the movement of the vessel causing a reduction in pressure around the vessel (squat). This can move the vessel towards the seabed, or towards the channel sides. Shorter period waves in the outer channels can also reduce the effective depth of the channel, so the outer channels have a design depth of 15.8 m that transitions to the inner channel depth of 14.5 m within Cutter Channel. Vessel movements at the Port of Tauranga are managed to minimize squat, but the calculations are based on the design depth and channel width.

Individual vessels were extracted from Port of Tauranga ship movement records for 2021-2025, which identified 1547 separate vessels, and for each of these the maximum draft and the length overall of the determined as the maximum length of a vessel's hull measured parallel to the waterline (LOA) was tabulated. Figure 12 shows the distribution of vessel dimensions as a scatterplot of draft versus LOA. Since multiple vessels have the same dimensions, the frequency of maximum draft and LOA values is indicated by the density curves parallel to the corresponding axes. The peak in LOA is mostly associated with log carriers. Container vessels tend to have larger LOA values. Larger vessels carry more cargo, and tend to visit less frequently than smaller vessels.

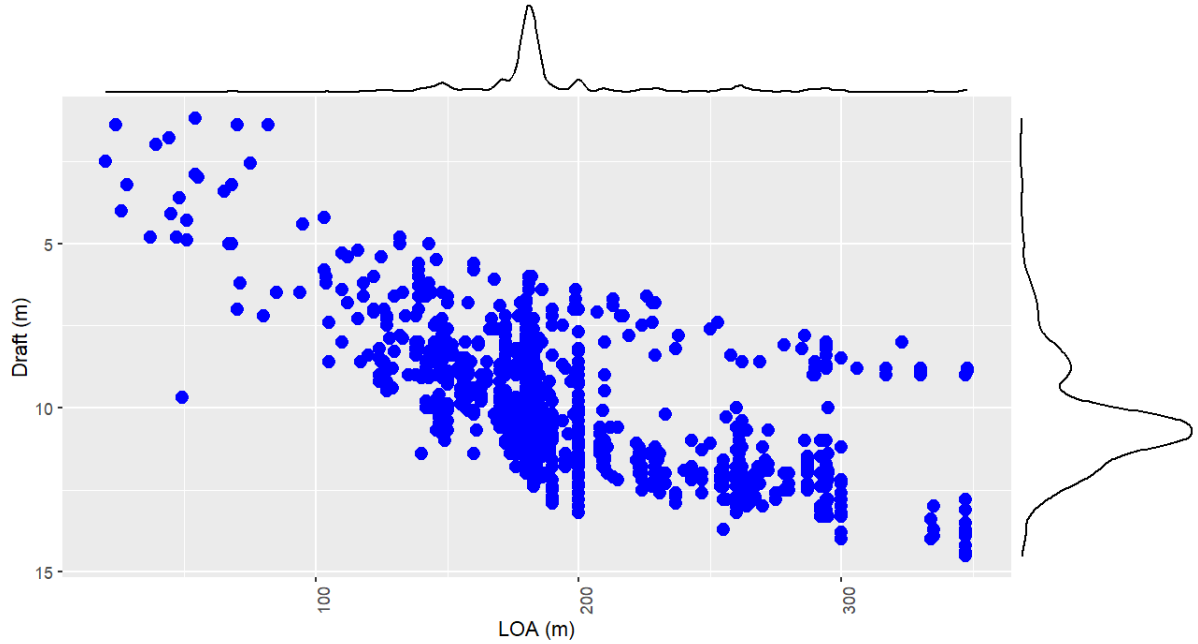



*Figure 12 – Scatter plot of the maximum draft and LOA for 1547 individual vessels that berthed at the Port of Tauranga between 2021-2025. The density curves above and at right indicate the frequency of vessels with the correspond LOA and draft respectively.*

With the maximum accretion rate of 0.08 m per month (0.96 m per year), the longer and deeper vessels plotted can potentially run aground without carefully managing vessel speed and state of the tide a year after maintenance dredging. In particular, the vessels in the lower right corner (Panamax container ships) are already limited to high tide when the channels are at design depth. Further, 13 of the vessels have the maximum LOA the channels were designed for, and would be affected if sediment accretion narrowed the channel width (AMC, 2012, 2013; Port of Tauranga, pers. comm.).

[33] Goring, D. G. (2005). Rissaga (long-wave events) on New Zealand's eastern seaboard: A hazard for navigation. Coasts and Ports 2005: Coastal Living-Living Coast; Australasian Conference; Proceedings.

If the maximum rate continued for ~5 years, about 50% of the vessels would be limited to high tide conditions. If the accretion patterns remain the same as shown in Figure 11, the longer vessels would require assistance to maneuver around the sharper bends in the channels at all stages of the tide (Port of Tauranga, pers. comm.). Without maintenance dredging, the channel dimensions with likely converge towards those existing before dredging began. However, the long-term shoaling of the Lower Western Channel in response to the accretion of southeastern Matakana Island will contribute extra ebb tidal discharge to channels on the eastern side of Te Paritaha so they are likely to be larger than before dredging. Without modelling this scenario, the eventual equilibrium channel dimensions are uncertain, although it is likely that the majority of vessels plotted in Figure 12 would be unable to enter the port.

## 3.0 Sediment extraction impacts

The dredging is likely to be undertaken mainly using a trailing suction hopper dredge (TSHD), with a back-hoe dredge (BHD) used in difficult to reach areas[34]. During the extraction phase a typical TSHD, can generate turbid plumes (Figure 13) in three distinct ways (Figure 14) (Mills & Kemp, 2016)[35]:

- At the seafloor as the cutter head disrupts the sediment to allow it to be pumped up into the dredge hopper;
- From the overflow discharge of water pumped into the hopper along with the sediment; and
- In shallow conditions, the propellor wash or jet can disturb sediment on the seafloor, and disrupt the settling process for the plumes produced by the other two sources.

In Figure 13, all three processes have contributed to the turbidity evident after the dredge has made a pass southward (towards the right) into Stella Passage, turned and continued dredging northwards towards the harbour entrance (towards the left).

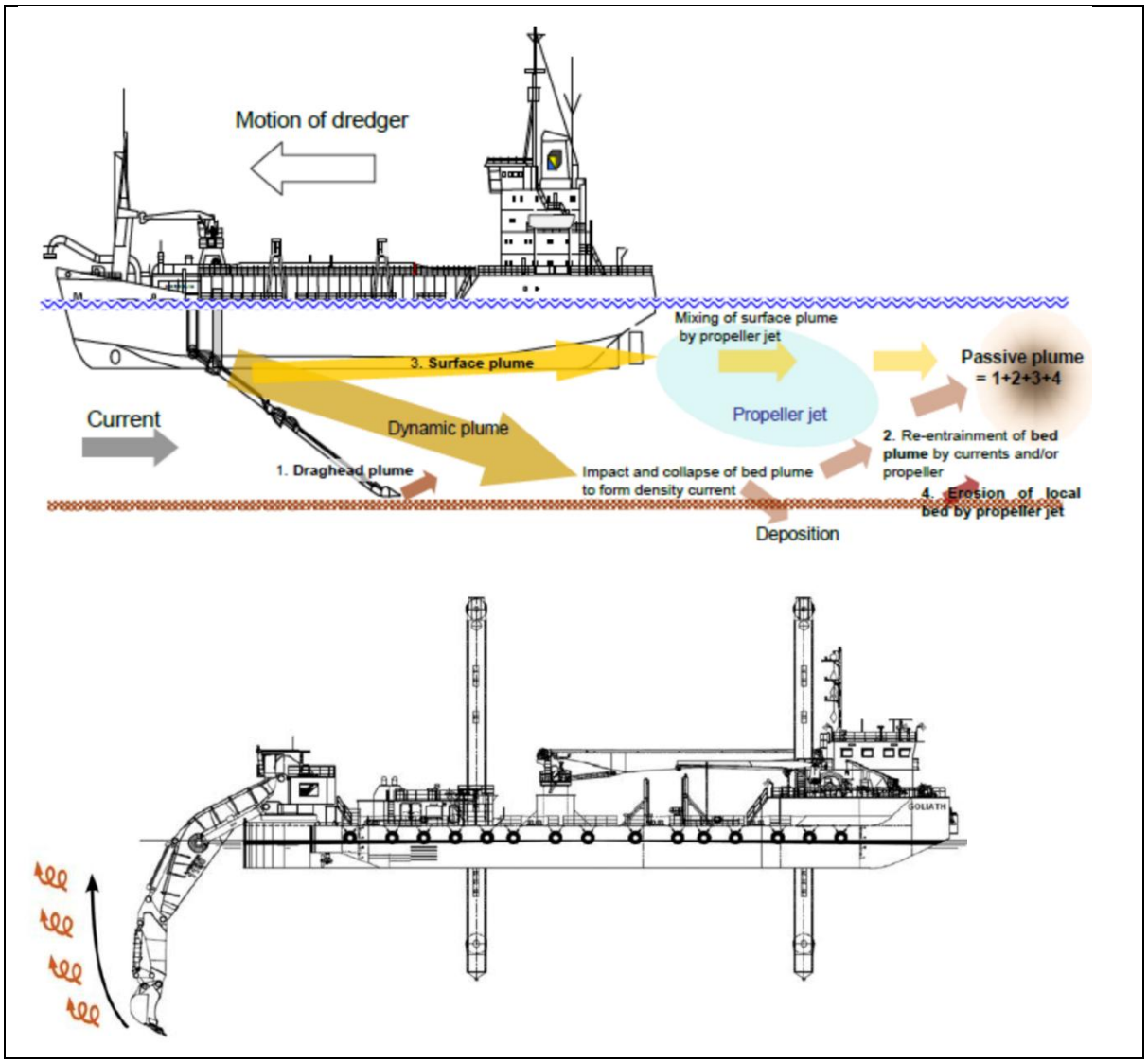



*Figure 13 – Trailing suction hopper dredge operating on a flood tide at the junction of the Maunganui Roads and Stella Passage during the 1991/92 Capital dredging Programme. There were very low levels of background turbidity at the time.*

[34] For more information on the operations of a TSHD refer to the 'Description of the Activity' section of the AEE

[35] Mills, D., & Kemps, H. (2016). Generation and release of sediments by hydraulic dredging: a review. WAMSI Dredging Science Node, Report, Theme 2, Project 2.1. 77 pp.

Figure 14 illustrates the sources of the plumes and the processes involved. In particular, it distinguishes between the surface plume that results from mixing of the overflow sediment with the water around the dredge, and the dynamic plume that involves a density current transporting most of the overflow sediment. Plume generation and behaviour was measured during dredging operations at the Ports of Auckland in 1992 and 1993 (Priestley, 1995)[36]. The observations showed that the increased density within the plume due to suspended sediment resulted in most discharged sediment being transported directly to the seabed, with the majority being rapidly redeposited as the plume collapsed and dispersed (Figure 14). This led to the conclusion by Priestley (1995) that the environmental effects were minimal. However, as illustrated in Figure 13 and Figure 14, the propellor wash can disrupt the dynamic plume causing mixing, and re-entrain the sediment from the sea floor, which adds sediment to the passive plume dispersing behind the dredge.




[36] Priestley, S. (1995). Measured environmental impacts of dredging operations. WIT Transactions on The Built Environment, 8, 283-290.

*Figure 14 – Release of sediment arising from dredging by (top) a trailing suction hopper dredge (TSHD) and contributions to the suspended sediment (Figure 9 from Mills & Kemps, 2016[37]), and (bottom) a backhoe dredge (BHD (Figure 6 from Becker et al, 2015[38]).*

One implication of the processes summarized in Figure 14, is that the overflow and dynamic plume effectively export fine sediment from the dredge hopper and return it to the seafloor in the area being dredged. This potentially increases the proportion of fines over time; most likely in response to frequent maintenance dredging, and not capital dredging that is essentially a one-off event. There does not appear to be published work assessing whether this is occurring and having an impact on benthic biota at any location worldwide being regularly dredged.

Figure 15 is a schematic diagram of the three plume sources, with density of the shading indicating the proportion contributed to the overall turbidity of the total near-field plume. This indicates the propellor wash is a significant factor in determining the turbidity in the vicinity of the dredge; primarily due to the interaction between the propellor wash and the dynamic plume, since without overflow and the water being sufficiently deep to prevent the propellor wash directly eroding the seabed, the turbidity is greatly reduced.

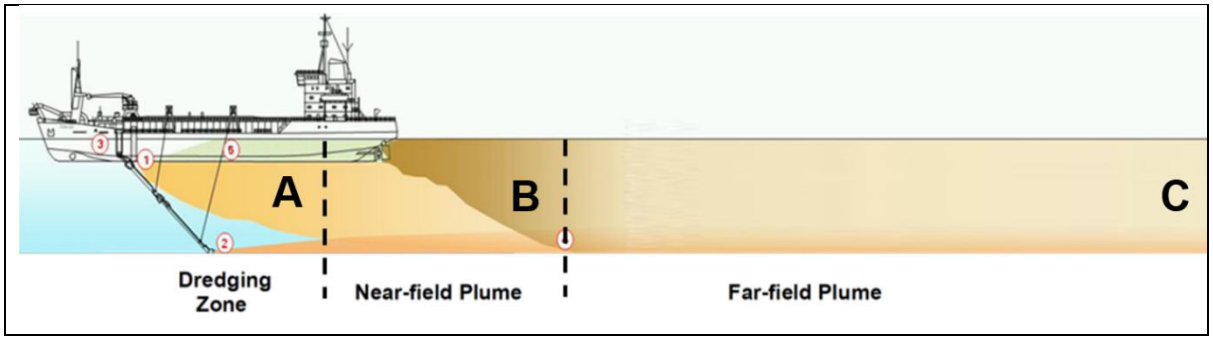



*Figure 15 – Release of sediment arising from dredging by (top) a trailing suction hopper dredge (TSHD) and contributions to the suspended sediment (Figure 9 from Mills & Kemps, 2016), and (bottom) a backhoe dredge (BHD (Figure 6 from Becker et al, 2015).*

As the plume moves away from the near-field, the concentration of suspended sediment within the plume declines as the plume disperses and, more importantly, the sediment settles to the seabed (Figure 16). Dispersion is less important for the excavation phase than the disposal phase, as the flow is generally concentrated in deep channels, particularly during ebb tide (e.g. Figure 17). Settling of larger grain and clast sizes, typically fine sand and coarser, is rapid (order of seconds) so this material returns to the seabed close to the dredge. Generally, this material is captured within the dredge hopper during the excavation phase, and does not contribute to the plume.

[37] Mills D, & Kemps H, 2016. Generation and release of sediments by hydraulic dredging: a review, WAMSI Dredging Science Node, Report. Theme 2: Project 2.1. 77 p.
[38] Becker J, van Eekelen E, van Wiechen J, de Lange W, Damsma T, Smolders T, & van Koningsveld M, 2015. Estimating source terms for far field dredge plume modelling. Journal of Environmental Management, 149, 282-293.

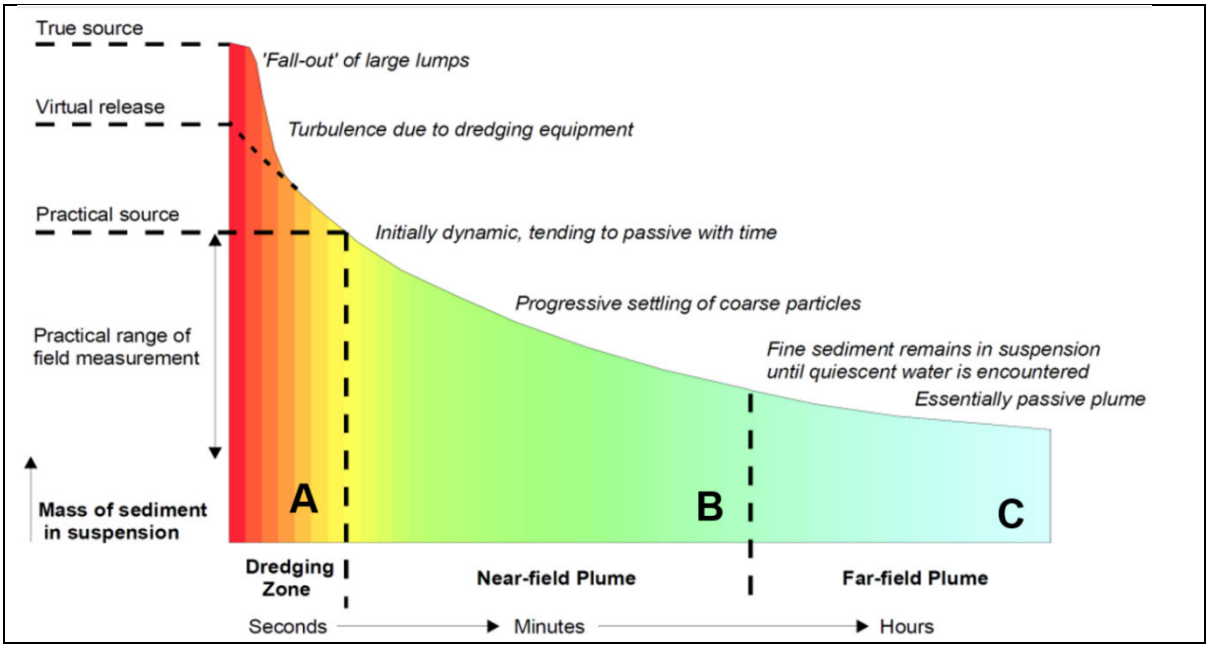



*Figure 16 – Schematic diagram of the sources of turbid plumes for a trailing suction dredge, where the overflow consists of two components: a concentrated discharge from a pipe at the stern of the dredge, and some discharge over the sides of the hopper. Propellor wash is not specifically shown. The zones A, B, and C correspond to the zones in Figure 15 that shows the plume behaviour with time/distance from source.*





*Figure 17 – A persistent turbid plume resulting from dredging a weathered ignimbrite in the Stella Passage during the 1991/92 Capital Dredging Programme. There are two vessels in the harbour entrance: (left) the THSD heading to the disposal site; and (right) a barge moored over Tanea Shelf to extract boulders for relocation to form a new reef closer to Pilot Bay.*

Very fine sand to fine silt takes minutes to settle to the seabed (depending on water depth and level of turbulence), and the time/distance taken for this to occur defines the extent of the near-field plume. Previous consent conditions for the Port of Tauranga have defined a mixing zone, which represents the maximum likely extent of the near-field plume.

The remaining sediment (very fine silt and clay) tends to remain in suspension if there is any turbulence present, unless the grains form larger aggregates (flocculation, or incorporation into marine snow), and forms the far-field plume. Very fine material may take hours to days to settle, which means that it is generally exported from estuaries. Sediment plumes are also formed in Te Awanui due to other processes, such as rainfall, landslides and waves, that add sediment to freshwater inflows into the harbour, directly deposit sediment in the harbour, or entrain fine sediment from the intertidal areas. Figure 18 shows a plume of very fine sediment discharged by the Wairoa River and Waikareao Estuary after heavy rain, heading seaward through the Otumoetai Channel on an ebb tide.



*Figure 18 – Turbid plume consisting mostly of clays derived from weathered tephra and discharged after heavy rain by the Wairoa River, and the Waikareao Estuary catchment.*

The concentration of suspended sediment in far-field plumes is low, and for the plumes measured by the Ports of Auckland (Priestley, 1995) and the Port of Tauranga (Bryan et al, 2013[39]; Coppede Cussioli, 2018[40]), the concentrations are reported as being at the lower end of the natural range. Although, the concentrations are low, the sediment grains involved may have a significant effect on the visual appearance of the water (Figure 13 & Figure 17). This results from the scattering of light, which is a function of the grain size (very fine grains are more efficient scatters than coarser grains), grain shape, and colour (Cussioli et al, 2020[41]).

The very distinct plume formed during the dredging of a weathered ignimbrite in 1992 (Figure 17) was due to the presence of bladed glass shards in the fine silt and very fine silt fraction. White sediment scatters light efficiently (followed by orange) so it results in a greater impact on photosynthesis at the sea bed (Cussioli et al, 2020). This means that assessing turbidity solely on the suspended sediment concentration is not reliable. The sensors used by the Port of Tauranga measure light attenuation, which is more useful but ideally is supplemented by Photosynthetically Active Radiation (PAR) sensors to monitor the available light near the surface.

Coppede Cussioli (2018) focused primarily on the impacts of turbidity on seagrass (nana, eelgrass, *Zostera mulleri*), so her data are presented as the light attenuation coefficient, $K_d$(PAR). She presents a standard relationship relating this with NTU, and also developed an empirical relationship specifically for Te Awanui/ Tauranga Harbour. She also derived relationships between TSS and NTU for different sediment colours, which were:

$$Grey\ sediment \quad NTU = \frac{TSS - 9.637}{1.412}$$

$$White\ sediment \quad NTU = \frac{TSS - 2.594}{3.012}$$

[39] Bryan KR, Douglas E, Pilditch CA, & Cussioli MC, 2014. *Setting water quality limits and monitoring turbidity for the Port of Tauranga. Part A: Preliminary Investigation*. ERI report 25. Environmental Research Institute, Hamilton, New Zealand. 22 pp + appendix

[40] Coppede Cussioli M, 2018. *Ecological effects of turbidity variations in and around dredging areas in the Port of Tauranga*. PhD Thesis, The University of Waikato, Hamilton, New Zealand.

[41] Cussioli, M. C., Seeger, D., Pratt, D. R., Bryan, K. R., Bischof, K., de Lange, W. P., Bornman, J. F., & Pilditch, C. A. (2020). Spectral differences in the underwater light regime caused by sediment types in New Zealand estuaries: implications for seagrass photosynthesis. Geo-Marine Letters, 40(2), 217-225.

These equations indicate that the relationship between NTU and TSS is not straightforward, and comparing results obtained by different sensors without information about their calibration is unreliable. Measurements of TSS are not affected by the sediment characteristics, and are more reliable if a standard procedure is followed. However, TSS generally requires laboratory analysis, and, hence, is not a normally reported in real time. NTU can be reported in real time, but should utilize the same types of sensors throughout the monitoring network. This is the case with the Port of Tauranga turbidity sensors. Periodic acquisition of water samples to determine TSS is a useful supplement, and is provided for in the Dredge Management Plan that includes periodic sampling at the mixing zone boundaries when the dredge is excavating.

Numerical modeling of dredge plume behaviour predicts TSS, and this will predominantly be used in the following sections. To provide a context for the values being discussed, Table 3 summarises the NTU and TSS observations reported by the Bay of Plenty Regional Council via their Environmental Data Portal[42]. These data indicate that the variation in NTU and TSS values tends to increase with distance from the harbour entrances. The Mount Maunganui and Bridge Marina sites are the closest to the Port of Tauranga.

*Table 3– Summary univariate statistics for the turbidity and total suspended solids observations reported by the Bay of Plenty Regional Council for their estuarine and tidal sites within Te Awanui.*

| | Turbidity (NTU) | | | Total suspended solids (mg/l) | | |
|---|---|---|---|---|---|---|
| Location | Minimum | Median | Maximum | Minimum | Median | Maximum |
| Tanners Point Jetty | 0.3 | 1.8 | 10.1 | 2.1 | 9.2 | 53.0 |
| Kauri Point Jetty | 0.5 | 2.8 | 66.6 | 2.9 | 14.0 | 165.6 |
| Omokoroa Wharf | 0.5 | 3.2 | 22.0 | 2.2 | 15.0 | 123.0 |
| Wairoa at SH2 | 0.8 | 3.8 | 55.0 | 0.8 | 8.0 | 166.0 |
| Tilby Point | 0.7 | 2.6 | 169.0 | 1.1 | 11.0 | 498.0 |
| Waikareao | 0.6 | 2.0 | 15.3 | 1.4 | 10.3 | 41.7 |
| Kopurererua at SH2 | 0.5 | 7.1 | 203.0 | 1.4 | 13.6 | 350.0 |
| Mount Maunganui | 0.4 | 2.0 | 16.0 | 2.0 | 10.8 | 63.5 |
| Bridge Marina | 0.6 | 2.0 | 11.5 | 2.6 | 10.3 | 48.0 |
| Maungatapu Bridge | 0.8 | 3.0 | 68.0 | 2.8 | 12.7 | 205.0 |
| Overall Te Awanui | 0.3 | 2.7 | 203.0 | 0.8 | 10.9 | 498.0 |

Table 4 summarises the median turbidity measured by the Port of Tauranga network of ANALITE sensors between January 2013 and October 2016. This includes two periods of maintenance dredging (M1 between 1 October 2014 and 1 November 2014; and M2 between 18 August 2015 and 9 September 2015), and a period of capital dredging from 1 October 2015 to 1 September 2016 (CP). The TSS corresponding to the measured NTU values was estimated with the equations for grey and white sediment given above, and the medians calculated for the estimated TSS values

*Table 4 – Median statistics of turbidity data recorded by Port of Tauranga ANALITE sensors from January 2013 until October 2016. Periods analysed are all dataset (ALL, n~106), excluding dredging periods M1, M2 and CP (NO, n~106), maintenance dredging period 1 (M1, n~104), maintenance dredging period 2 (M2, n~104) and capital dredging period (CP, n~104). TSS is estimated for gey and white sediment plumes used the ANALITE calibration equations given in the text. From Table A.2 in Coppede Cussioli (2018).*

| Site | Location | Period | Turbidity (NTU) | Grey sediment (mg/l) | White sediment (mg/l) |
|---|---|---|---|---|---|

[42] https://www.boprc.govt.nz/environment/maps-and-data/environmental-data/

| | | | | | |
|---|---|---|---|---|---|
| S1 | Harbour entrance | ALL | 3.1 | 6.6 | 8.1 |
| | | NO | 3.2 | 6.8 | 8.6 |
| | | M1 | 3.4 | 7.2 | 9.3 |
| | | M2 | 1.7 | 3.7 | 2.8 |
| | | CP | 2.9 | 6.3 | 7.7 |
| S2 | Lower Western Channel | ALL | 2.4 | 5.1 | 5.4 |
| | | NO | 2.3 | 4.9 | 5.1 |
| | | M1 | 2.3 | 4.9 | 5.1 |
| | | M2 | 1.5 | 3.3 | 2.1 |
| | | CP | 2.6 | 5.5 | 6.2 |
| S3 | Cutter Channel | ALL | 2.5 | 5.4 | 6.0 |
| | | NO | 2.6 | 5.5 | 6.1 |
| | | M1 | 1.7 | 3.6 | 2.7 |
| | | M2 | 2.1 | 4.5 | 4.4 |
| | | CP | 2.5 | 5.4 | 6.0 |
| S4 | Whareroa Point | ALL | 4.4 | 9.4 | 13.4 |
| | | NO | 4.3 | 9.2 | 13.0 |
| | | M1 | 3.8 | 8.1 | 11.0 |
| | | M2 | 3.8 | 8.1 | 10.9 |
| | | CP | 4.7 | 10.1 | 14.6 |
| S5 | Stella Passage near Bridge Marina entrance | ALL | 3.3 | 7.1 | 9.1 |
| | | NO | 3.0 | 6.4 | 7.8 |
| | | M1 | 3.2 | 6.9 | 8.8 |
| | | M2 | 1.8 | 3.9 | 3.3 |
| | | CP | 4.1 | 8.8 | 12.3 |
| S6 | Otumoetai Channel near marina entrance | ALL | 2.7 | 5.8 | 6.7 |
| | | NO | 2.7 | 5.8 | 6.8 |
| | | M1 | 2.3 | 5.0 | 5.3 |
| | | M2 | 2.0 | 4.4 | 4.2 |
| | | CP | 2.7 | 5.8 | 6.8 |

Sites S1 and S3 are located within the areas subjected to dredging and potentially affected by near field and far field dredge plumes. The remaining sites are outside the dredged area and potentially affected by far field dredge plumes. Site S2 is the furthest from the dredged area, and is likely to be the least affected by dredge plumes. The measured data do not show any detectable increase in NTU due to dredged (since TSS is estimated from NTU, it can only show the same pattern).

For the 2015/16 Capital Dredging Programme, improved dredging technology and methodology was employed to avoid a repeat of the turbid plume shown in Figure 14. This included a 3-dimensional model of the subsurface geology that allowed the dredge operators to adjust their dredging methodology for the predicted sediment characteristics before they excavated material, an array of turbidity sensors surrounding the area being dredged to detect any potentially adverse plume, observers on board the dredges to monitor the water appearance, and improved management of overflow from the hopper (including stopping overflow completely if necessary).

Environmental sensor data are often noisy and may drift over time. Bryan et al (2014) reported that this was true for the turbidity sensor array used in Te Awanui by the Port of Tauranga. The Port regularly cleans the sensors to minimize the drift due to overgrowth by biota, and Bryan et al (2014) used several

techniques to remove the noise, including manual removal of data gaps, automated removal of large spikes (attributed to drifting seaweed obscuring the sensors), and different data smoothing algorithms for providing information on real time trends. The main approaches to smoothing were a 6-hour and 2-week moving average, and an Exponentially Weighted Moving Average (EWMA). The EWMA was utilized by the Port of Melbourne for the purpose of real time tracking of turbidity (Port of Melbourne Corporation, 2008)[43].

The EWMA is a first order infinite impulse filter, and may be expressed as

$$\bar{x}_i = \lambda \bar{x}_{i-1} + (1 - \lambda) x_k$$

Essentially the weighted (1-λ) current value is added to the weighted (λ) previous average value to determine the current average. This means that it can be continuously updated as new observations become available. The Port of Tauranga applies it to the average turbidity in 6-hour long data windows, with λ=0.6, as illustrated in Figure 19.

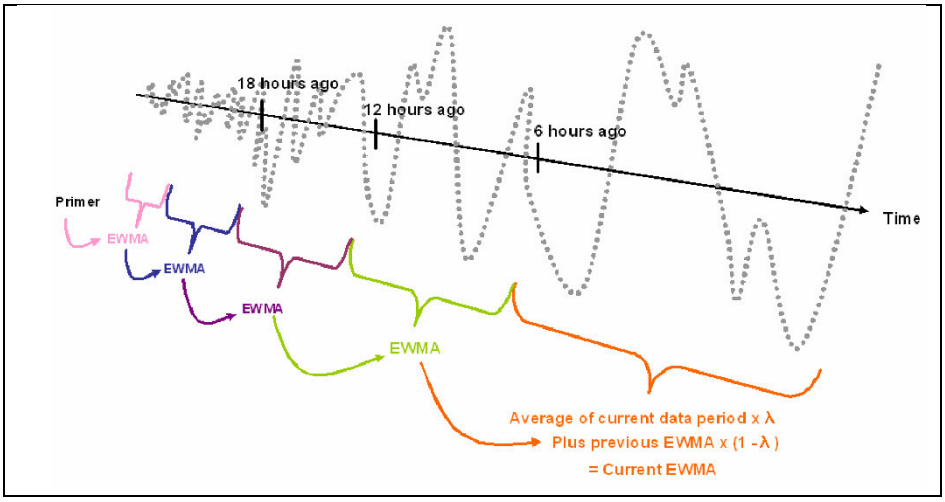



*Figure 19 – Conceptual summary of the EWMA approach applied to averages of 6-hour long data windows. (Figure 3, Port of Melbourne Corporation, 2008).*

Figure 20 summarises three approaches to dredging available and their effects on turbidity. The THSD used for the 1991/92 Capital Dredging Programme operated with a standard overflow. The THSDs used for the 2015/16 Capital Dredging Programme used a low turbidity valve, which can restrict the overflow to reduce air bubbles that keep sediment in suspension, limit the amount of fine sediment entering the overflow, and strengthen the dynamic plume to enhance redeposition on the seabed. The low turbidity valve significantly reduced the extent of the near-field plume in 2015/16, and a far-field plume was not observed. If necessary, overflow can cease completely so that only the near-bed draghead plume is generated.

[43] Port of Melbourne Corporation (2008) Turbidity - Detailed Design. CDP_ENV_MD_024 REV 2. Port of Melbourne Corporation, Melbourne, Victoria. 45 pp.

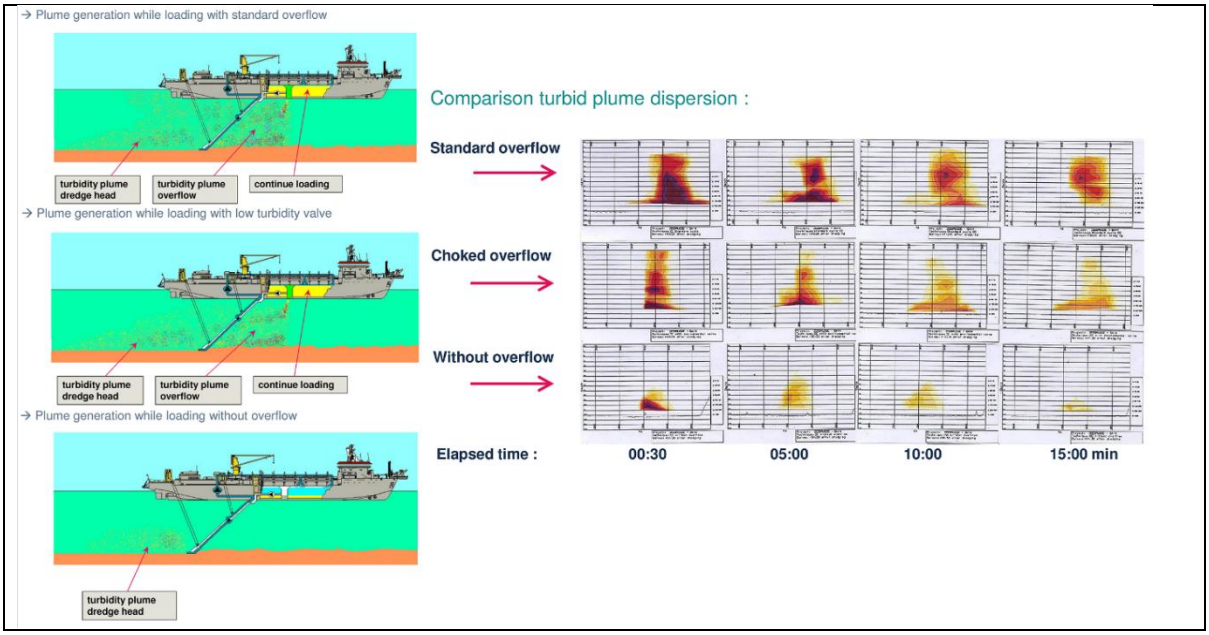



*Figure 20 – Schematic diagram of the sources of turbid plumes for a trailing suction dredge, where the overflow consists of two components: a concentrated discharge from a pipe at the stern of the dredge, and some discharge over the sides of the hopper. Propellor wash is not specifically shown. The zones A, B, and C correspond to the zones in Figure 11 that shows the plume behaviour with time/distance from source.*

Montaño (2024)[44] presents the results of numerical modelling of plumes generated by a large TSHD and a BHD for the shipping channels in Te Awanui. They simulated a TSHD with a 15,000 $m^3$ maximum hopper capacity, compared to the *Balder R* with a 6,000 $m^3$ hopper capacity used for the 2015/2016 capital dredging and the *Albatros* with an 1,800 $m^3$ hopper capacity used for maintenance dredging. The BHD was assumed to excavate a maximum of 5,000 $m^3d^{-1}$. The TSHD most likely to be used for the proposed capital and maintenance dredging will similar in size similar to the *Albatros* and hence the modelled plumes for the large TSHD are much larger than actually would be produced.

Dredging was simulated for 7 locations along the shipping channels (Figure 21): 6 locations for the TSHD, and 1 for the BHD. Different scenarios were used for the 7 locations as summarised in Table 5.

For the dredging scenarios, coarse sands and gravels were assumed to be retained within the hopper, or settle immediately for the drag head plume, any silt present was assumed to be discharged, and clays were ignored due to the very low proportions of clay (~0.3%) present in the sediment being excavated. Sampling of dredge hopper sediments after excavation shows that a proportion of silt (and clay) is retained within the hopper, so the actual silt contents of the discharge would be lower than assumed for the modelling. Two TSHD scenarios were modelled for Stella Passage, which corresponded to the state of the tide. During flood tide, no overflow was simulated, and during ebb tide, overflow was simulated.

*Table 5 – THSD dredging scenarios simulated. The sites correspond to Figure 17. From Table 2.2, Montaño (2024).*

| | Stella Passage No overflow | Stella Passage Overflow | Maunganui Roads | Cutter Channel | Entrance Channel |
|---|---|---|---|---|---|
| Sites | L1 | L1 | L2 | L3, L4 | L5, L6 |
| Hopper volume ($m^3$) | 13,000 | 13,400 | 13,400 | 13,400 | 13,400 |
| Overflow duration (min) | 0 | 15 | 15 | 15 | 15 |
| Hopper fill time (min) | 30 | 45 | 45 | 50 | 50 |
| Full dredging cycle (min) | 125 | 140 | 120 | 115 | 110 |

[44] Montaño, M., 2024. *Dredge plume modelling: Dredging plume dispersion over existing and proposed port configurations*. Report prepared for the Port of Tauranga. MetOcean Solutions, December 2024.

| | | | | | |
|---|---|---|---|---|---|
| Disposal duration (min) | 10 | 10 | 10 | 10 | 10 |
| Production rate ($m^3s^{-1}$) | 7.22 | 4.96 | 4.96 | 4.47 | 4.47 |
| Medium sand (%) | 53 | 53 | 51 | 79 | 84 |
| Fine sand (%) | 5 | 5 | 8 | 2 | 2 |
| Silt (%) | 42 | 42 | 41 | 19 | 14 |

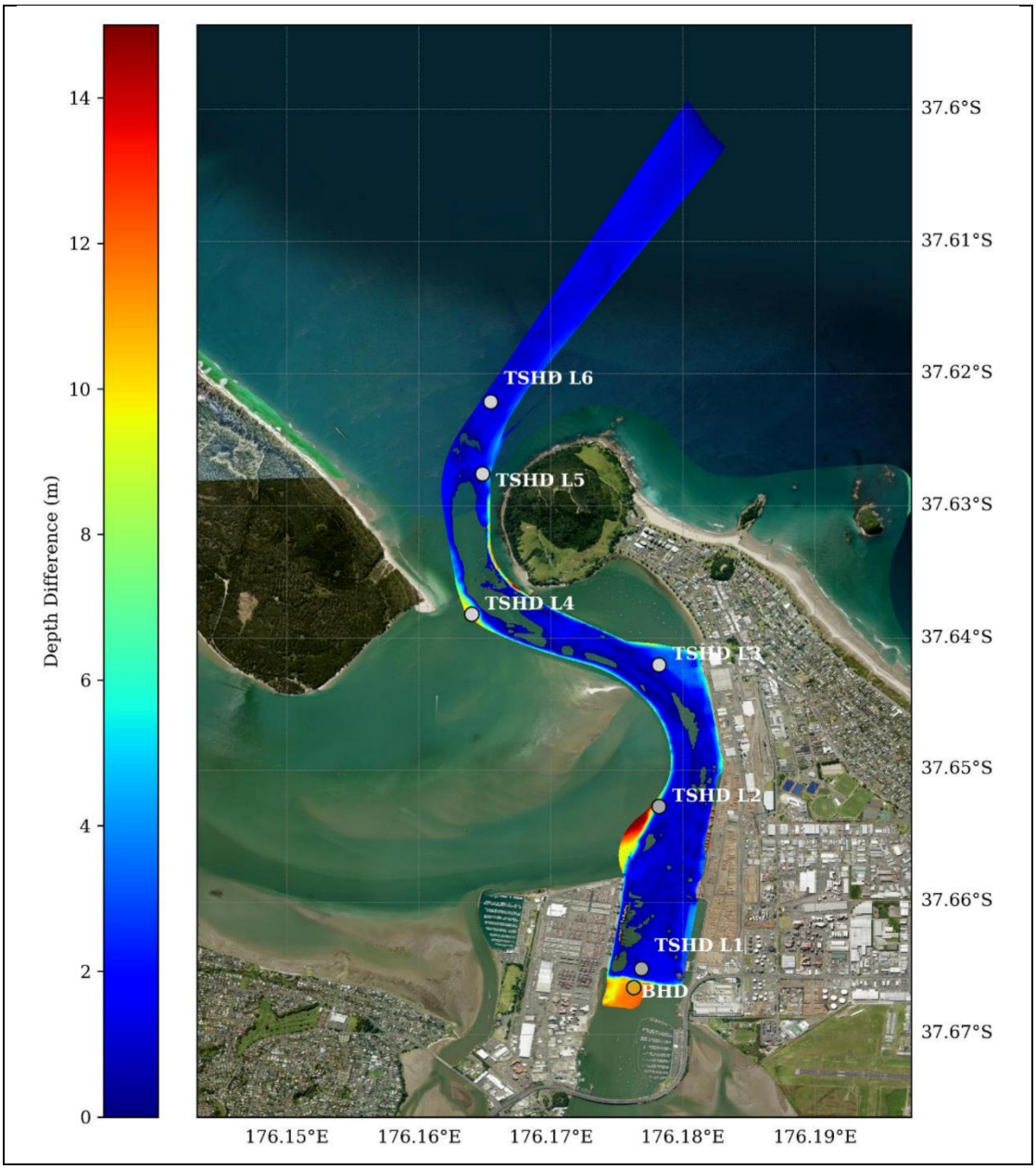



*Figure 21 – Locations for dredging simulations for the large TSHD (L1-L6) and the BHD. Figure 2-1, Montaño (2024). The colours indicate the thickness of sediment proposed to be removed by capital dredging (expressed as a depth difference after dredging).*

Modelling involved estimating the initial dredge plume contributions from different sources (Figure 14) as a proportion of the production rate (Table 6). The production rate is based on the 15,000$m^3$ TSHD, which is an order of magnitude larger than the TSHD expected to be used. Hence, the modelling exaggerates the plumes the dredge could produce.

*Table 6 – Summary of plume source contributions as a proportion of the production rate (Montaño, 2024).*

| Plume source | Release depth | Source radius (m) | Proportion (%) |
|---|---|---|---|
| TSHD | | | |
| - Draghead | Near bed 2 m | 10 | 3 |
| - Propellor wash | Near bed 2 m | 10 | 3 |
| - Overflow surface plume | Near surface | Point source | 4.75 |
| - Overflow dynamic plume | Near bed 2 m | 60 | 19 |
| BHD | | | |
| - Bucket losses | Entire water column | 32 | 4 |
| - Surface losses | Near surface 3 m | 10 | 1 |

The modelling assumes that the largest contribution to the dredge plume is the impact of the dynamic plume with the seabed forming a density current (Figure 14), which is consistent with the observations presented in Figure 20. The modelling also assumes that all of the dredging occurs at the modelled locations during an excavation pass. This is true for a BHD, whereas a TSHD continually moves along the channel. This means that the mixing zone for a TSHD is not static, but moves with the dredge.

Since most of the sediment entering the water column is located within a near-bed density current, it tends to be trapped within the channels being dredged as illustrated by Figure 17, whereas suspended sediment discharged into the harbour from the surrounding catchments tends to be associated with a low density (fresher water) surface layer (Figure 18). Suspended sediment within the near-bed density current can be transferred to the surface by turbulence if the vertical velocity exceeds the sediment settling velocity. The main sources of turbulence are propellor wash from vessels crossing the plume, and strong tidal currents.

This means that the surface suspended sediment concentrations may be higher for spring tides than neap tides, and in areas of strong turbulence such as the tidal inlet and associated flood and ebb tidal jets. Due to the interactions between the main lunar and solar tidal constituents, Te Awanui experiences different consecutive spring and neap tidal ranges (Figure 22). Typically, there is one large spring tide and one small neap tide per lunar month, with the remaining spring and neap tide having similar tidal ranges. This pattern of tidal behaviour limits the periods of maximum turbulence per lunar month.

Montaño (2024) used the OpenDrift framework for Lagrangian particle tracking and the SCHISM hydrodynamic model predictions to simulate the dispersal of the suspended sediment from the TSHD and BHD sites. The modelling did not include the influence of waves, but due to the small amplitude of waves within the harbour and the depth of the density current, wave turbulence is negligible. Modelling was undertaken for the summer/winter El Niño/La Niña combinations modelled by Watson and Berthold (2024a) to assess if there are differences due to seasonality and climate variability

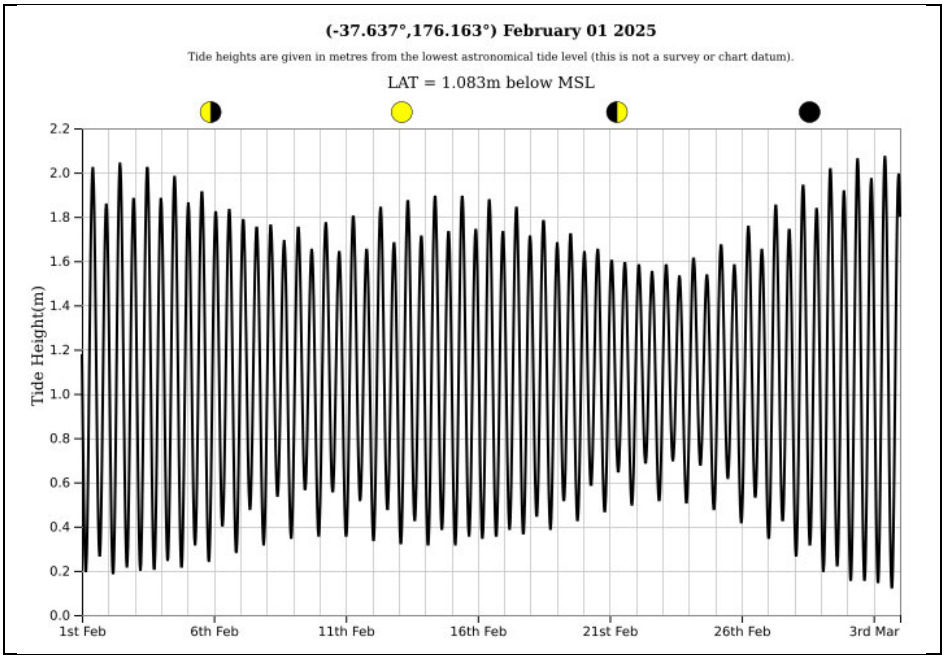



*Figure 22 – Predicted tides for the Tauranga Harbour Entrance for February 2025 from the NIWA tide forecaster[45].*

As an example, Figure 23 shows the TSHD overflow (ebb) and no overflow (flood), and BHD, surface and near bed (seafloor) plumes for La Niña summer conditions. Montaño (2024) also presents results for the other combinations of conditions, but no seasonal or climate variation effects were evident. The plumes are confined to the channels, and do not extend over Te Paritaha or into Waipu Bay through any of the channels draining the Bay. This is consistent with observations during the 2015/16 Capital Dredging Campaign.

Figure 23 also shows that the highest suspended sediment concentrations occur close to the dredge, with higher concentrations associated with the TSHD that is shifting larger volumes of sediment per unit time than the BHD. The TSHD colour scale extends up to 75 $mgl^{-1}$, which is the threshold for impacts on pipi (*Paphies australis*) as determined by Coppede Cussioli (2018). In this example, the threshold is reached at the seafloor where the dynamic plume impacts, which is almost underneath the dredge (Figure 14). In practice, due to a smaller TSHD capacity and the movement of the dredge, the concentrations in the dynamic plume will be lower than modelled. Strictly, the ecological impact of the dredge plume is dependent on the duration of the exceedance, which will be considered further below.

Modelling shows that the potential for adverse impacts from the dredge plume is dependent on the distance between the dredge and the areas of concern. Figure 23 shows that for a BHD the 200 m mixing zone is sufficient to avoid adverse impacts (strictly the suspended sediment concentrations are always well below 75 $mgl^{-1}$). For a large TSHD with no overflow, the 200 m mixing zone distance is also sufficient, while with overflow the 600 m mixing zone is sufficient. Due to the lower production rates, a small TSHD similar to the *Albatros* would require a smaller mixing zone.

For ecological impacts it is necessary to consider the duration of threshold exceedance, and also the ambient levels of suspended sediment, as the dredge plumes are additional. Considering the duration of exceedance, Montaño (2024) assessed the hourly suspended sediment concentrations from each of the dredging sites at 3 locations (Figure 24): Te Paritaha; the northern side of the Bridge Marina; and the channel by Whareroa Marae. This was done for La Niña summer (2012) and winter (2011)

[45] https://tides.niwa.co.nz/

conditions. However, since these corresponded to different time periods, the sequence of tidal elevations differed. Hence, there are differences between the summer and winter combinations that are a consequence of the different tidal ranges (different turbulence) and their timing.

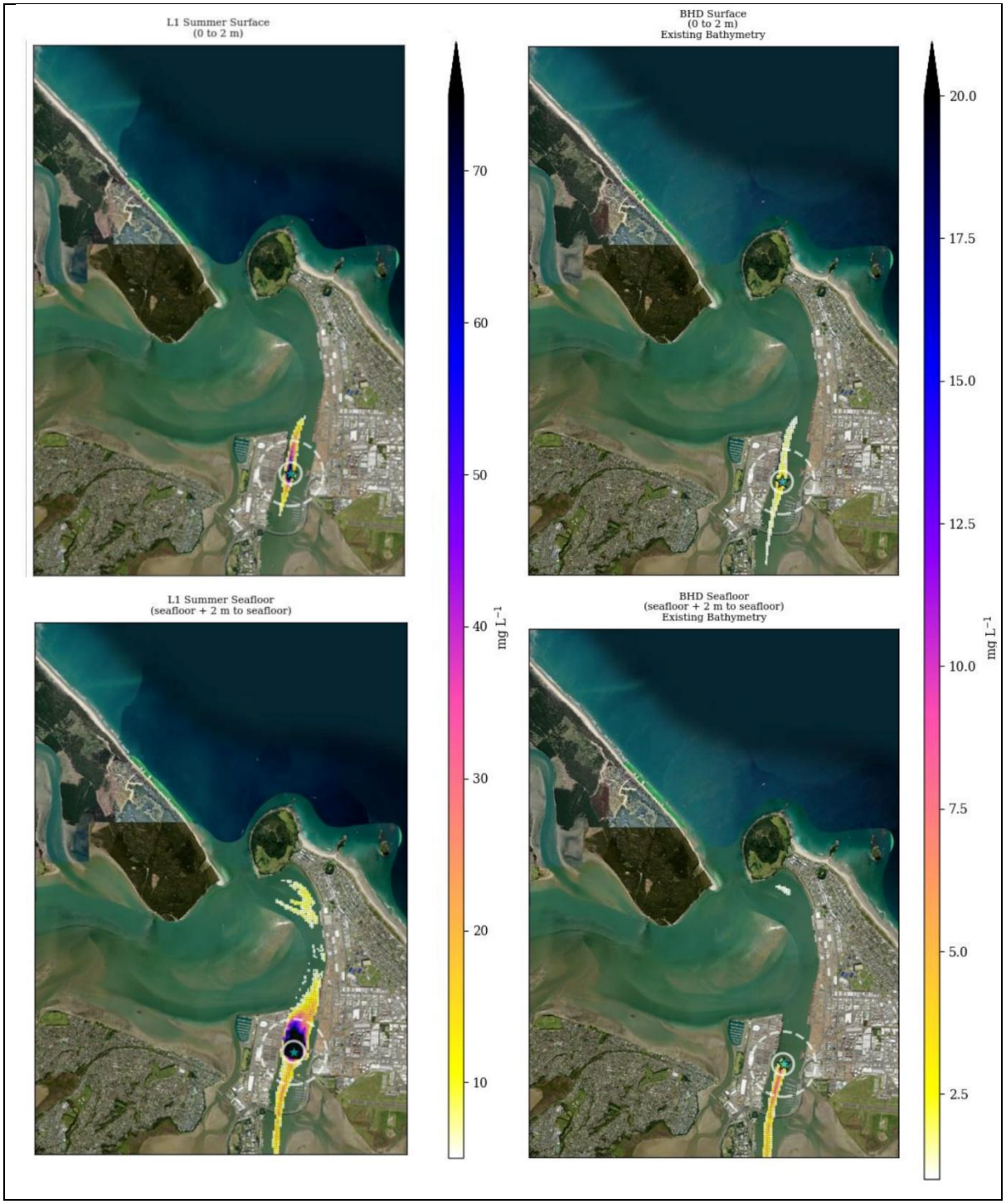



*Figure 23 – Modelled sediment plumes (mean TSS in mgl$^{-1}$) for a large TSHD (left column) operating with no overflow during flood tide and overflow during ebb tide, and a BHD (right column), excavating sediment from the southern Stella Passage. The surface plume represents the surface 2 m of the flow, and the seafloor plume represents the deepest 2 m. The point of release is marked by a star, and surrounding circles represent a 200 m (solid line) and a 600 m (dashed line) circumference to identify the mixing zone. Concentrations <5 mgl$^{-1}$ are masked. (Figures 3.11 and 3.16 from Montaño, 2024).*

Modelling of the large TSHD and BHD only recorded one instance of suspended sediment concentrations exceeding 75 mgl$^{-1}$ at the Te Paritaha site, as shown in Figure 25, for La Niña summer

conditions (from site L5). The threshold was also exceeded twice for La Niña winter conditions: 1 exceedance from site L5 and 1 exceedance from site L6, but at different times. The time series cover 62 days, or 1488 hours of dredging.

Interestingly, the exceedances for Te Paritaha only involved dredging in the Entrance Channel (L5 and L6) during flood tide with overflow, and didn't involve dredging at L2, L3 and L4 closer to the margins of the flood delta. Montaño (2024) includes plots of the mean and 90$^{th}$ percentile plots of the near-bed and surface plumes for all sites. All plots show the plumes following the channels (Western Channel, Cutter Channel, and Maunganui Roads), so the suspended sediment is transported away from Te Paritaha.




*Figure 24 – Sites used to assess the hourly total suspended sediment concentrations due to dredging at the BHD and TSHD sites in Figure 17 (Figure 2-5, Montaño, 2024).*

Considering the timing of the modelled exceedances reported, they appear to occur when dredging at L5 and L6 coincided with maximum spring tide flood flows into Te Awanui. It is most likely that the modelled turbulence at those times was sufficient to entrain some of the near-bed density flow into the flood tidal jet over Te Paritaha. This is not likely to occur with a smaller capacity TSHD, and has not been observed with previous dredging campaigns.

It should also be noted that the plume modelling is conservatively based on a much larger TSHD and even then, there were no periods of consecutive exceedances, and it is extremely likely that any remaining flood tide surface plume extending onto Te Paritaha will be swept away during the following ebb tide.

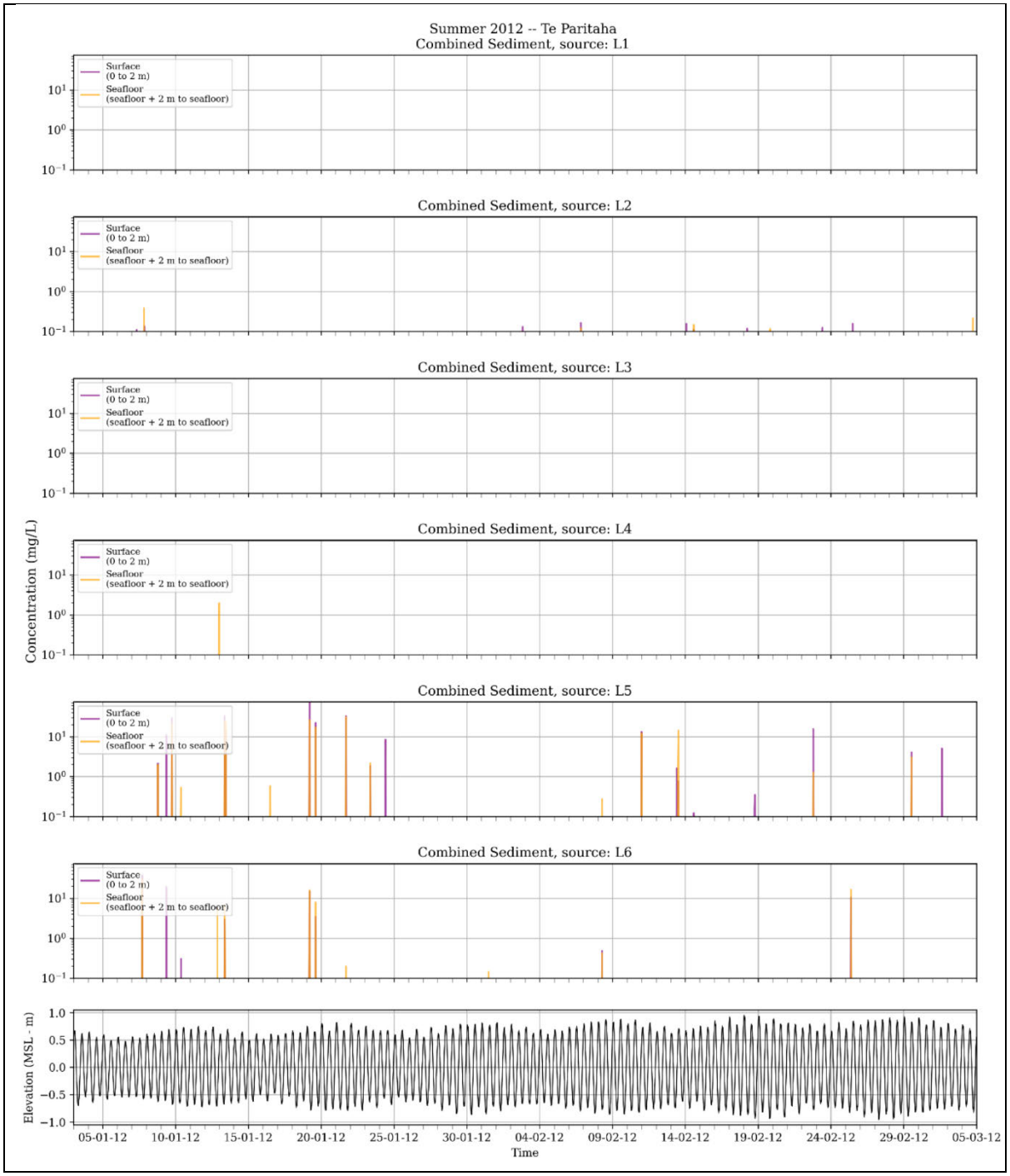



*Figure 25 – Time series of hourly total suspended sediment concentrations on Te Paritaha (Figure 20) due to a large TSHD operating at the locations in Figure 17 during La Niña summer conditions. The vertical scale is logarithmic from 0.1 to 75 mgl$^{-1}$, so bars reaching the top of the graph represents an exceedance. The bottom panel is the tidal elevation in Stella Passage. (Figure 3-6 from Montaño, 2024)*

The additional impact of the dredge plumes has previously been managed by the use of real time monitoring of turbidity. The results of Montaño indicate that the additional suspended sediment due to dredging using a Large TSHD and BHD is unlikely to boost ambient levels above the threshold level under normal weather conditions. Previous capital dredging campaigns have indicated that it may be possible under stormy weather conditions that high sediment discharge from catchments into the harbour could produce sufficiently high background suspended sediment levels within Stella Passage that may combine with dredge plumes to exceed threshold levels. The use of real time monitoring and appropriate consent conditions can be applied to prevent this from occurring in Stella Passage, such

as restricting dredging with no overflow during peak flood tidal flows, or only dredging on an ebb tide, or ceasing dredging while background levels are above threshold.

It should also be noted that the plume modelling is conservatively based on a much larger TSHD and even then, there were no periods of consecutive exceedances, and it is extremely likely that any remaining flood tide surface plume extending onto Te Paritaha will be swept away during the following ebb tide.

The additional impact of the dredge plumes has previously been managed by the use of real time monitoring of turbidity. The results of Montaño indicate that the additional suspended sediment due to dredging using a Large TSHD and BHD is unlikely to boost ambient levels above the threshold level under normal weather conditions. Previous capital dredging campaigns have indicated that it may be possible under stormy weather conditions that high sediment discharge from catchments into the harbour could produce sufficiently high background suspended sediment levels within Stella Passage that may combine with dredge plumes to exceed threshold levels. The use of real time monitoring and appropriate consent conditions can be applied to prevent this from occurring in Stella Passage, such as restricting dredging with no overflow during peak flood tidal flows, or only dredging on an ebb tide, or ceasing dredging while background levels are above threshold.

As noted above, sediment entrained into the water column during excavation is predominantly deposited within the mixing zone within the channels being dredged. However, the very fine sediment within the far field plume may be transported some distance before being deposited, particularly if there is sufficient turbulence to prevent deposition. This suggests that there is a potential cumulative impact due to the deposition of the fine sediment in the upper reaches of the harbour.

Figure 26 shows the mean surface and near-bed sediment dispersal patterns for a large TSHD operating at locations L4, L5 and L2 over a 2-month long period in a La Niña Summer. The modelling includes changing tidal and weather conditions, and hence the mean shows the potential range of dispersal paths. Dredging involved overflow, and was not restricted to either ebb or flood flow. TSS values <5 $mg.l^{-1}$ have been masked as there are too few particles per grid cell to simulate reliably. This value is also about 50% of median TSS values recorded in Te Awanui (Table 3). As noted by Montaño (2024), the results shown represent a worst-case scenario.

The highest TSS values occur within the near-bed plume and predominantly within the mixing zone indicated by the dashed circle. However, all 3 locations are subjected to strong tidal currents, which increases the length of the dispersal plumes. As discussed above, the near-bed plume is constrained to the dredged channels, except that there are two areas (Pilot Bay and the Entrance Channel) where the model predicted near-bed plume that are not connected directly to the dredge discharge plumes. The TSS for these two areas is <10 $mg.l^{-1}$. The most likely mechanism for their occurrence is that flow convergence causes the model to combine the suspended sediment in the distal plume (TSS <5 $mg.l^{-1}$) into a smaller volume and increasing the TSS above the masking threshold. This has not been observed during previous maintenance or capital dredging.

Considering the surface plume, the dispersal is also largely constrained to the main tidal channels (dredged channels, Lower Western Channel, and Otumoetai Channel). This is due to the strength of the tidal flows relative to wind-induced currents. This means that on a flood tide surface plume dispersal from most dredged areas is confined to the upper harbour to the east of the Tauranga tidal inlet (e.g. locations L5 and L2 in Figure 26). Dredging close to the entrance to the Lower Western Channel (L4) results in plumes that are transported towards the upper harbour west of the Tauranga tidal inlet.

The final destination of the fine sediment in surface plumes that initially travel towards the upper harbour areas of the Tauranga Basin depends on the flushing time, which is the time required to replace the existing water in an estuary or embayment with new, oceanic water. Fast flushing times mean suspended sediments are removed quickly, while slow flushing times allow time for suspended sediment to be deposited.

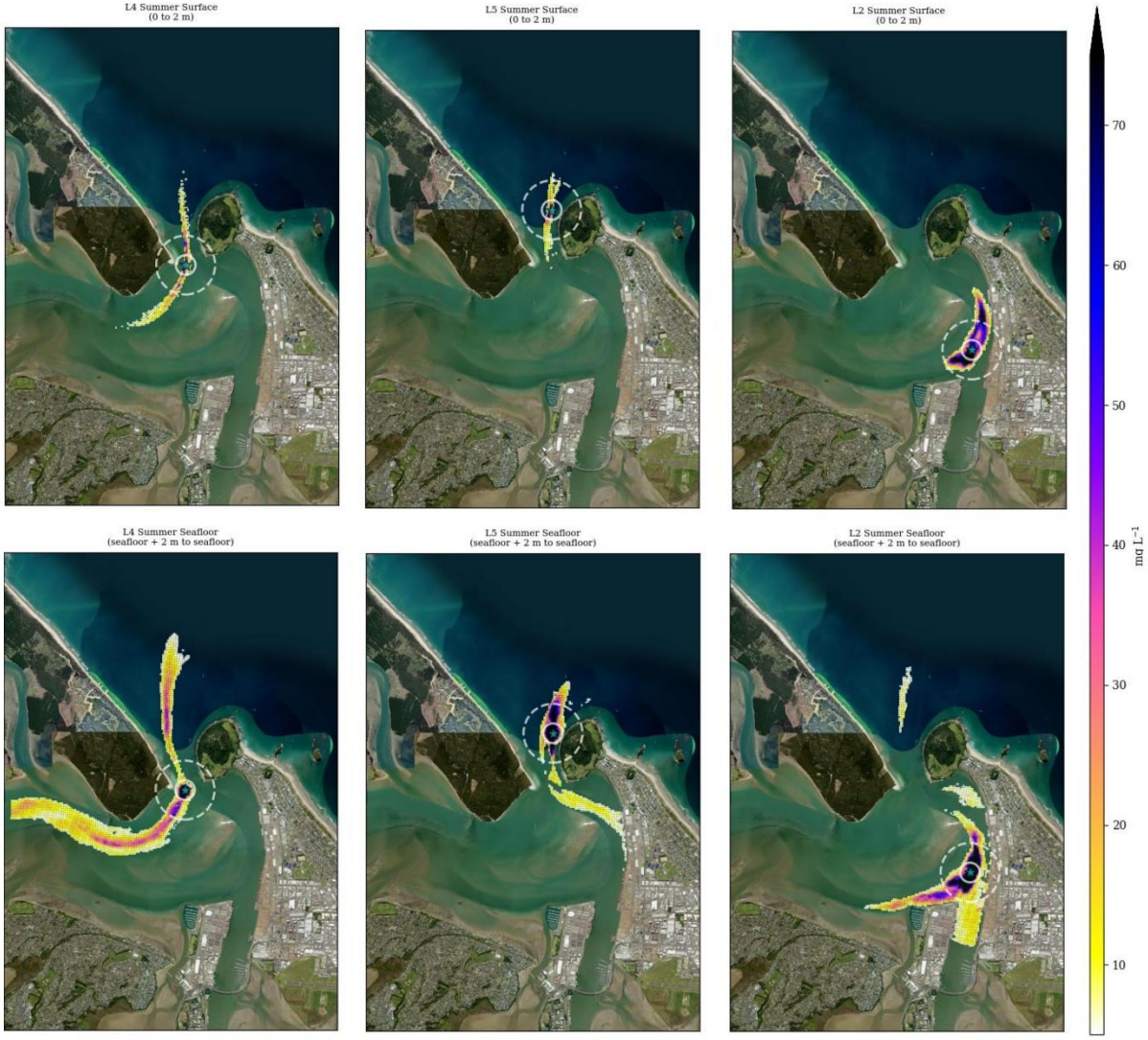



*Figure 26 – Dispersion of sediment discharged by a large TSHD (Mean TSS over 2 months) for locations L4, L5 and L2). TSS values < 5 mg.l$^{-1}$ are masked so do not appear. From Figures 5.4, 5.5 and 5.2 of Montaño (2024).*

Tidal flushing within estuaries, such as Te Awanui, depends on the tidal range, freshwater discharge, wind stress on the water surface, and rainfall on the estuary. Stewart (2021)[46] is the most recent study investigating tidal flushing within Te Awanui using a combination of isotopic tracers and numerical modelling. His study considered a range of scenarios to investigate the influences of these factors in response to climate change. 24. Stewart (2021) found that tidal flushing within Te Awanui is correlated with the Southern Oscillation Index (SOI) with statistical significance of r2=0.43 with p≤0.001. This indicates that in the long term, changes in tidal flushing are predominantly a function of weather patterns.

[46] Stewart, BT, 2021. *Investigating groundwater derived nutrient fluxes within Tauranga harbour, New Zealand*. PhD Thesis, University of Waikato, Hamilton, New Zealand. 166 pp.

Figure 27 shows the annual average flushing times for the Tauranga Basin of Te Awanui, and it highlights that flushing time is a function of the distance from the harbour entrance and proximity to freshwater discharges into the harbour. With respect to the surface plumes produced by dredging, the flushing times are of the order of 1 day at the temporal resolution of the Figure 27. This means that any residual suspended sediment is flushed from the harbour by ebb tides.

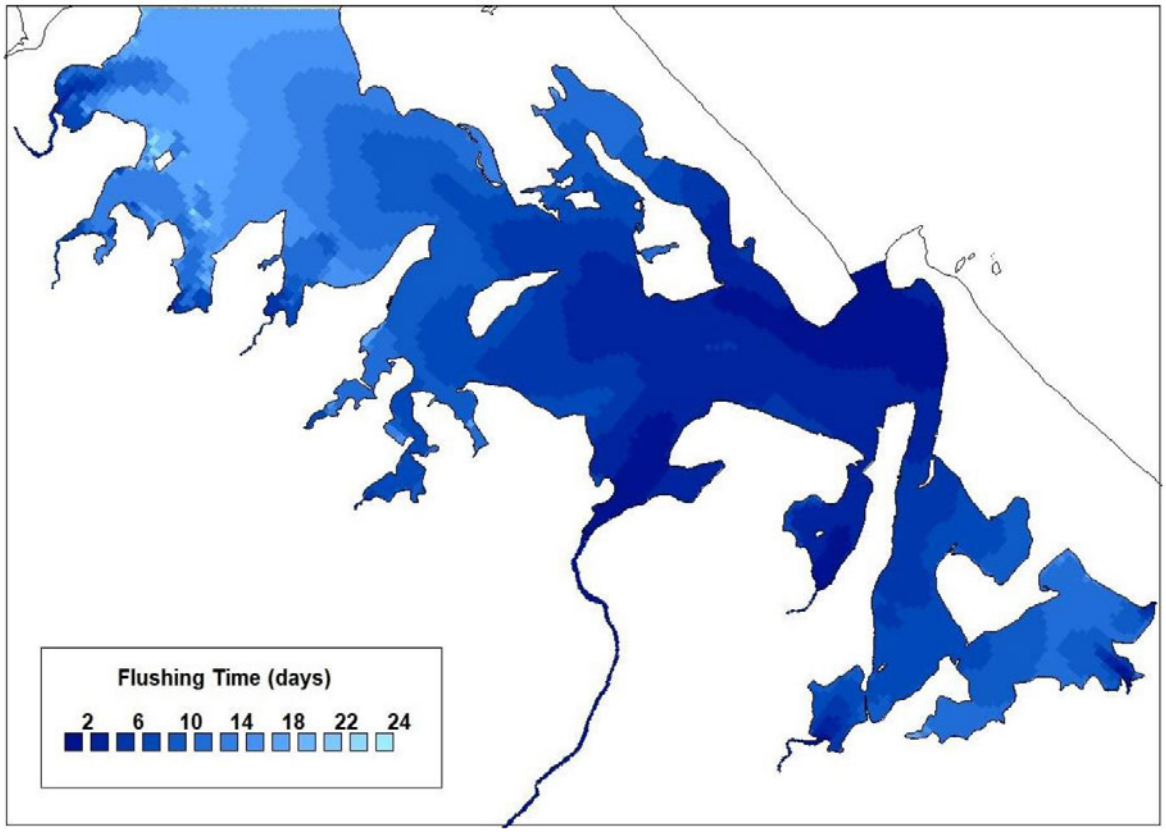



*Figure 27 - Annual average flushing time for the Tauranga Basin of Te Awanui. Figure 3.7 from Stewart (2019).*

Figure 27 also highlights areas where fine sediment derived from catchments around Te Awanui is likely to accumulate. The results of Stewart (2019) are consistent with those of the NIWA sediment study (Pritchard et al, 2009) and de Ruiter (2022).

Overall, the available evidence and modelling indicates that dredge plumes do not contribute to fine sediment accumulation within the upper harbour areas of Te Awanui because:

- Sediment from the plumes is predominantly deposited within the dredged area (gravel, sand, and silt); and
- Very fine sediment in suspension (fine silt and clay) is transported out of the harbour by ebb tidal currents.

It should also be noted that the dredge plumes are a short duration source, with low volumes of suspended sediment., compared to freshwater discharges that are long duration and may deliver very large volumes of suspended sediment.

# 4.0 Sediment disposal impacts

The generation of turbid plumes during disposal is a little simpler to analyse than the extraction phase, as there is only one source of sediment (Figure 28). A split hopper TSHD releases the bulk of the sediment at once, while other hopper designs take a little longer to release the sediment. The release of hopper contents results in a high-density pulse of sediment and water descending into the water column.

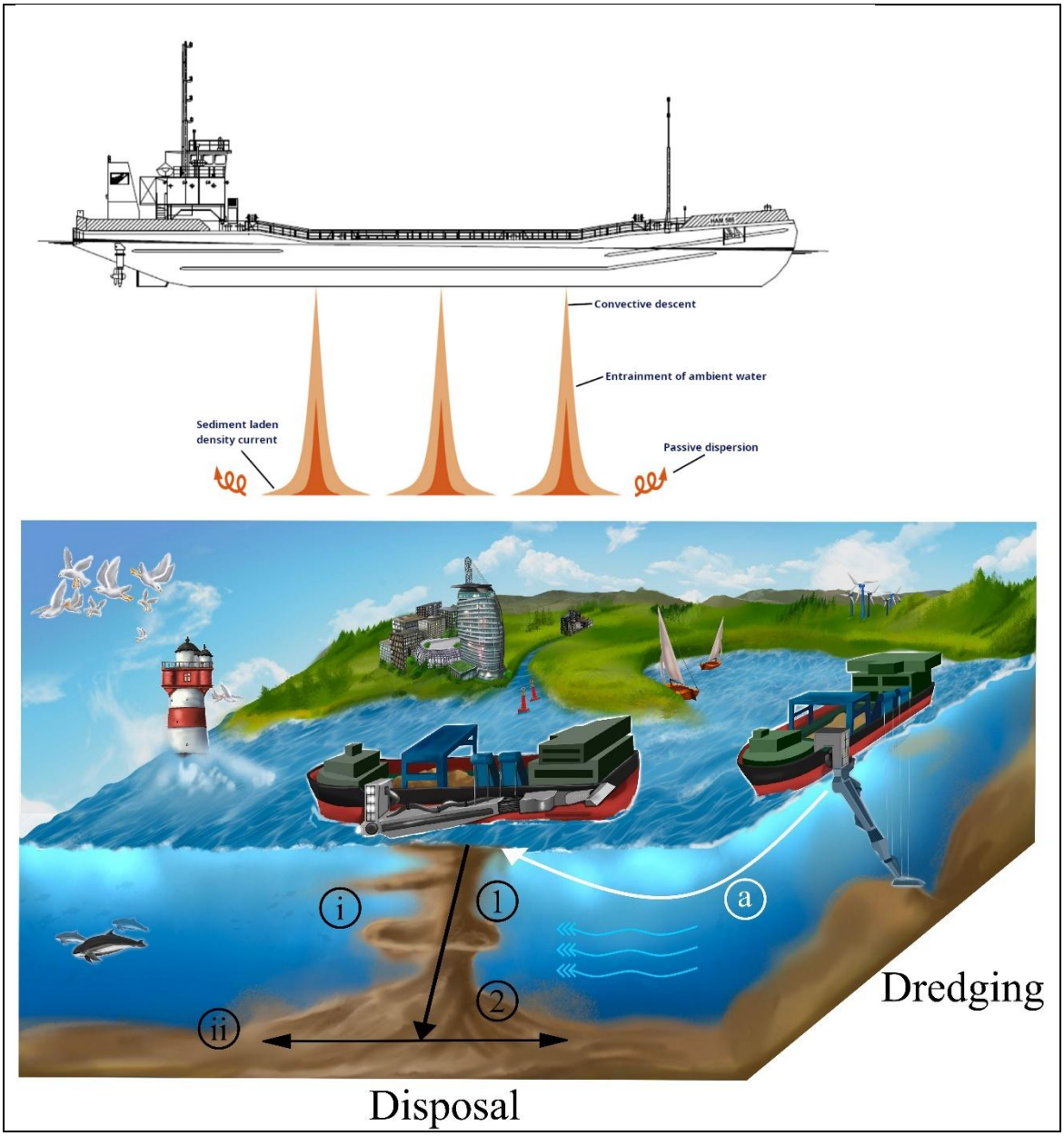



*Figure 28 – Schematic diagrams of the behaviour of turbid plumes after disposal from a hopper. The labels 1 & 2 in the bottom figure correspond to convective descent and dynamic collapse; i refers to stripping at a pycnocline; and ii refers to the near-bed radial density current formed by dynamic collapse.*

There are 3 distinct phases of behaviour:

- Convective descent - initially convective circulation draws surrounding water into the descending plume producing a density current that spreads laterally with increasing depth.
- Dynamic collapse - in relatively shallow water, the sediment plume impacts the sea floor creating a radial density current that spreads outwards along the sea floor. This is analogous

to the seabed impact of the dynamic plume in Figure 14 for the extraction process by a TSHD. In deep-water disposal sites, some finer sediment is removed from the descending plume when it reaches a zone of rapidly increasing fluid density (a pycnocline), a process known as stripping. This means that there may be multiple horizontal spreading layers of fine sediment. For a continental shelf disposal site, this situation normally is associated with the formation of a seasonal pycnocline due to heating of surface water during summer months. For the Bay of Plenty, the summer seasonal pycnocline develops at ~30 m depth in December, progressively moving down to ~100 m depth by late March (Longdill, 2008)[47].

- Passive dispersion - while most sediment is rapidly deposited on the seafloor during dynamic collapse, the finest sediments mixed into the surrounding water during convective descent and dynamic collapse is dispersed by diffusion and advection by any currents present.

The behaviour with time/distance illustrated by Figure 16 also applies for disposal, with the main differences being that the ambient currents are generally weaker, and the abiotic processes that produce marine snow are more effective. Hence, in general the far-field extent is more restricted (of order twice the near-field extent at the seabed). For the Port of Tauranga, the original disposal sites D and G were designed so that disposal of muddy sediment near the center of the sites would result in a far-field plume that remained well within the boundaries of the site.

The Port of Tauranga currently has 5 consented sites for disposal of dredged sediment consisting of sites A, B C, H1 & H2 (Figure 29). Site H1 and H2 overlay previous sites D and G. These sites are utilized for different types of sediment textures:

- Sites A, B, C are intended to supply sediment to replenish any losses from Mount and Ocean Beaches due to natural coastal processes (Foster et al, 1996[48]). The sediment deposited in these sites is required to have a very similar texture to the natural beach sediments, with <5% fines. The only difference between the dredged and natural sediment is in the presence of estuarine fauna, mostly shellfish (eg. tuangi, pipi, papatai). Monitoring of older sites and during the trials with Site A showed that adult estuarine shellfish did become established within the disposal sites, but no juveniles were found to appear over time (Foster et al, 1991[49]).
- Sites D and H1 are consented for the disposal of sandy sediment with <5% fine (silt and clay; also referred to as mud) content; and
- Sites G and H2 are consented for the disposal of sediment with >25% fine content, and also sand material with <5% fine content suitable for sites D and H2 to ensure an even distribution of dredged sediment over H1 & H2 is achieved.
- Clean sand (<25% fines) may also be used for beach renourishment (e.g. Pilot Bay beach and in front of Whareroa Marae)

All the disposal sites were chosen using two main criteria:

- The sediment texture of the seabed - the philosophy was to have natural characteristics as similar as possible to the deposited dredged sediment, so that the disposed sediment would behave the same way in response to natural processes and preserve the natural habitat for any biota present; and

[47] Longdill PC, 2008. Environmentally Sustainable Aquaculture: An Eco-Physical Perspective. PhD Thesis, The University of Waikato, Hamilton, New Zealand. 280 pp.

[48] Foster GA, Healy TR, & de Lange WP, 1996. Presaging beach renourishment from a nearshore dredge dump mound, Mt. Maunganui Beach, New Zealand. Journal of Coastal Research, 12(2), 395-405.

[49] Foster DM, Healy, TR, & Warren SK, 1991. Environmental impacts of a recent dredge spoil dumping operation off Tauranga, New Zealand. Coastal Engineering - Climate for Change: 10th Australasian Conference on Coastal and Ocean Engineering, Auckland, New Zealand. 141-145.

- Whether the sites would be non-dispersive or dispersive – which characterizes the mobility of the dredged sediment and determines whether sediment would stay where it was put, or would spread outside the disposal site.

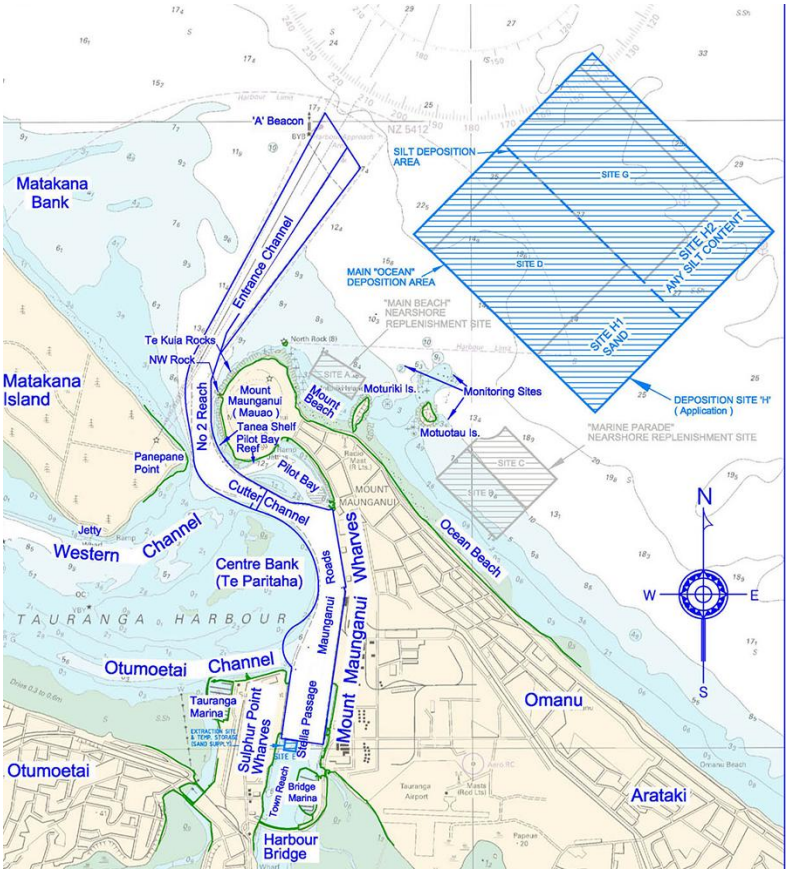



*Figure 29 – Section of Figure 1 showing the main areas involving dredging extraction and disposal for the Port of Tauranga.*

The proportion of fines present affects the geotechnical characteristics of sediment, primarily to changes to infilling of pore spaces between sand grains by finer sediments. This typically results in an abrupt change in behaviour when a critical proportion of fines is exceeded. The critical proportion is known as the threshold, limiting or critical fines content in different studies (Polito & Sibley)[50]. Below this critical value, the sediment behaves like sand; while above this value, the sediment behaves like cohesive silt. The critical value is not constant, but varies depending on the shape and size of the sand and fines fractions of the sediment, which affects the pore shape and size, and amount of fine infilling. However, for most sand-fine mixtures the critical proportion of fines varies between 20-28%. Hence, the dredged sediment from Te Awanui with fines contents >25% are likely to behave like cohesive silts and form non-dispersive spoil mounds. Similarly, sediment with <5% fines will be non-cohesive and form dispersive spoil mounds.

The critical proportion of fines raises an issue with the definition of clean sand for the purposes of beach renourishment, in addition to the conflict where shallow water deposition involves a threshold of <5%, while subaerial deposition on an adjacent beach involves a threshold of <25%. Sediment with a fines content approaching 25% behaves like a silt, so the sediment will be cohesive and is likely to change the characteristics of the beaches renourished as they typically are non-cohesive. Further,

[50] Polito, CP, & Sibley, ELD, 2019. Threshold fines content and behavior of sands with nonplastic silts. Canadian Geotechnical Journal, 57(3), 462-465.

under sufficiently strong wave swash action, the fines can be removed from the sediment forming a turbid fringe along the surf zone and contributing the rate of volume loss from the renourishment area. A sediment fines threshold of <5% consistent with shallow water dispersive dredge disposal sites would be more appropriate.

Sites A, B and C were intended to be dispersive sites, which would allow the sediment to move onshore and renourish the beach. A methodology was developed for Tauranga based on the thresholds of sediment motion due to wave-induced currents, the annual distribution of wave heights, and the depth of the spoil mound within the disposal site (de Lange and Healy (1994[51]). This was used to identify zones where sediment: would be exchanged with the beach (sites A and B); could slowly exchange with the beach (site C, D, H1); and would not disperse (sites G and H2).

Monitoring indicates these sites are behaving as intended. For dispersive sites, the sediment deposited is entirely/predominantly marine sand (mostly beach sands) transported into and out of the harbour by tidal currents, the volumes are small, and the overall rate of sediment dispersal is low. Apart from the differences in shellfish present and a higher pumice, there is no obvious way to tell the dredged sediment from the natural sediment. These differences diminish over time as the shellfish die and pumice is destroyed and removed by wave action.

Non-dispersive sites are used to contain sediment that may have adverse effects if it moves beyond the boundaries of the disposal sites. If sediment is considered particularly hazardous, the deposited sediment can be capped by a layer of benign sediment.

To date, all analyses of sediment dredged from the port area indicate that potential contamination is associated with fines (clay mostly) that can absorb pollutants. The guidelines used to assess some contaminants, particularly heavy metals, do not account for sediments that naturally have elevated levels (mostly because they are based on international guidelines from countries with different underlying geology). This is an issue for the volcanic sediments that are predominant in the Bay of Plenty, and it mostly affects sand-sized sediment.

Sites G and H2 were selected for disposal of sediment with >25% fines as they correspond to the depth where fines content naturally exceeds 25%. Potentially contaminated sediment disposed at sites G and H2 is associated with maintenance dredging, so involves small volumes deposited at a low rate over time. Capital dredging involves older sediments that are not contaminated unless previously disturbed and contaminants introduced. For the development of the non-dispersive sites, it was assumed that: any contaminant present would be diluted; and any contaminants that were present would be retained and buried within the sites. This also justifies a higher proportion of fines than the 5% threshold allowed for shallower dispersive sites (A, B, C, D & H1).

Due to the issues with position fixing when they were established (before radio-based and GPS navigation) the disposal sites were larger than required for the volumes deposited to allow for incorrect placement of the sediment. This is not really necessary now, but it means that the boundaries of the sites are effectively the boundaries of the sediment mixing zone for all sites.

The sediment thresholds used to determine the minimum depth for a non-dispersive disposal site were those defined by Hallermeier (1981[52]), which allowed for movement at greater depths for up to 12 hours per year. The thresholds are also a function of the sediment density, such that denser sediment grains such as titanomagnetite are immobile at shallower depths while lower density sediments such

[51] de Lange WP, & Healy TR, 1994. Assessing the stability of inner shelf dredge spoil mounds using spreadsheet applications on personal computers. Journal of Coastal Research, 10(4), 946-958.
[52] Hallermeier RJ, 1981. A profile zonation for seasonal sand beaches from wave climate. Coastal Engineering, 4, 253-277.

as carbonates and pumice are mobile at greater depths than those predicted for quartz and feldspar (the dominant minerals present).

Badesab et al (2012[53]) identified coast parallel bands of titanomagnetite between Maketu and Waihi Beach that demonstrate that denser sediments are effectively immobile at depths shallower than assumed for sites H1 and H2. Kulgemeyer et al (2018[54]) demonstrated that the titanomagnetite bands were placer deposits resulting from the preferential removal of lower density sediments by wave action.

Side-scan sonar and multibeam surveys of the Bay of Plenty inner continental shelf show the presence of alternating zones of fine and coarse sediment (Hume et al, 1995[55]). Initially it was considered that these represented the reworking of sediments by episodic severe storm waves (once a year or less). However, coring of these zones offshore from Tairua and Pauanui Beaches showed no relationship with storm activity. Instead, it was suggested that they resulted from feedback associated with small scale movements of bedforms due to smaller waves than previously inferred (Trembanis and Hume, 2011[56]). If this is the case, then it is possible that sites H1 and H2 are partially dispersive. This may explain the higher-than-expected onshore movement of sediment at the northern end of Waihi Beach (Bear, 2009[57]).

Studies by Harms (1989[58]) and Warren (1992[59]) investigated dispersion from the dredge spoil sites used by the Port of Tauranga before the 1991/92 Capital Dredging Campaign. They demonstrated the sites used were dispersive, which led to the establishment of deeper sites (now H1 and H2, Figure 29). Michels and Healy (1999) reported on the investigations undertaken to select the deeper sites. They assumed dredging would occur using a BHD or bucket dredge, so the sediment discharged onto the disposal site would be in cohesive clumps. Their theoretical analysis suggested that coarser sediment would be moved during large wave events, while the finer sediment would be unaffected due to cohesion. Limited current measurements indicated the presence of a weak wind-driven net southerly current (towards Ocean Beach), which suggested dispersion of coarser sediment towards the beach might occur.

Blacker (2024[60]) undertook the first detailed assessment of the dispersion from the disposal sites since the establishment of sites H1 and H2. She used a combination of shallow seismic surveys, surficial sediment sampling, and vibracores to examine the D, G, H1 and H2 disposal sites and the surrounding seafloor (Figure 30 left). The seismic survey identified 3 stratigraphic boundaries:

[53] Badesab F, von Dobeneck T, Bryan KR, Müller H, Briggs RM, Frederichs T, & Kwoll E, 2012. Formation of magnetite-enriched zones in and offshore of a mesotidal estuarine lagoon: An environmental magnetic study of Tauranga Harbour and Bay of Plenty, New Zealand. Geochemistry, Geophysics, Geosystems, 13(6). 20 p.

[54] Kulgemeyer T, Bryan KR, & von Dobeneck T, 2018. Formation of coast-parallel heavy mineral enrichments investigated by exploratory numerical modelling. GSA Bulletin, 130(11-12), 1875-1888.

[55] Hume TM, Beamsley B, Green MO, de Lange WP, & Hicks DM, 1995. Influence of seabed topography and roughness on longshore wave processes. Coastal Dynamics '95', International Conference on Coastal Research in Terms of Large-Scale Coastal Experiments, Gdansk, Poland. 975-986

[56] Trembanis AC, & Hume TM, 2011. Sorted bedforms on the inner shelf off northeastern New Zealand: spatiotemporal relationships and potential paleo-environmental implications. Geo-Marine Letters, 31(3), 203-214.

[57] Bear AL, 2009. Erosion and Sedimentation Processes at Northern Waihi Beach. MSc Thesis, The University of Waikato, Hamilton. 214 p.

[58] Harms C, 1989. Dredge spoil dispersion from an inner-shelf dump mound. MPhil Thesis, The University of Waikato, Hamilton. 177 p.

[59] Warren SK, 1992. The geomechanics and dispersion of dredge spoil dumped in open water on the inner shelf, Tauranga, New Zealand. MSc Thesis, The University of Waikato, Hamilton. 281 p.

[60] Blackler C, 2024. Assessing dredge spoil dispersion on the inner shelf off the coast of Tauranga Harbour, Aotearoa New Zealand. MSc Thesis, The University of Waikato. Hamilton. 186 p.

A. The seabed where there is a sharp change in density from seawater to sediment;
B. An increase in density from soft poorly consolidated sediment to harder sediment, which was inferred to be the contact between dredge spoil and the original seabed; and
C. An increase in density that was inferred to be the contact between marine sediments and terrestrial sediments representing the land surface before the post-glacial sea level rise.

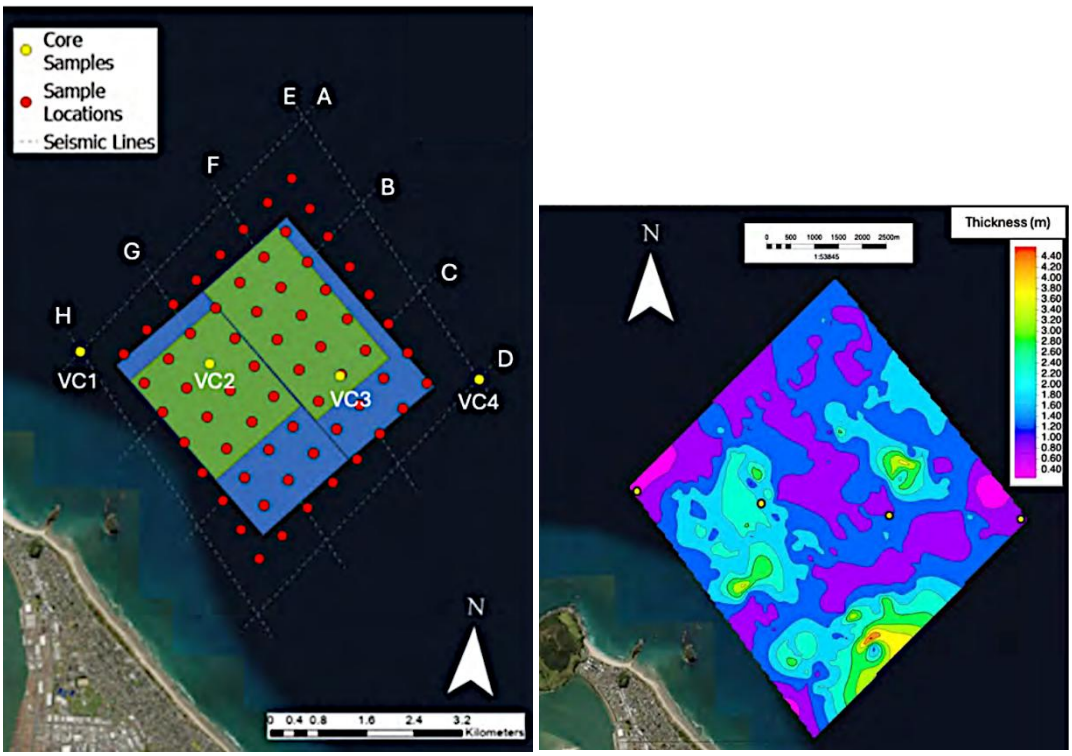



*Figure 30 – (Left) location of vibracores, surficial sediment samples, and seismic survey lines collected by Blackler (2024), and (Right) isopach map of dredged sediment thickness in 0.5 m increments. (Figures 2.1C and 2.4D from Blackler, 2024)*

The depth difference between boundaries A and B was taken to be the thickness of the dredge spoil deposit (Figure 30 right). The deposit varied in thickness from 0.5-4.5 m, with most being in the range 1-1.5 m. There are 3 areas of greater thickness of between 3.5 and 4.5 m, which all occur within the existing disposal sites (D, G & H1).

The vibracores show that the dredge mounds are structureless, indicating that there has been little reworking since deposition on the seafloor. Surficial samples show that overall, the seabed is covered with medium moderately sorted sand, with a composition similar to the original seabed as reported by Michels and Healy (1999). There are variations in grain size and organic content (Figure 31), which are most marked at the edges of disposal sites where the dredge deposit is thinnest, and may mostly represent the original characteristics of the seabed before disposal commenced. The analysis by Michels and Healy (1999) doesn't provide sufficient information to allow a comparison with the observations of Blackler (2024). The area with the highest organic content overlies a buried fluvial channel, but it is not clear if this has affected the results or not.

The results presented by Blackler (2024) indicate that there is limited movement of the dredged material deposited in sites D, G, H1 and H2. There appears to be some reworking of the surficial sediment, but there is no evidence of dispersion from the sites.

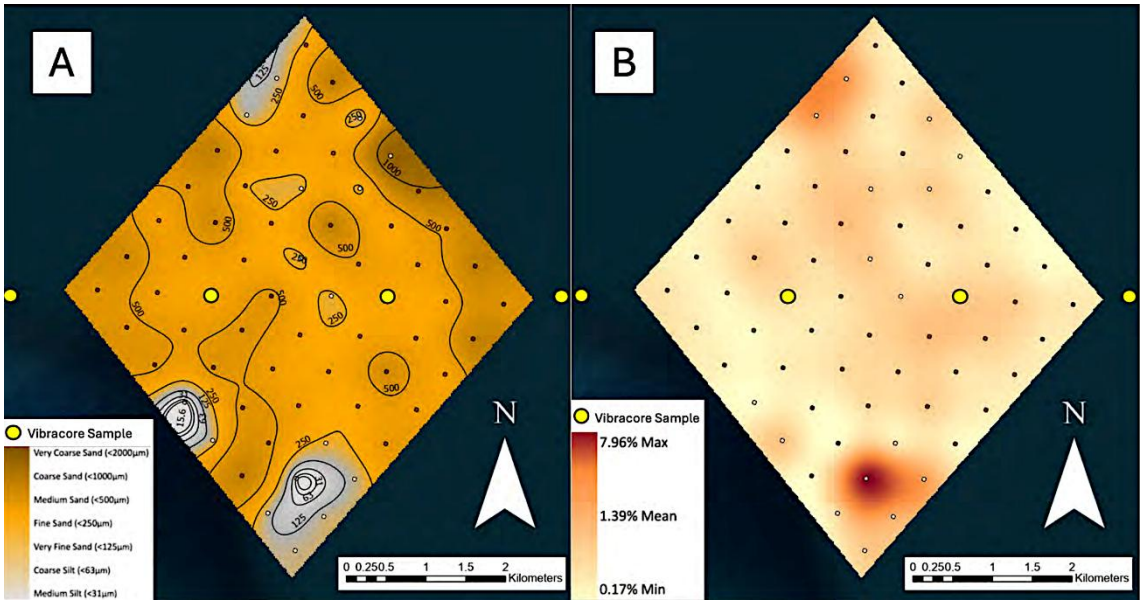



*Figure 31 – Mean surficial sediment grain size (A) and loss on ignition (LOI), which provides an estimate of organic content. (Figure 2.7 from Blackler, 2024)*

Berthot et al (2024)[i61] modelled the dispersion of nutrients and sediments from the disposal site, as well as locations within the harbour, by releasing a fixed quantity of material into the water column. They found that released sediment initially formed a near bed concentrated layer, while soluble nutrients were more uniformly dispersed in the water column. The dissolved and suspended material was then dispersed by ambient currents. This resulted in material within the harbour being exported, while offshore releases were dispersed along the inner continental shelf. During El Niño conditions, some offshore near bed suspended and dissolved material moved shoreward towards the harbour entrance, which is consistent with upwelling associated with onshore winds. In contrast during La Niño conditions, some material moved further offshore. Further, there was a tendency for offshore material to move westward during the Summer, and eastward during the Winter.

Montaño (2024) modelled the formation and dispersion of sediment plumes during the disposal of dredged sediment at the center of the combined sites D and H1 (Figure 29) from a large TSHD hopper. Disposal from a BHD hopper barge will behave in the same manner, but involves much smaller volumes of sediment (assumed to be up to 5,000 $m^3$ per day for BHD, versus up to 15,000 $m^3$ per dredging cycle for TSHD). The source terms for the sediment plume (Figure 28) simulated were defined as a proportion of the hopper volume, and consisted of:

- Density current following seafloor impact affecting deepest 20% of the water column over a radius of 20 m – 21%
- De-entrainment of sediment during convective descent affecting all of the water column over a radius of 160 m – 5%
- Turbulent entrainment caused by the moving vessel as sediment is discharged affecting the surface with a radius of 20 m – 1%.

Due to the water depth and low current velocities, no sediment was assumed to be entrained back to the surface from the near-bed density current. Hence, any visible plume was assumed to be caused by entrainment from the near surface descending sediment by convective descent and vessel turbulence only.

[61] Berthot A, Watson H. & Cussioli M, 2024. Tauranga Harbour Nutrient and Sediment dispersal, Report prepared for Port of Tauranga, MetOcean Solutions, August 2024. 38 p.

The modelling shows that under the conditions simulated the surface sediment plume is restricted to a small area around the release point (Figure 32). The near-bed plume travels further due to the initial momentum of the density current releasing sediment into the water column, but is still confined to the disposal site. If the sediment was released close to the boundaries of the sites, then the near-bed plume would extend beyond the boundaries. However, this is not normal practice as shown by the results of Blackler (2024) where most sediment has been deposited in relatively restricted areas within the disposal sites.

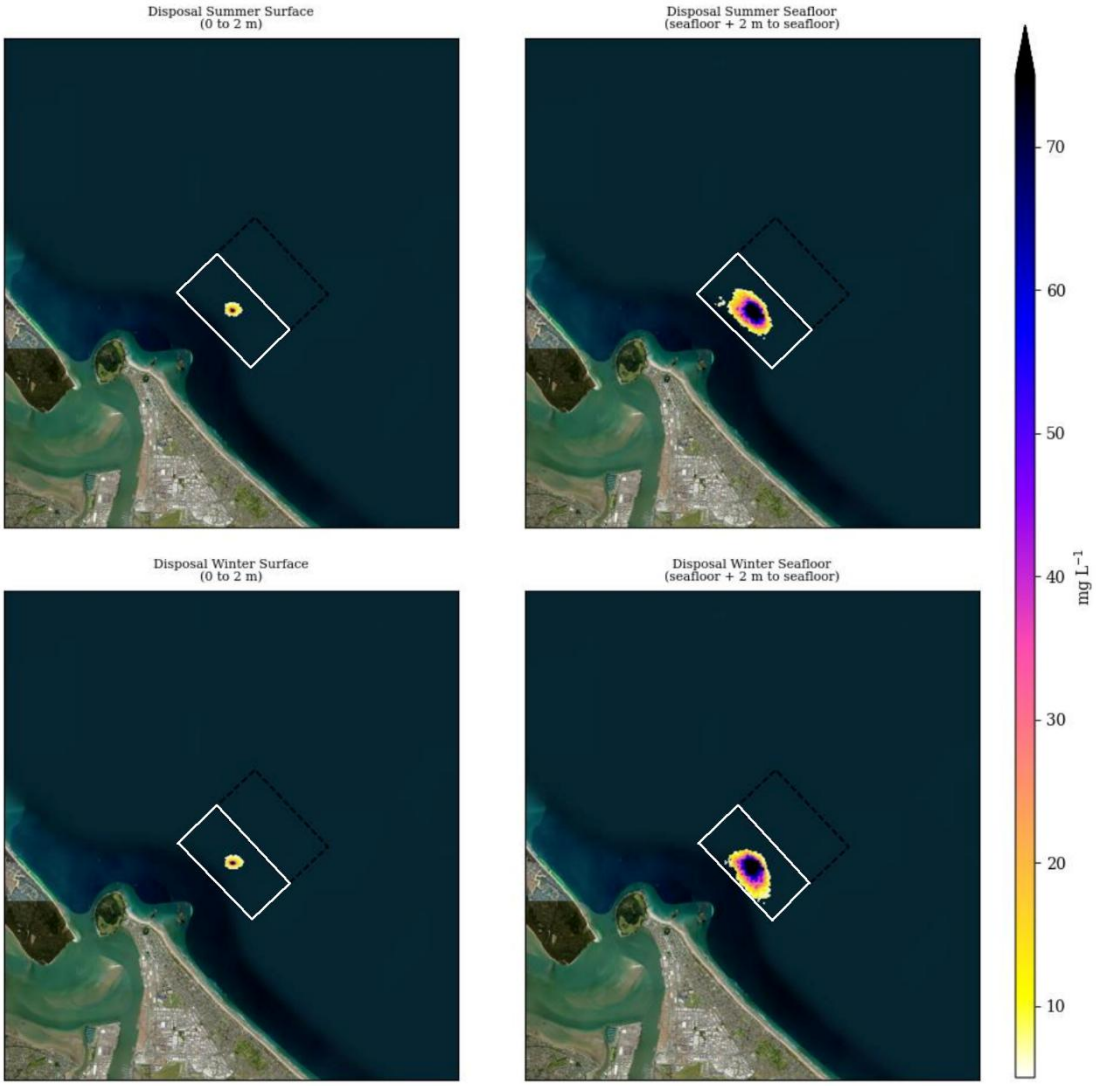



*Figure 32 – 90th percentile of total suspended sediment concentration following the emptying of a large TSHD hopper at the centre of the combined D and H1 disposal sites (white rectangle). Plots show the surface and near bed plumes for La Niña summer and winter conditions. . Concentrations <5 mgl-1 are masked. (Figure 3-15 from Montaño, 2024)*

Unlike the extraction phase results where concentrations exceeding the 75 mg.l$^{-1}$ threshold only occurred during specific tidal conditions for short non-consecutive periods, the patterns shown in Figure 32 occur for every sediment release. The modelling indicates that for a large TSHD the suspended sediment concentrations can exceed the threshold within ~100 m of the release point for a limited time after release. The affected area is within the disposal site, and ~70% of the released sediment is deposited on the seafloor within this area burying any benthic biota present.

Foster et al (1991[62]) and Foster (1992[63]) examined the effects of sediment disposal on benthic fauna for an existing disposal site (within site D). They concluded that burial was the main adverse effect, which was linked in a reduction of biodiversity 6 months after disposal. However, there was limited movement of the sediment, so they assessed the site as stable and it was expected that the site would recover quickly as suggested by Dr Roger Grace in Healy et al (1988).

Ecological monitoring of the disposal site was undertaken annually after the 1991/92 Capital Dredging Campaign, and Cole and Healy (1997[64]) reviewed 3 years of data as part of an analysis of the effectiveness of the sampling design. While the data showed the recovery of the main species present before the campaign, they identified that the sampling design didn't adequately address the natural variability in species presence and abundance, particularly for rare species.

# 5.0 Post-dredging impacts

Post-dredging impacts are predominantly due the changed morphologies resulting from excavation and mass emplacement the sediment at disposal sites. The volumes of sediment associated with the dredging plumes during excavation and disposal are usually too small to alter the morphology sufficiently to affect hydrodynamics. The main potential impacts are: changes to the tidal circulation and sediment transport within and outside the harbour; changes to the behaviour of depth-dependent phenomena, such as waves and storm surges; changed patterns of erosion and accretion; and dispersal of sediment from the disposal site. Changes to tidal circulation may primarily occur within the harbour, but can affect the ebb-tidal delta, and manifest as changes to the shape of the tidal elevation curve (affecting tidal range, the timing of high and low tide, the duration of flood and ebb tidal flows, and tidal flushing).

Dredging involves the extraction of sediment, and the subsequent disposal of the sediment. For Te Awanui, most sediment dredged since 1960 has been deposited in either offshore disposal grounds, or within reclamations. A small proportion has been used to renourish beaches and establish bird roosting areas. Outside of the areas of direct sediment deposition within Te Awanui, the dredging does not provide a source of sediment for accretion.

As the coastal lagoons, such as Te Awanui, evolve naturally over time, the balance between terrestrial and marine sediment changes from a marine dominated system to a terrestrial dominated system. Overall, they are sediment sinks, which creates potential issues with the accumulation of contaminants. Te Awanui sedimentation is terrestrial dominated, so that sediment is derived primarily from terrestrial sources (local catchment discharges and coastal mass movement), except in the immediate vicinity of the two tidal entrances that contribute marine sediment.

The current hydrodynamic regime favours the export of very fine sediment from the harbour, and the accumulation of medium to coarse sediment. The exceptions are areas of restricted turbulence and tidal flushing at the heads of sub-estuaries, particularly those enclosed or partially enclosed by causeways. This suggests that construction of the railway line around the harbour has accelerated the accumulation fine sediments in some areas.

[62] Foster DM, Healy TR, & Warren SK, 1991. Environmental impacts of a recent dredge spoil dumping operation off Tauranga, New Zealand. Coastal Engineering - Climate for Change: 10th Australasian Conference on Coastal and Ocean Engineering, Auckland, New Zealand. 141-145.

[63] Foster DM, 1992. Environmental impacts of recent dredging and inner shelf spoil disposal at Tauranga. MSc Thesis, The University of Waikato, Hamilton. 230 p.

[64] Cole RG, & Healy TR, 1997. Dredge spoil disposal off Tauranga and sampling designs to detect its impacts. Pacific Coasts and Ports' 97: Proceedings of the 13th Australasian Coastal and Ocean Engineering Conference and the 6th Australasian Port and Harbour Conference; Volume 2, 586-590

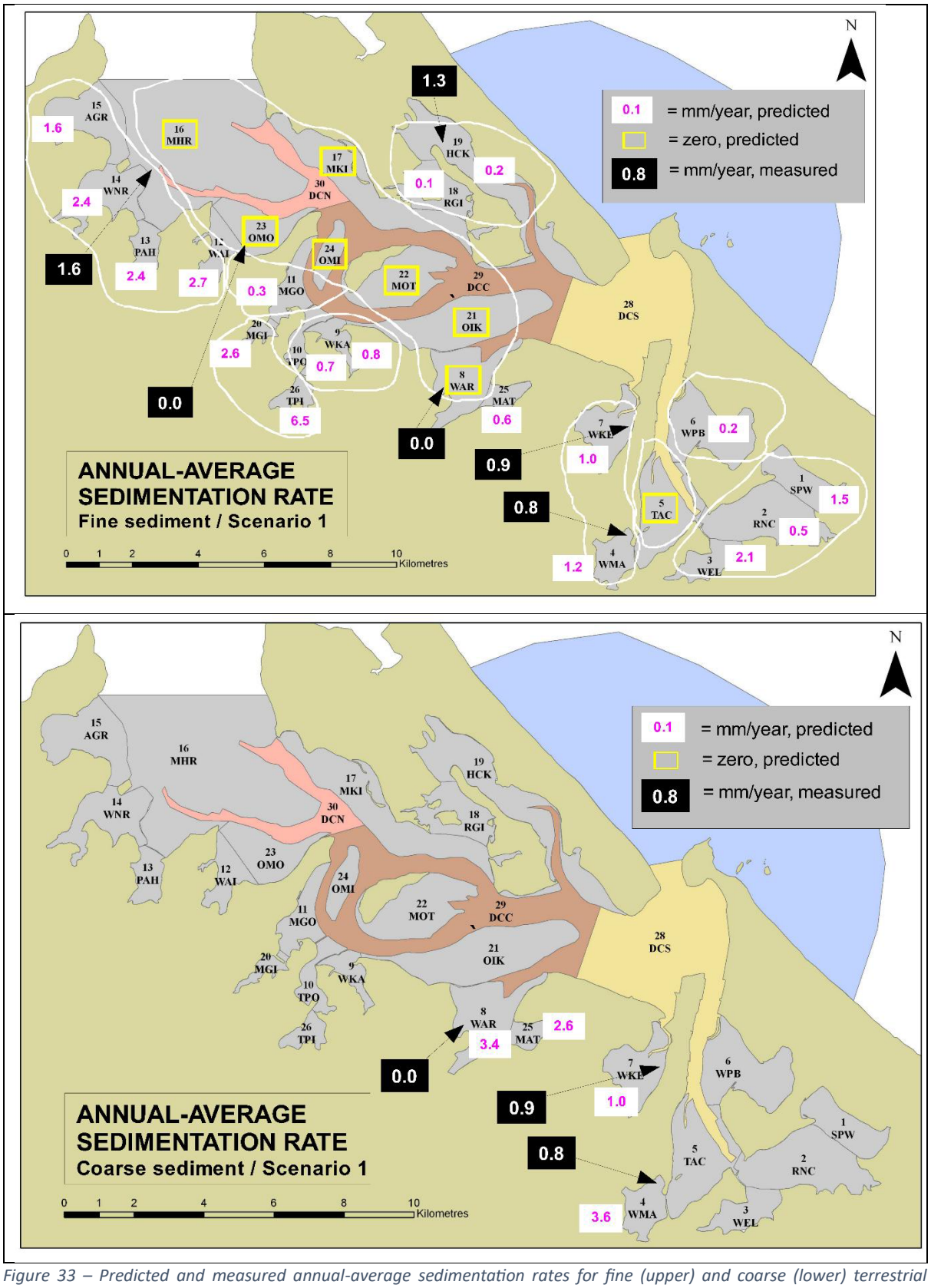



*Figure 33 – Predicted and measured annual-average sedimentation rates for fine (upper) and coarse (lower) terrestrial sediment. (Figures 4-5 and 4-6 from Green, 2010).*

Figure 33 shows the deposition of fine and coarse terrestrial sediment patterns within sub-basins and sub estuaries of the Tauranga Basin of Te Awanui determined by the NIWA sediment study from

historical sedimentation rates and numerical modelling (Scenario 1)[65]. These figures do not include the sediment exported from the harbour (42% of the fine sediment entering the harbour), and the contribution from shoreline erosion within the harbour (predominantly landslides).

The hydrodynamics of Te Awanui can be affected by small changes in forcing conditions, and the bathymetry. Modelling and observations indicate that the dominant driver of hydrodynamic changes is weather (*viz*. Green, 2010), which varies at a range of time scales from decadal to millennial. However, unlike the weather, the hydrodynamic effects of dredging are confined to the immediate vicinity of the dredged channels, and do not extend over the entire harbour.

Appendix 1 summarises the observed erosion and siltation changes within Te Awanui associated with the development of the Port of Tauranga prior to 2022. This section reviews the processes involved in post-dredging impacts and summarises more recent observations, measurements and modelling results.

Tides are important drivers of estuarine processes. The observed tide at any location represents the combination of multiple tidal constituents caused by the gravitational attraction of celestial objects (predominantly the Moon and Sun), and the interactions with the boundaries of the water bodies they form in. In the deep ocean, the tides travel as a progressive wave that rotates about an axis (amphidromic point). The magnitude and direction of the currents produced by the moving wave (tidal streams) can be plotted as a rose diagram, which is known as a tidal hodograph (). A deep-water tidal hodograph is close to circular with the strongest currents occurring at high (HW) and low water (LW).

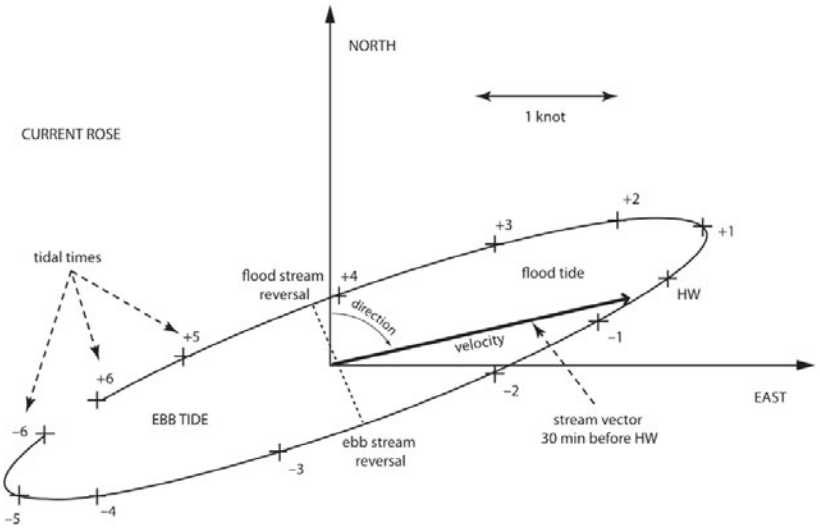



*Figure 34 – Example of a tidal stream hodograph that illustrates the direction and magnitude of tidal currents at each stage of a tidal cycle (Figure 10.6 from Simon, 2013[66]).*

As the water depth decreases, the tidal wave begins to shoal just like wind-generated swell waves do as they approach the shore to form surf (the tidal equivalent to surf is a tidal bore). Shoaling changes the progressive tidal wave into a standing wave. In Figure  this transformation has started so the maximum currents no longer occur at high and low water (about 1 hour after HW and LW in this example). As the tidal wave continues to shoal, the hodograph becomes a very narrow ellipse with dominant ebb and flood directions, as can be observed in the entrances to Te Awanui. When the tide is constrained by channels, the ebb and flood directions may no longer be 180° apart and the maximum

[65] Green, M.O., 2010. Tauranga Harbour Sediment Study: Predictions of harbour sedimentation under future scenarios. Report prepared for Environment Bay of Plenty. NIWA Client Report HAM 2009-078. 68 pp.
[66] Simon B, 2013. Coastal tides. Institut océanographique éd, Monaco. 411 p.

speeds may differ. This results in a net transport of water (a residual current) and sediment over a tidal cycle, and the presence of circulation systems within an estuary.

Eventually when the tide has transformed into a standing wave, the maximum currents occur at mid-tide, and the stream reversals shown in Figure 34 occur at HW and LW. This is essentially the situation in the Tauranga Harbour inlet. An important consequence of the tide behaving as a standing wave is that the tidal currents are now forced by slope of the water surface, and not by the orbital motions within the tidal wave. This means that within Te Awanui, the tidal currents are a result of the water level differences throughout the harbour, so the main tidal control on current velocity is the tidal range (the difference in water level between HW and LW).

However, the water depth can also affect the current velocity due to the friction exerted in the moving tide. The Gironde Estuary in France is a classic example of the shoaling changes that occur within an estuary (Figure 35). As the tide travels from Le Verdon to Bordeaux the timing of HW and LW gets later and the time intervals between HW and LW change as the duration of flood tide decreases and the duration of ebb tide increases. This results in steeper water surface slopes during the flood tide driving faster currents than occur during the ebb tide. In the Gironde Estuary the tidal range also increases with distance from the entrance. If the friction is sufficiently high (very shallow estuary for example) the tidal range may decrease.

Similar changes occur within Te Awanui, but they are much smaller than those shown in Figure 35. This is expected as the Gironde Estuary is a 75 km long, narrow (3-12 km), macro-tidal (mean spring tidal range of 5 m) river mouth estuary, while Te Awanui is a microtidal lagoonal estuary (maximum spring tidal range < 2 m). For example, as the tide travels through relatively deep channels between the harbour entrance and Ōmokoroa (~12 km), both HW and LW are delayed by 45-48 minutes and the tidal range is slightly increased by ~0.05 m. Tide gauges between A Beacon and the Bridge Marina show that the tidal range is not significantly changed, but the tide is increasingly delayed with distance along the channels from A Beacon (~20 minutes for LW & HW).

Stephens (2017)[67] and Tyler (2018)[68] both analysed tidal characteristics at Moturiki, Tug Berth, Sulphur Point, Omokoroa, Hairini, and Oruamatua. They only reported the amplitudes of the constituents, and did not provide the phases that are required to determine the timing changes throughout the harbour. However, Reeve et al (2019)[69] do provide a table of measured $M_2$ amplitudes and phases for 27 locations throughout the entire harbour including those examined by Stephens (2017) and Tyler (2018). The phases show the delays caused by the propagation and shoaling of the tide within the harbour, and also indicate that the two basins are effectively separate.

[67] Stephens SA, 2017. Tauranga Harbour extreme sea level analysis. Report for Bay of Plenty Regional Council. NIWA Client Report 2017035HN.
[68] Tyler MJ, 2018. *Storm surges in Tauranga Harbour*. MSc Thesis, The University of Waikato, Hamilton, New Zealand.
[69] Reeve G, Stephens S, & Wadhwa S, 2019. Tauranga Harbour inundation modelling. Report for Bay of Plenty Regional Council. NIWA Client Report 2018269HN.

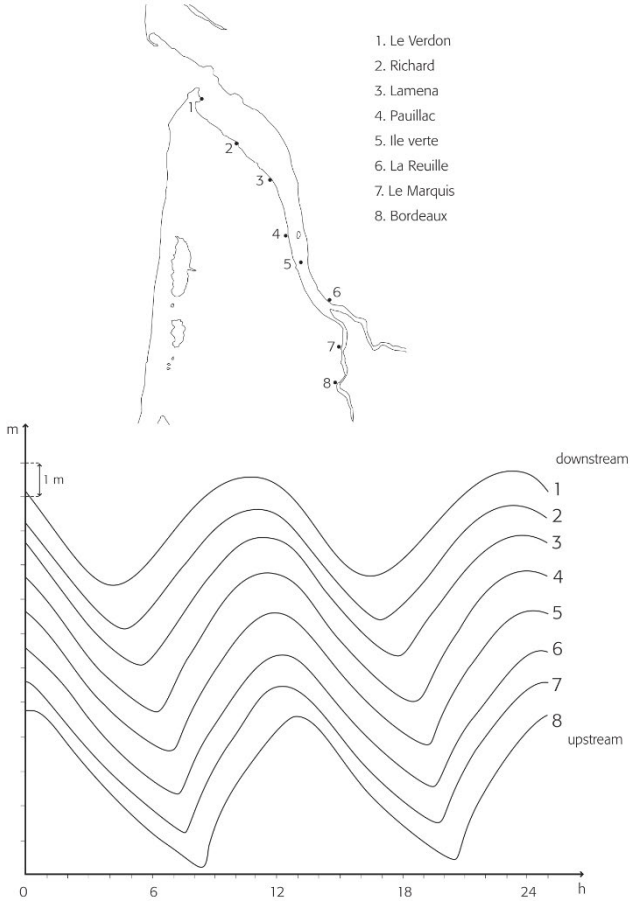



*Figure 35– Example of the shoaling transformations of the tidal wave as it travels into the Gironde Estuary, France (Figure 1.8 from Simon, 2013).*

In addition to the slope of the water surface the velocity water flows in a channel also depends on the area of the channel, and the wetted perimeter. It is generally assumed that the discharge (volume of water moved per unit time) along a channel remains constant, unless water is added or removed. Discharge is determined by the channel wetted cross-sectional area multiplied by the velocity. If the area increases then the velocity decreases, and vice versa. The wetted perimeter is an indication of the frictional resistance. This is only significant when comparing flows in channels with flows across shallow intertidal flats.

Dredging can change:

- the tidal range by changing the friction and/or constrictions affecting the movement of the tide, which changes the water slope. Increasing tidal range increases current velocities, and vice versa;
- the timing of high and low tide within the harbour, as the tidal wave propagates faster in deeper water. Hence, dredging tends to reduce the time difference between corresponding tidal stages at either end of the channels;
- the duration of flood and ebb flow, which also changes the water slope. Decreasing duration of either ebb or flood flow increases current velocities, and vice versa;
- the wetted cross-sectional area and wetted perimeter length of the channels. Decreasing cross-sectional area and perimeter length increases current velocities, and vice versa.

There are other processes that can cause the same changes including large freshwater floods, shoaling of channels, and construction of causeways, reclamations and wharves.

Measurements following previous capital dredging in Te Awanui showed that the dredging increased the channel cross-sectional areas, which was the purpose of the dredging. There were also very small effects (within the error bounds of the models) on tidal range, timing of high and low water, and durations of flood and ebb flows due to a slight reduction in the total friction and constrictions experienced by the tide: tidal ranges decreased slightly, and the differences in flood and ebb tide durations decreased slightly. These changes resulted in a reduction in current velocities, restricted to the dredged channels. Analysis of the tidal constituents measured at locations further up harbour and outside the harbour showed no change in amplitude or phase (Tyler, 2018).

There are limited observational data to assess changes in tidal velocities, with most available measurements collected before and shortly after the 2015/16 Capital Dredging Campaign. For example, Watson (2016)[70] examined the impacts of the dredging on Stella Passage and areas further upstream within the harbour, and found no measurable changes beyond the dredged channels. Based on available data, changes in velocities beyond dredged channels were due to construction of causeways (e.g. Tauranga Harbour Bridge approaches), shoaling of channels in the shallower areas of the harbour, and in areas of shoaling on Te Paritaha. The areas of shoaling associated with increased velocities have been undergoing shoaling over the entire period of available bathymetric data from 1852 to the present, and are consistent for the natural tendency for estuaries to infill over time. This pattern of behaviour was demonstrated by the analysis of historic circulation within Te Awanui by Brannigan (2009)[71] and Moffat (2021)[72]

Watson and Berthot (2025) modelled three historic bathymetric configurations – 2015 pre-capital dredging, 2016 post-capital dredging, and 2023 – and one proposed capital dredging scenario. The proposed capital dredging scenario planned to be undertaken in 2026 and involved greater modification than the capital dredging now proposed to be reconsented. They undertook simulations using the same La Niña summer and winter conditions as the other modelling studies undertaken by MetOcean Solutions. Water level and current velocity data were saved for locations with instrumental observations (stations) and areas of interest (map output) as shown in Figure 36. These locations are all within the tidal inlet flood and ebb tidal delta system, and shipping channels. Changes beyond these locations were smaller than the MAE values in Table 1, and therefore, are considered negligible.

Only 2 of the station output locations lie within dredged channels (Entrance ADCP and Stella Passage S4), where current velocity and water level observations are available. The remaining 3 station output locations correspond to operational water level recorders (Sulphur Point, Tug Berth, and A Beacon). The map output locations are in areas where either limited or no observational data are available.

Tables 4.1 and 4.3 in Watson and Berthot (2025) summarise the La Niña summer and winter surface current speed statistics for the station locations, including the mean, 80$^{th}$ percentile, 90$^{th}$ percentile, 95$^{th}$ percentile, 98$^{th}$ percentile, and maximum. The maximum values are based on a single value in the time series and should not be considered robust. The model results show negligible change at A Beacon, which is expected as the discharge is unconfined by the channel at that point. The remaining stations show a reduction in surface current speeds as a consequence of dredging as expected from theory as discussed above.

[70] Watson HM, 2016. *Potential impacts of wharf extensions on the hydrodynamics of Stella Passage and upstream regions of Tauranga Harbour, New Zealand*. MSc Thesis, The University of Waikato, Hamilton, New Zealand.

[71] Brannigan AM, 2009. *Change in geomorphology, hydrodynamics and surficial sediment of the Tauranga Entrance tidal delta system.* MSc Thesis, The University of Waikato, Hamilton, New Zealand.

[72] Moffat A, 2021. *The ecological implications of reconstructed historic hydrodynamic conditions in Tauranga Harbour (1852-2006)*. MSc Thesis, The University of Waikato, Hamilton, New Zealand.




*Figure 36 – SCHISM/WMM time series output locations for assessing changes potentially linked to capital dredging (Figure 1-2 from Watson and Berthot, 2025).*

Figure 37 shows time series of hourly depth averaged current speeds for the model station locations over 2 days of spring tide during La Niña winter conditions. The water elevation is plotted as well to provide an indication of ebb and flood tidal stage. The plots show that the tidal behaviour at some sites is modified by the dredged channels. The Entrance ADCP and Stella Passage S4 sites are showing patterns that occur normally in tidal channels, with the ebb and flood flows differing in strength. Both sites show a stronger ebb flow than the flood flow. Since the total ebb and flood discharge (referred to as tidal prism) is the same over a tidal cycle, this means that the opposite side of the channel should have a stronger flood flow than the ebb flow. This is the case for the harbour entrance. In Stella Passage, the ebb flow forms a narrow jet as the water passes between the Bridge Marina and Sulphur Point causing the higher ebb velocities at the station. The flood flow in Stella Passage is not concentrated into a jet and occurs over a larger area, resulting in lower velocities. The more extreme modelled capital dredging reduces the overall velocities at the Stella Passage S4 site, but enhances the influence of the tidal jet as it will flow directly over the site, resulting in a narrow ebb-tide peak before mid-tide.

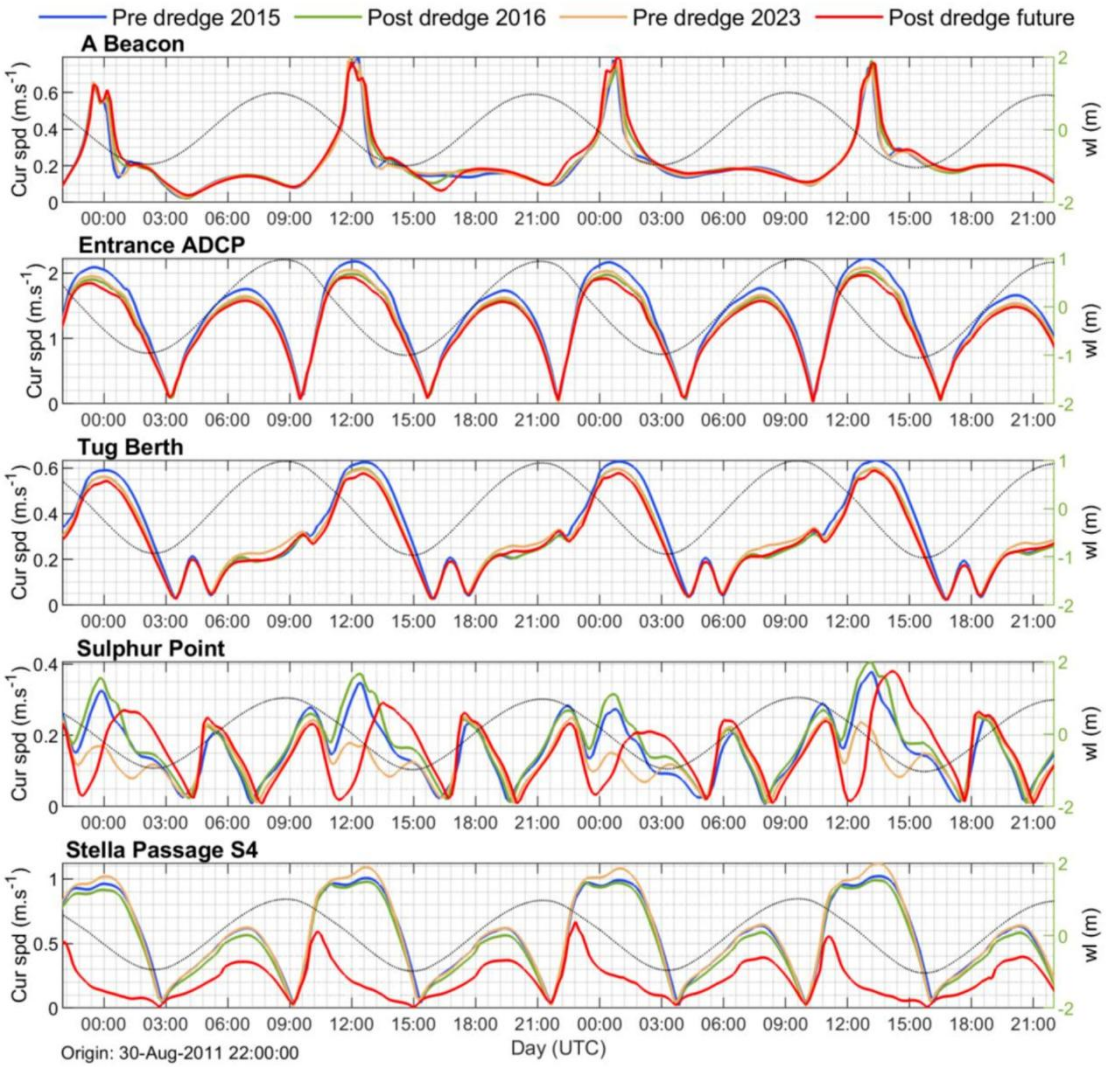



*Figure 37 – Time series of 10-minute current speeds and reference water level at the station sites, over 2 days of a spring tide under La Niña winter conditions for the 4 historical and future bathymetric conditions (Figure 4-3 from Watson and Berthot, 2025).*

The tidal flow at A Beacon is also affected by an ebb tidal jet formed as the water exits Te Awanui. This jet is directed northward, but some of the flow is deflected out through the Entrance Channel during the peak jet flow after mid-tide. Flood flow into the harbour occurs across a wide area of the ebb tidal delta (Matakana Bank), and the velocities are very low at A Beacon.

The Tug Berth and Sulphur Point locations are affected by converging flow from two channels during flood and ebb tide respectively, and the formation of tidal eddies that are associated with lower velocities than the main tidal flows. The pattern at the Tug Berth resulted from the formation of the Cutter Channel during the first capital dredging in the 1960s, and hasn't changed much since then (only a decrease in maximum speeds as the channels were enlarged). Sulphur Point has been progressively modified by reclamation and capital dredging over the last 50-60 years, and also a long-term natural trend that is shifting the ebb discharge from the upper harbour to the Otumoetai Channel from the Western Channel. The modelling shows a decrease in ebb flows between 2016 and 2023, which will be discussed further below with the modelling results for the Western and Otumoetai Channels. The modelled dredging resulted in a reduction of ebb flow speeds and a shift in timing due to the extension of the Stella Passage dredged channel, but little change to flood flow.

However, the proposed capital dredging being reconsented is only a small component of the modelled proposal, which means that the likely effects would be less than the model results.

The Stella Passage S4 site is a little unusual as the flows are affected by the channel connecting to Waipu Bay at Whareroa Point. Both flood and ebb flows through this channel vary with water level due to the flooding and drainage of the intertidal flats. When the water level is below the level of the intertidal flats, the flow is limited by the restricted volume in the tidal channels in Waipu Bay. This results in the double peak during the ebb tide, and the delayed peak during flood (compared to the Harbour Bridge site in Figure 37 for example). The model results show that the influence of Waipu Bay moves further north and it is no longer evident at the Stella Passage S4 site.

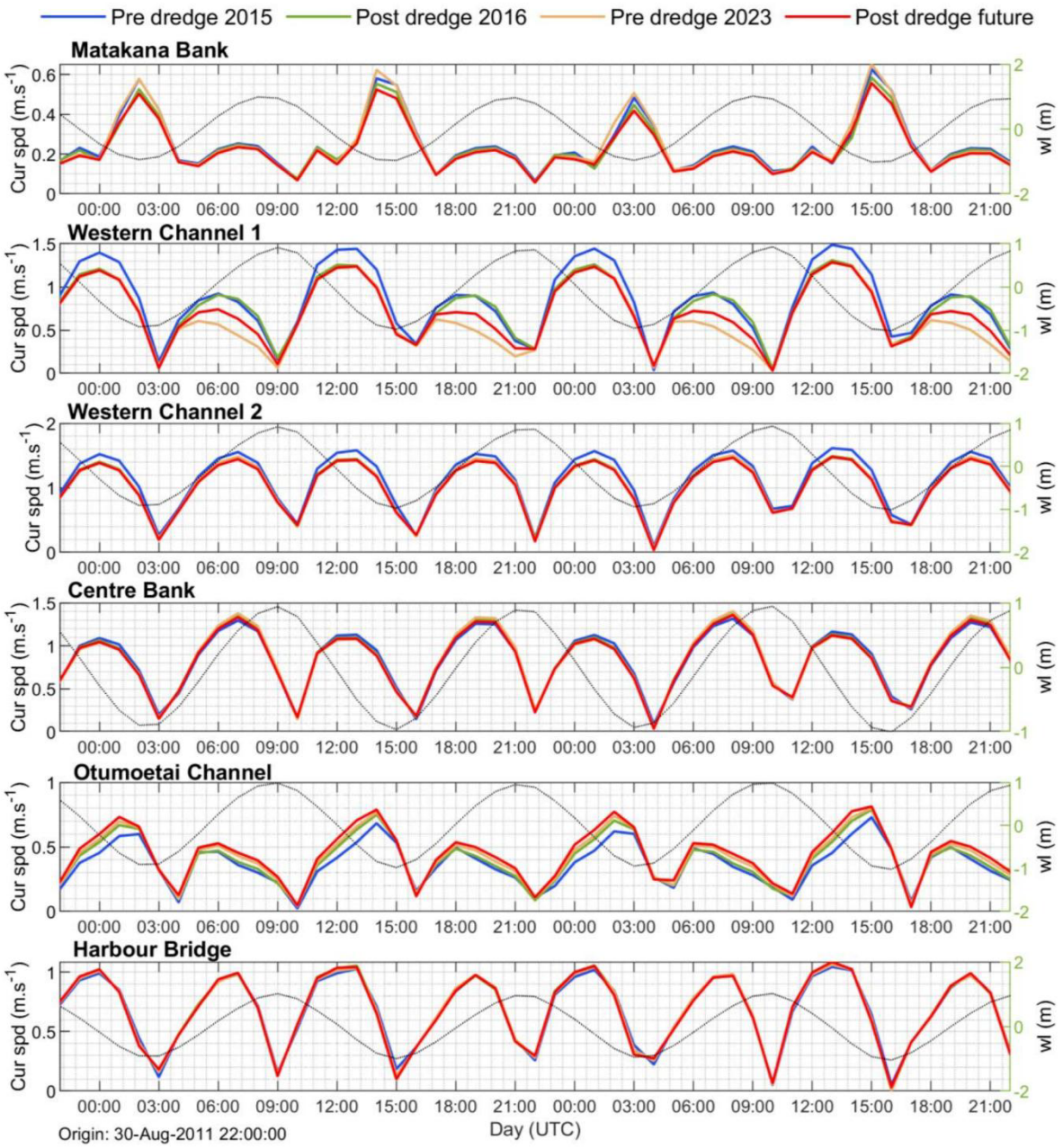



*Figure 38 – Time series of hourly current speeds and reference water level at the map output sites, over 2 days of a spring tide under La Niña winter conditions for the 4 historical and future bathymetric conditions (Figure 4-4 from Watson and Berthot, 2025). Refer Figure 28 for locations.*

The model map output locations are sites that are not dredged, but may show changes as a consequence of dredging. Figure 38 is the corresponding plot to Figure 30 for the model map output locations. The sites plotted show a change from a predominantly progressive tidal wave over the Matakana Banks (peak flows at LW), and a predominantly standing wave at the Harbour Bridge (peak flows at mid-tide). The station plots (Figure 36) fit into this progression, with the Entrance ADCP showing a shift in peak flows away from HW and LW towards mid-tide level and Stella Passage S4 showing a standing wave pattern with peak flows at mid-tide level.

The Matakana Bank site shows the strongest currents occur at LW when the ebb tidal jet leaving Te Awanui weakens, and initial flood flow into the harbour is established along the Matakana Island foreshore. Overall, the tidal currents are much weaker than those inside Te Awanui, but sediment transport rates can be high with the larger waves outside the harbour being responsible for entraining the sediment that the tidal currents transport.

The Centre Bank site is located at the landward end of a geomorphic feature referred to as the flood ramp (Figure 39 ). Flood flows entering the harbour are focused into a flood tidal jet that accelerates up the ramp as water depth decreases. When the flow has reached the Centre Bank site, the flood tidal jet is starting to spread out over Te Paritaha and the velocities are decreasing. The strength and orientation of the flood tidal jet is the main control of tidal current velocities across Te Paritaha, and the eddies it forms control the deposition of sediment on Te Paritaha. Hence, most of Te Paritaha is dominated by flood flows.

Any deposition during a flood tide, is modified by the following ebb tide resulting in sand banks (ebb shield and ebb spits, Figure 39) on the margins of Te Paritaha flanking the main channels. The current velocities at the Centre Bank site are sufficiently high to prevent shoaling and there is negligible change between the 4 bathymetries simulated.

The Harbour Bridge site is constrained by the infrastructure lining the channel, and shows negligible change between all the bathymetries simulated.

The Western and Otumoetai Channels form the western and southern margins of Te Paritaha, while the dredged Maunganui Roads forms the eastern margin. These 3 channels are ebb-dominated. The remaining dredged Cutter Channel on the northern margin is flood channel dominated, and prior to dredging was a blind flood channel. Water ebbing from the upper harbour via the Upper Western Channel can leave the harbour through either the Lower Western Channel, or the Otumoetai Channel/Maunganui Roads/Channel Route. Hydrographic charts and numerical modeling of Te Awanui since 1852 (Brannigan, 2009) shows that there has been a gradual displacement of ebb flow from the Lower Western Channel to the Otumoetai Channel associated with the southeastward growth of Matakana Island and particularly Panepane, which has increasingly blocked the channel. This has been occurring since the formation of the Purakau Shoreline on Matakana Island dated to 582±66[73] cal y BP (de Lange et al, 2015[74]).

[74] de Lange WP, Moon VG, & Johnstone R, 2015. Evolution of the Tauranga Harbour Entrance: Influences of tsunami, geology and dredging. 22nd Australasian Coastal and Ocean Engineering Conference and the 15th Australasian Port and Harbour Conference, 235-241.

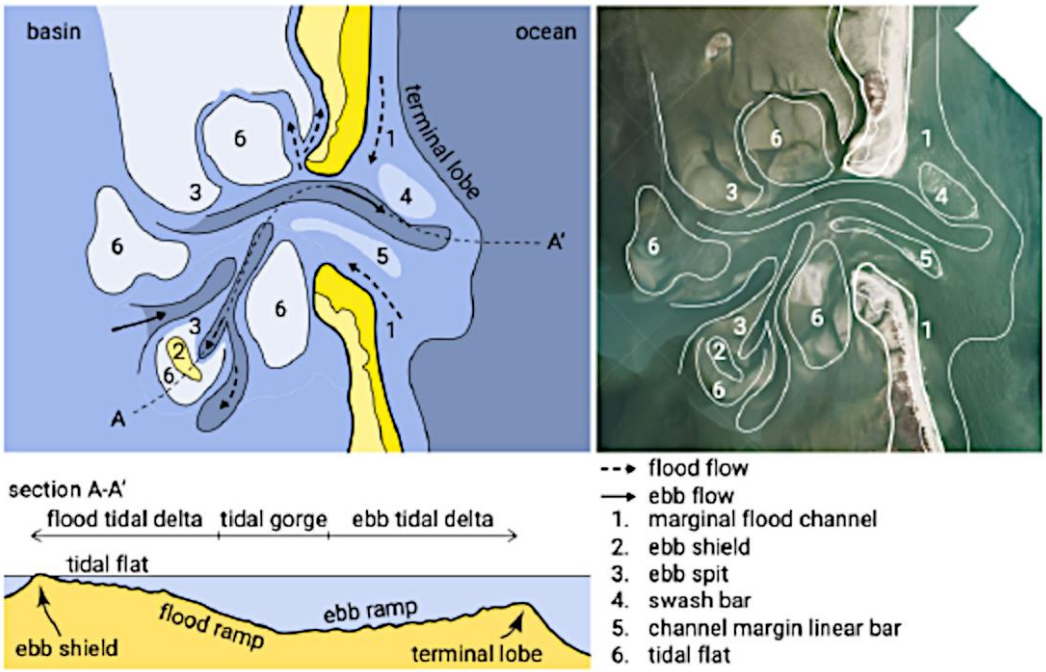



*Figure 39 – Sketch of the morphological elements of a tidal inlet based upon a photo from an inlet near Sheep Island, North Carolina. The lower part of the figure shows a cross-section along the inlet[75]. The Tauranga tidal inlet is simplified by the presence of Mauao, which prevents eastward migration of the inlet.*

Although there has been an overall trend of reducing flow in the Lower Western Channel, there have been periods of increased flow. Figure 38 shows that between 2016 and 2023, tidal currents increased in speed at site Western Channel 1, on the western side of the channel close to Matakana Island. Site Western Channel 2 closer to Te Paritaha did not show any increase or decrease, while the Otumoetai Channel site showed a slight decrease. The increase in speed at the Western Channel 1 mostly occurred during flood tides.

de Lange (2024[76]) reported on shoreline changes at Panepane, and noted that the recent erosion of the shoreline at Panepane and westwards along the Matakana Island foreshore was associated with the development of a marginal flood channel (Figure 39) that would transport sediment into the Lower Western Channel. Figure 40 shows the bathymetry of the Lower Western Channel and Te Paritaha measured by multibeam surveys in 2011, 2017, 2021, and 2024.

[75]https://geo.libretexts.org/Bookshelves/Oceanography/Coastal_Dynamics_%28Bosboom_and_Stive%29/9%3A_Coastal_inlets_and_tidal_basins/10.03%3A_The_main_morphological_elements/9.3.2%3A_Tidal_deltas

[76] de Lange WP, 2024. Morphological changes for south-eastern Matakana Island (Panepane) and Matakana Banks (ebb tidal delta) 2016-24. Report prepared for Port of Tauranga Ltd, December 2024. 10 p.

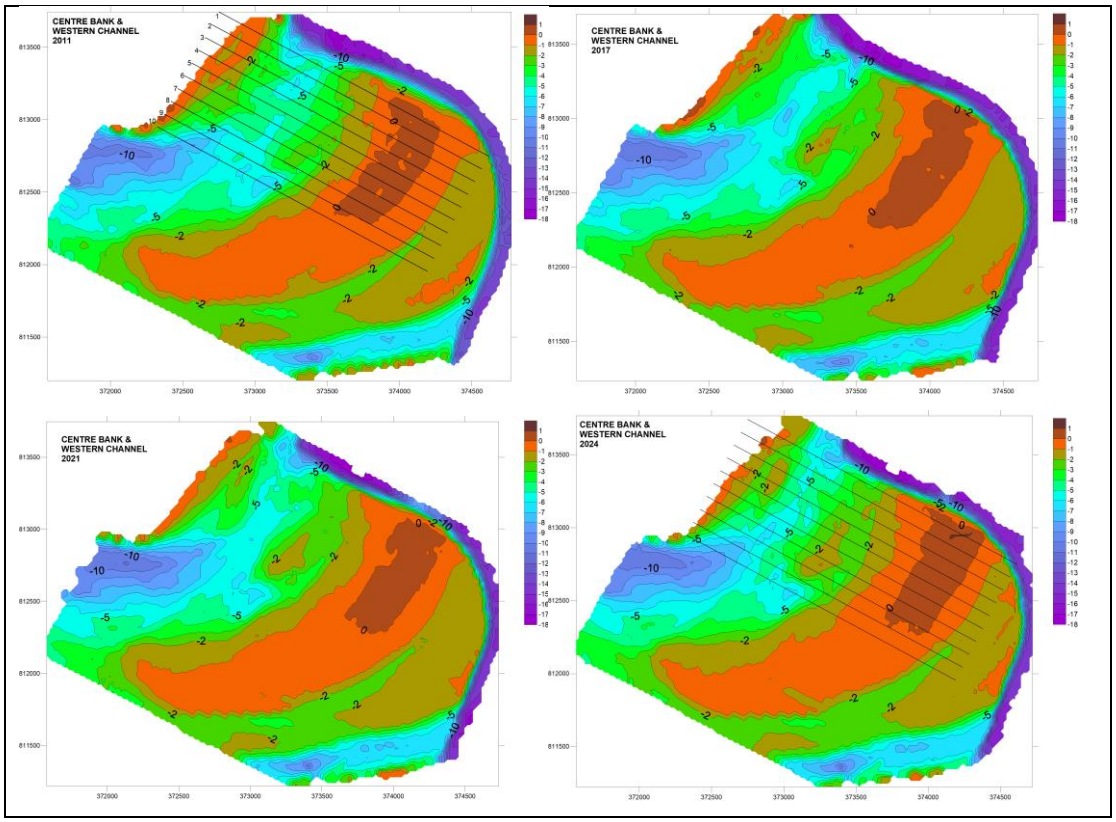



*Figure 40 – Bathymetry of the Lower Western Channel and Te Paritaha in 2011, 2017, 2021 and 2024. Figures provided by Greg Cox for Port of Tauranga Ltd. (Figure 6, de Lange, 2024)*

Ten transects were sampled across the Lower Western Channel to determine the changes in wetted cross-sectional area (the map output sites correspond to transect 3). Examples of the profiles along the transects and calculated cross-sectional area are shown in Figure 41. The profiles (left column) show that Te Paritaha was stable over the period 2011 to 2024, but the Lower Channel experienced localized erosion and accretion of up to 2 m depth. The cross-sectional areas change with the erosion and accretion, but there is no consistent trend for the whole channel. Tidal current speeds tend to increase when the cross-sectional area decreases, and vice versa.

Given the localized changes evident in Figure 40 and all of the transect data (Figure 41), the results of the comparisons done by Watson and Berthot (2025) will depend on where the map output sites are located in the Lower Western Channel. Hence, the different behaviour of the Western Channel 1 and 2 sites in Figure . Nonetheless, the results suggest that there may be a link between erosion of Panepane and the changes in the Lower Western Channel. This will be examined further below.

Capital dredging does not include shaping of the batter slopes at the side of the channels. These slopes may change in response to the dredging resulting in erosion or accretion, with a consequential change in the batter profile. Note that maintenance dredging removes accumulated sediment to restore the design channel dimensions, and would not affect the batter slope unless there is a high rate of accretion.

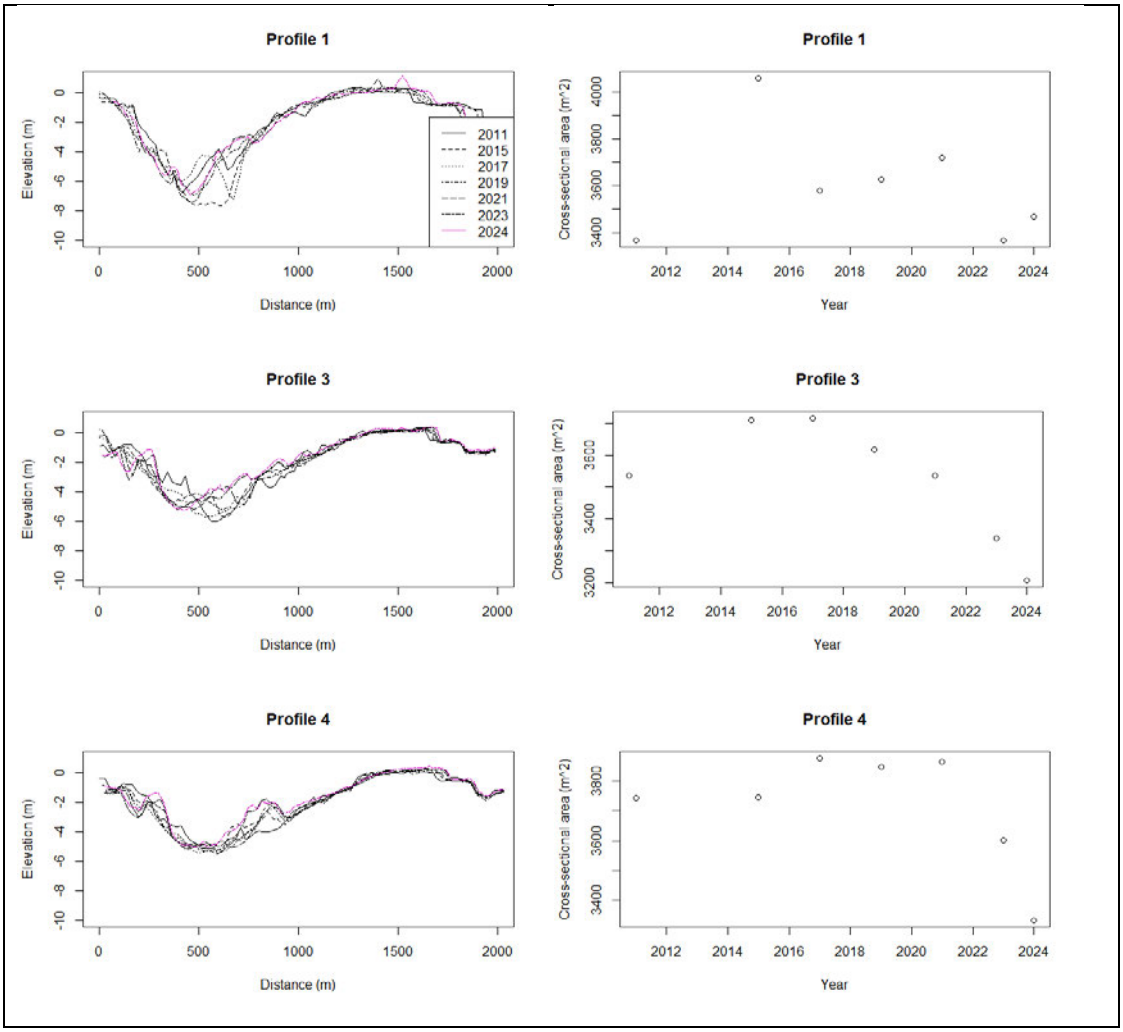



*Figure 41 – (Left) Stacked plots of transect cross-sections of the Lower Western Channel and Te Paritaha from 2011-2024; and (Right) corresponding time series of channel cross-sectional areas for the transects. The transects are marked in Figure on the plots for 2011 and 2024.*

Capital dredging may involve deepening and/or widening the channel; either of which results in removing sediment from the base of the batter slopes. The effect of this removal is dependent on the geotechnical characteristics of the batter slope, predominantly the in-situ strength. de Lange et al (2014) assessed the sub-surface characteristics of the shipping channels, including the batter slopes, using a combination of shallow seismic profiling and vibracoring. The geotechnical characteristics of the subsurface units have been assessed by CPT profiles (Moon et al, 2013[77]; de Lange et al, 2014; Jorat, 2014[78]; Jorat et al, 2017[79]; Moon & de Lange, 2019 OPUS, 2019[80]). These results indicate that:

[77] Moon, VG, de Lange, WP, Jorat, E, Christophers, A, & Moerz, T, 2013. *Sub-surface stratigraphy of Stella Passage, Tauranga Harbour*. ERI Report 28. Client report prepared for Port of Tauranga. Environmental Research Institute, Faculty of Science and Engineering, University of Waikato, Hamilton, New Zealand.

[78] Jorat, ME, 2014. *Advanced CPTu and laboratory investigation of geotechnically critical on-shore and near-shore soft sediments in Germany and New Zealand*. PhD Thesis, University of Bremen, Bremen, Germany. 123 pp.

[79] Jorat, ME, Moon, VG, Hepp, DA, Kreiter, S, de Lange, WP, Feldmann, S, & Mörz, T, 2017. Subseafloor Investigation of Sediments at Southern Tauranga Harbour, New Zealand, before Capital Dredging. *Journal of Coastal Research*, 33(2), 227-242.

[80] OPUS, 2019. *Sulphur Point Southern Wharf Extension – Port of Tauranga: Geotechnical factual report*. 359 pp.

- Where the batter slope consists only of sediment, the fines content increases with depth and age, so that cohesion increases with depth due to greater cohesion. This results in convex batter slopes as the stable angle increases with depth;
- In areas of high accretion, the batter slope is oversteepened by recent sediments with negligible fines content. The recent sediment has low strength and tends to produce a concave slope as the sediment slides downslope into the channel (requiring maintenance dredging).
- The Holocene sediments mostly overlie a ridge and valley topography formed in Pleistocene materials, which include harder units such as ignimbrites, iron pans, and gravel-cobble layers. In Pilot Bay, previous seismic surveys during the Tauranga Harbour study showed the presence of at least one buried rhyolite dome (Healy, 1985[81]). These units can form steep slopes, and are associated with stable convex slopes.

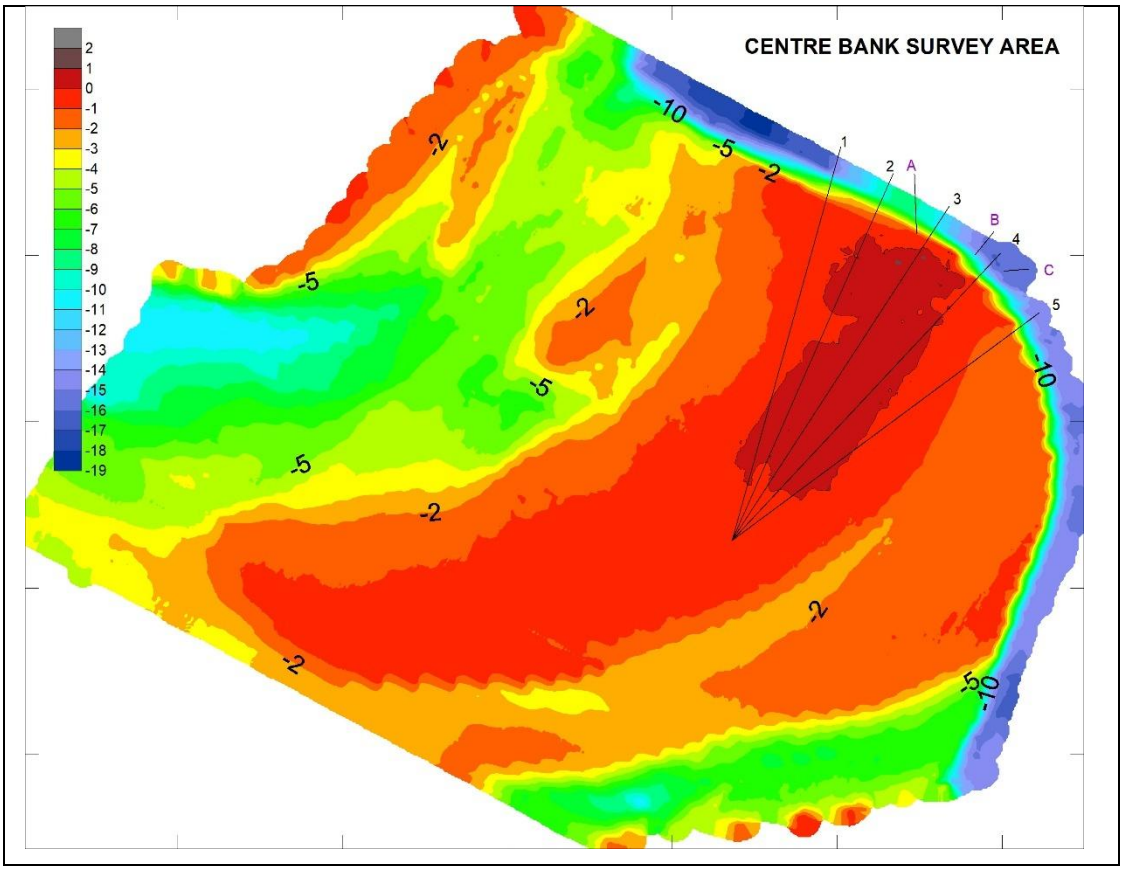



*Figure 42 – Contour map of Te Paritaha (Centre Bank) showing the locations of batter slope profiles (1-5) and pipi survey locations (A-C).*

The batter slopes for the Cutter Channel provide examples of all these situations. Figure 42 shows the locations of 5 profiles (numbered 1-5) of the batter slope near the junction of the Cutter Channel, Maunganui Roads, and Pilot Bay Channel. Also shown are the locations of pipi monitoring sites located on or near the batter slopes. Capital dredging in 2015-16 deepened (from 12.9 m to 14.5 m) and widened the Cutter Channel and Maunganui Roads. This involved excavation of the batter slopes on the southern side of Cutter Channel and western side of the Maunganui Roads (Figure 43). Note that

[81] Healy, TR, 1985. Field data collection programme and morphological study. Tauranga Harbour Study Parts II & V. Report to the Bay of Plenty Harbour Board.

the capital dredging programme also involved the relocation of most channel markers and buoys along the shipping channels in this area. The main exception is the No.7/P7 mark at the entrance to the Pilot Bay Channel.

Figure 43 shows the edges of the design channel, which involved removal of material along the edges of the flood tidal delta (Te Paritaha). Prior to the capital dredging, a zone of "hard white silty" material was identified at the base of the batter slope along the southern margin of the Cutter Channel (Transects 1-3 in Figure 42). This material is a slightly weathered ignimbrite that can be excavated by a TSHD but supports steep slopes. Transects 3 and 4 are located at the end of the ebb shield, where ebb tidal currents transported sediment northwards towards Pilot Bay before capital dredging. This resulted in an area of accretion that spilt down the batter slope and into the Cutter Channel. Transect 5 is located further away from the ebb shield, but was affected by flood tidal transport of sediment accumulating at transects 3 and 4 before capital dredging.

After the 2016-17 capital dredging, the batter slopes adjusted rapidly to the excavation of lower parts of the slope. The results were that transects 1-3 became more convex and had a steeper average slope than before dredging, while transects 4-5 had a similar shape, but translated by the amount of widening. Figure 44 shows the profiles for transects 2, 3 and 5 (1 & 2, and 4 & 5 are very similar to each other).

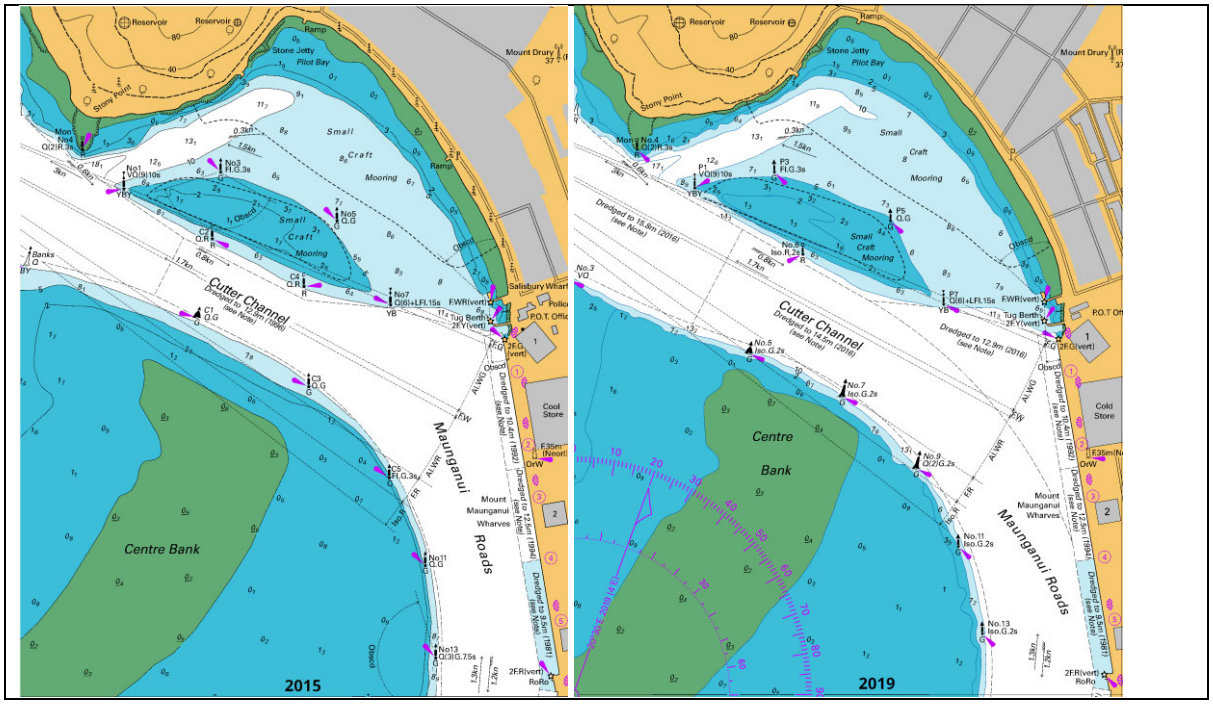



*Figure 43 – Sections of chart NZ5412 showing the junction of the Cutter Channel, Maunganui Roads and Pilot Bay channel in 2015 and 2019.*

All the transects showed accumulation of sediment in the sediment resulting in shallower depths than the 12.9 m design depth. This sediment was removed by maintenance dredging when the extent of shoaling became too great, particularly between transects 3 and 5. Note that the removal of sediment by maintenance dredging did not affect the adjacent batter slope.

After the capital dredging stable slopes were established at transects 1-3, while transects 4 and 5 showed accumulation of sediment at the base. This sediment accumulation is not associated with erosion of the batter slope, and is due to the sediment entering the channel from the ebb shield as before.

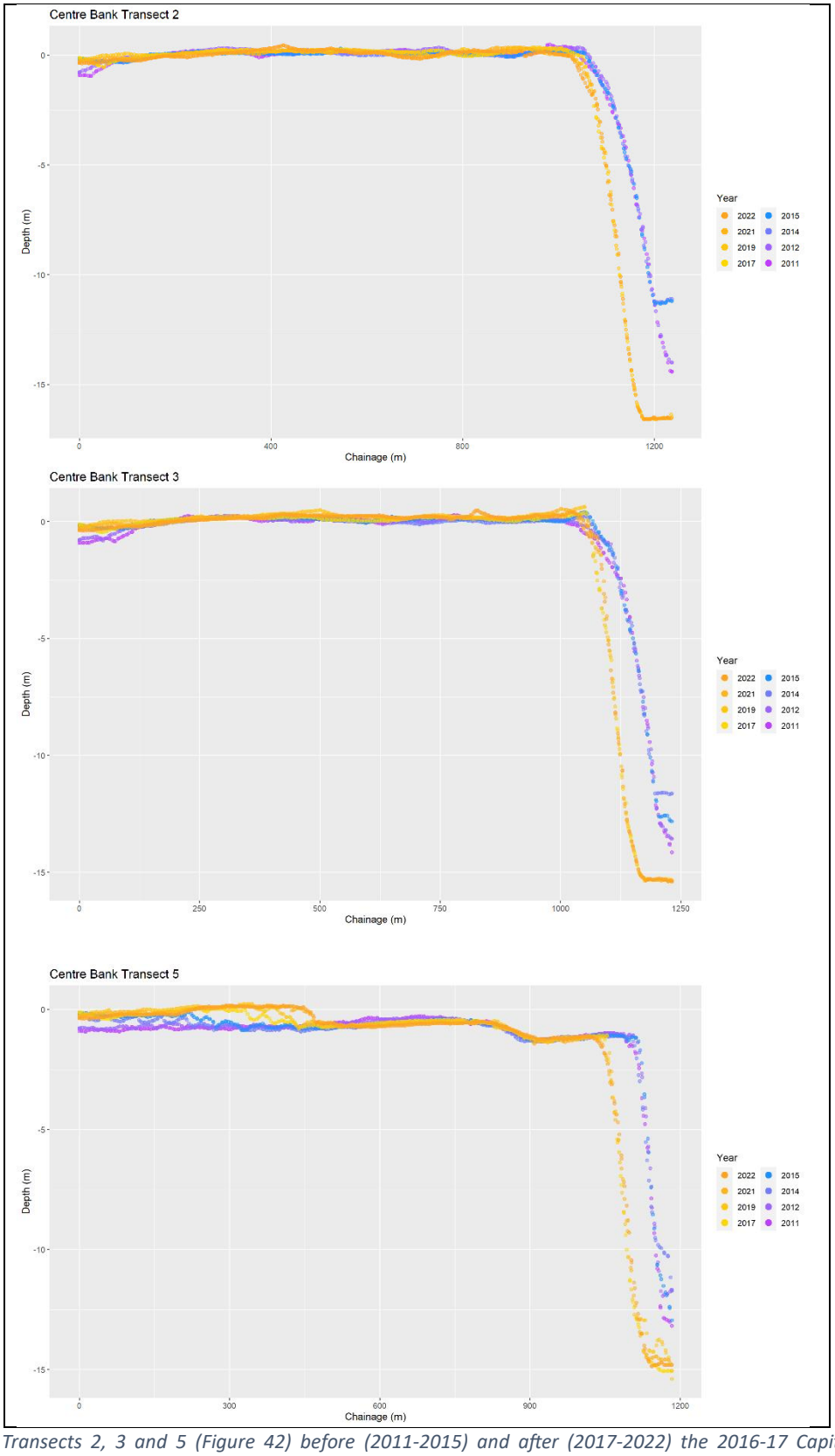



*Figure 44 – Transects 2, 3 and 5 (Figure 42) before (2011-2015) and after (2017-2022) the 2016-17 Capital Dredging Programme showing the changes to the batter slopes along the margin of Te Paritaha.*

Considering all the shipping channel areas without structures, the consistent pattern is a steepening of the batter slope as illustrated by transects 2 and 3 in , unless there is accretion due to movement of

sediment into the channel from the adjacent shallows. With a supply of sediment, the batter slope tends to retain the pre-dredging gradient, but requires maintenance dredging to remove sediment accumulating at the base of the slope.

While there was some loss of the margin of Te Paritaha due to the channel widening, as shown in  and transect 5 in , accretion continued along the Lower Western Channel and Otumoetai Channel margins () so that the overall area of the flood tidal delta increased. The post-dredging batter slope adjustments discussed above, had negligible impact on the extent of Te Paritaha, or the trend of shoaling that has been occurring since the 1852 hydrographic chart was surveyed.

Berthot et al (2024[82]) undertook an analysis of the shoreline movement of the Matakana Island shoreline focusing on Panepane. They included examination of high-resolution aerial photographic images from 1943-2023, analysis of satellite imagery from the 1990s to 2023 using CoastSat[83] software, and numerical modelling using the one-line ShorelineS model. This model is driven by wave processes using wave conditions from the SCHISM/WMM model simulations, and sea level rise via the Bruun Rule. The model did not include the effects of tidal currents, which may be more important close to the tidal inlet than wave induced longshore transport. Hence, Berthot et al (2024) also undertook an empirical analysis that combined wave and tidal currents to assess longshore sediment transport.




*Figure 45 – Transects used to assess shoreline movement from CoastSat analysis of shoreline positions from satellite images by Berthot et al 2024).*

Recent shoreline movement between 2000 and 2024 was assessed from the CoastSat extracted shoreline positions for a series of transects along the Matakana Island shoreline (Figure 45). The length

[82] Berthot A, Cussioli M, & Carle E, 2024. Shoreline change assessment, Report prepared for Port of Tauranga, MetOcean Solutions, December 2024. 66 p.
[83] https://github.com/kvos/CoastSat

of coast covered is longer and includes more data (2000-2024) than that included in the analysis of de Lange (2024), which corresponds with transects 2-6 in Figure 36 and only covers 2016 to 2024. The shoreline was defined as the boundary between water and sand (raw data in Figure 36), which was then adjusted for the tidal elevation at the time of the image (tidally-corrected data in Figure 36). This differs from the shoreline digitised from high resolution aerial photographs, which was the boundary between vegetation and sand. This can result in large differences in recorded shoreline positions in areas with poor vegetation coverage such as the spit at Panepane (Figure 45).

Figure 46 shows the raw and tidally corrected shoreline positions as departures from the long-term mean shoreline position (1943-2023) for the transects in Figure 45. The transect furthest from the tidal inlet (Matakana 8) shows a trend of slow erosion starting in late 2005, which slows down around 2014 within little change between 2016 and 2024. Transects Matakana 4 and 6 both show an erosion trend over the entire time series, although the rate of erosion is initially faster at Matakana 4. The rate of erosion increases towards 2024 for both transects, although the timing of rapid increase differs. Matakana 6 underwent an increase in erosion rate in 2020, after a period of relative stability from 2012 to 2020, and continued to erode until the end of the time series in 2024. The rate of erosion at Matakana 4 was negligible between 2013 and 2018, and increases rapidly resulting in the highest rate of erosion observed. The erosion rate slowed from 2021 until 2024.

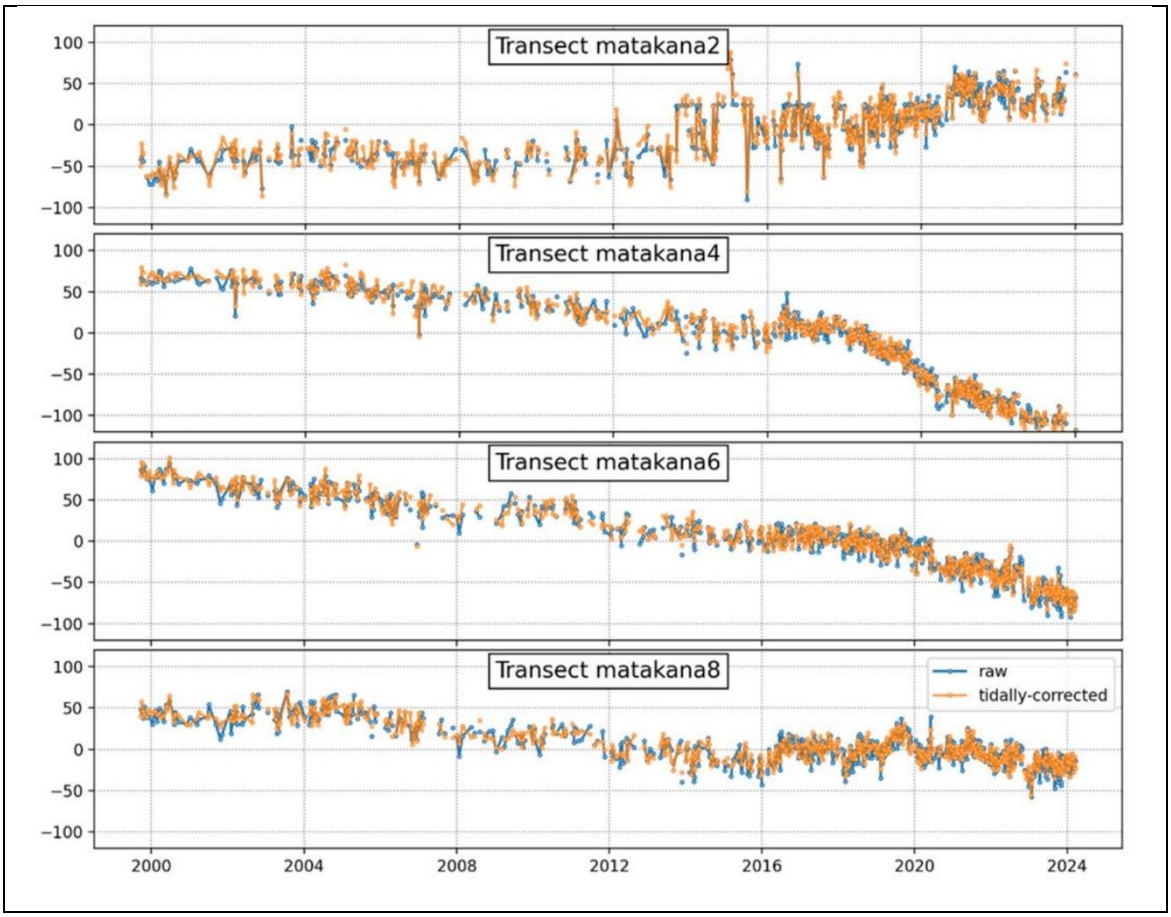



*Figure 46 – Time series of raw and tidally corrected shoreline positions relative to the long-term mean shoreline position for the transects in Figure 35. Capital dredging occurred during 2015-16. (Figure 4-7, Berthot et al, 2024)*

Transect Matakana 2 is located inside the harbour entrance, and shows an overall trend of accretion. However, there was little change in shoreline position from 2000 to 2013, followed by accretion from 2013 to 2021, and relative stability since. The general direction of longshore sediment movement in

the area analyzed is towards the tidal inlet, with accumulation at the spit tip particularly on the inner margin.

The results of the analysis of shoreline positions are consistent with wave-induced erosion of the beach and dunes, and transport of eroded sediment into the harbour as explained by de Lange (2022[84], 2023[85], and 2024). de Lange (2022) showed the relative movement of different depth contours (Figure 47), where the only contour movement that coincided with the 2015/16 Capital Dredging Campaign was the 0 m depth (drying line) contour at transect XS5. This is located close to transect Matakana 6 in Figure 46, which doesn't show any shift in shoreline position at that time.

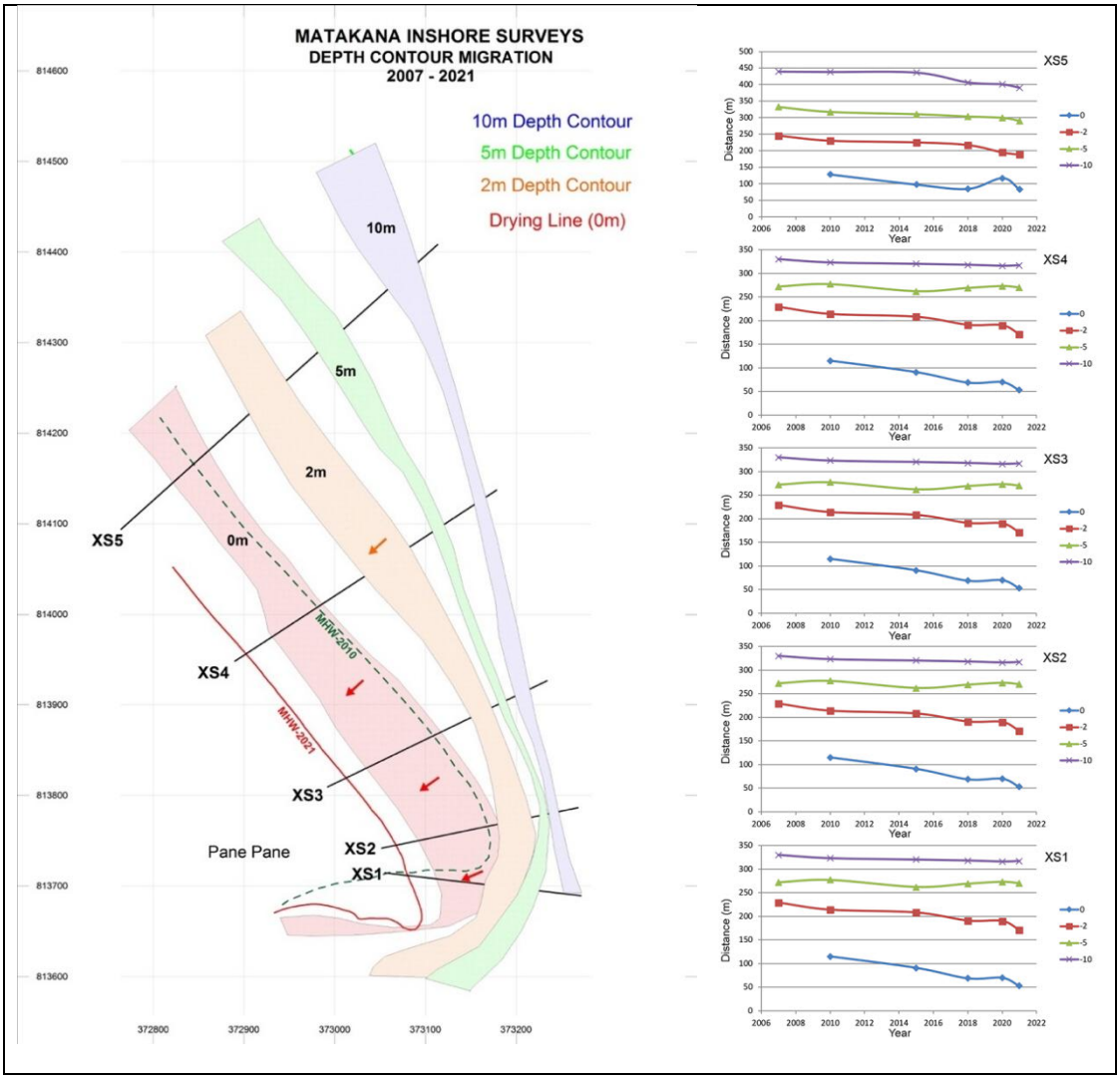



*Figure 47 – Migration of selected depth contours at Panepane, Matakana Island, between 2007, before capital dredging, and 2021, after capital dredging. Left-hand image is a plan view with the shaded areas representing the maximum excursions for each depth contour, while the right-hand images are time-series of excursion distances for the transects XS1-5. Figures and data provided by Greg Cox, GJC Consulting.*

de Lange (2023) suggested that the patterns of erosion and accretion at Panepane were associated with ENSO climate variability, with erosion occurring during La Niña. Figure 6 shows the different wave height patterns across the ebb tidal delta and along the Matakana Island coast under El Niño and La

[84] de Lange WP, 2022. Morphological changes for south-eastern Matakana Island (Panepane) and Matakana Banks (ebb tidal delta) 2016-22. Report prepared for Port of Tauranga Ltd, August 2022. 15 p

[85] de Lange WP, 2023. Morphological changes for south-eas tern Matakana Island (Panepane) and Matakana Banks (ebb tidal delta) 2016-23. Report prepared for Port of Tauranga Ltd, November 2023. 27 p

Niña winter conditions as reported by Watson and Berthot (2024a). This shows increased large waves reaching Panepane during La Niña conditions, and changes to the dominant wave approach directions.

Berthot et al (2024) modelled the shoreline response to La Niña conditions, using a year of wave forcing derived from each of the bathymetric scenarios modelled by Watson and Berthot (2024b). The shoreline model predicted that longshore sediment transport would be towards the southeast (towards the tidal inlet) under all bathymetric conditions (Figure 48). This would result in some erosion at the northwest end (near wave site W1), which may be an artefact of the model boundary conditions. The longshore transport results in slightly different spit configurations for the various bathymetric scenarios (Figure 48), with the 2015 and 2016 spits matching each other, and the same for the 2023 and future spits. This appears to be due to differences in the bathymetric grids as they are derived from surveys that captured the shape of the spit in 2015, 2016 and 2023, with the future spit modelled using the 2023 bathymetry.

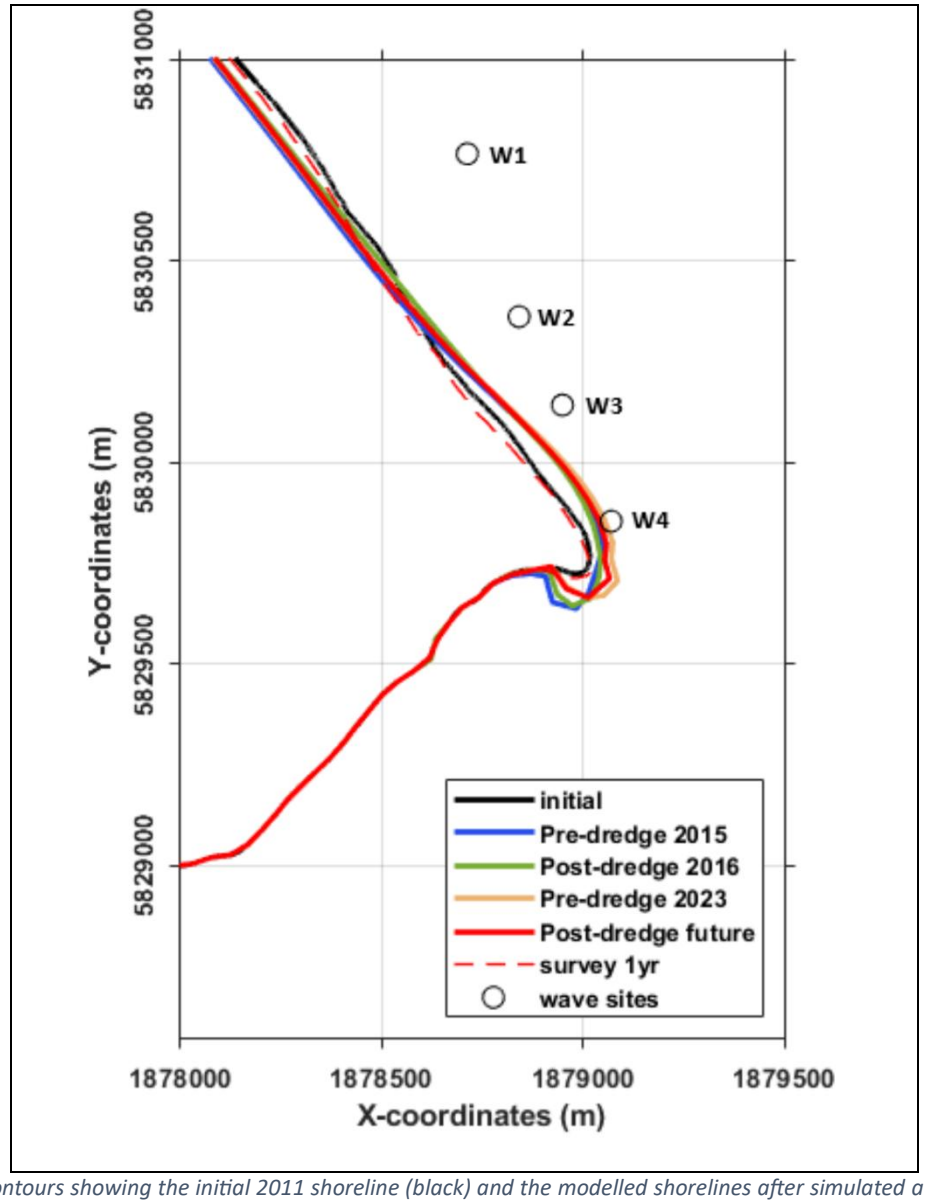



*Figure 48 – Contours showing the initial 2011 shoreline (black) and the modelled shorelines after simulated a year of waves in ShorelineS for pre-dredge 2015 (blue), post-dredge 2016 (green), pre-dredge 2023 (yellow) and post originally proposed 2026 capital dredging (red) wave scenarios. The red dashed line is the 2012 survey for reference. Black circles indicate location of wave parameters extracted from the SCHISM/WMM model (Figure 4-16, Berthot et al, 2024)*

Overall, the modelled shoreline response did not match the observed changes, although the incorporation of shoreline changes in the model bathymetries is a complication that may make the model predictions unreliable. The interpretation of the results is that dredging may reduce the wave heights in the area modelled, which may reduce the likelihood of erosion. However, Berthot et al (2024) recognize that a simple one-line model driven only by wave conditions may not fully capture the shoreline dynamics that may be response to other factors. There was no assessment of shoreline response to El Niño conditions for example, although this would have involved the same bathymetric scenarios and the issues raised above.

Berthot et al (2024) noted that there is a persistent flood-directed tidal residual current along the Matakana Island foreshore towards the harbour entrance. This could transport sediment entrained by waves away from the beach and into the harbour. The empirical modelling showed that if the deeper offshore tidal currents extended into the surf zone (possibly during large wave events when the surf zone width increases) the tidal currents would affect the direction and magnitude of longshore sediment transport. This influence was most important for sites W2-W4 (Figure 48). Overall, it would increase the transport of sediment into Te Awanui, but it could also reverse the direction of transport under some conditions. Overall, Berthot et al (2024) concluded the effect of originally proposed 2026 capital dredging could be a reduction in wave energy near Panepane, resulting in lower longshore sediment transport and reduced potential for erosion. This is the opposite of the trends evident from their shoreline analysis, and reported by de Lange (2022, 2023, 2024).

de Lange (2023) noted that this flood-tide directed current residual along the Matakana Island shoreline should produce a flood marginal channel (Figure 39 ), but this is not a permanent feature for the Tauranga tidal inlet. It is possible that when the longshore sediment transport rate from further west along the Matakana Island coast is sufficiently high, the rate of deposition exceeds the rate of removal so this channel is buried and the shoreline accretes. Figure 1 shows a series of aerial photographs and Google Earth satellite images that display erosional features that are rarely present along the Matakana Island ocean shoreline; specifically large erosional arcuate embayments and shore parallel flood marginal channels.

Stephens et al (1999)[86] discuss the formation of arcuate embayments along the southern end of Waihi Beach near the Katikati ebb tidal delta. They considered different mechanisms proposed in the literature for similar features worldwide, and concluded that the Waihi Beach embayments were due to wave focusing by submarine features offshore. These embayments were not always present, but once formed they took longer to recover than other erosional features because they modified the nearshore circulation. At Waihi Beach they are associated by large scale rip currents (megarips).

The erosion at Panepane begin with the formation of an arcuate embayment at the location marked by the yellow arrow in the satellite image for June 2018 (Figure 49), which was associated with the stronger than normal flood-directed flow along the shoreline towards Panepane (white open arrow). Subsequently a series of arcuate embayments developed to the west of this location (November 2023 image, Figure 49). There is no data available to indicate if there was a progressive or simultaneous development of these embayments between the two images. However, they all appear to associated with wave focusing by swash bars on the ebb tidal delta. Since this does not normally occur, it is possible that the focusing is in response to the movement of the swash bars, a change in the wave approach direction for large storm waves, or both.

[86] Stephens SA, Healy TR, Black KP, & de Lange WP. (1999). Arcuate duneline embayments, infragravity signals, rip currents and wave refraction at Waihi Beach, New Zealand. Journal of Coastal Research, 15(3), 823-829.

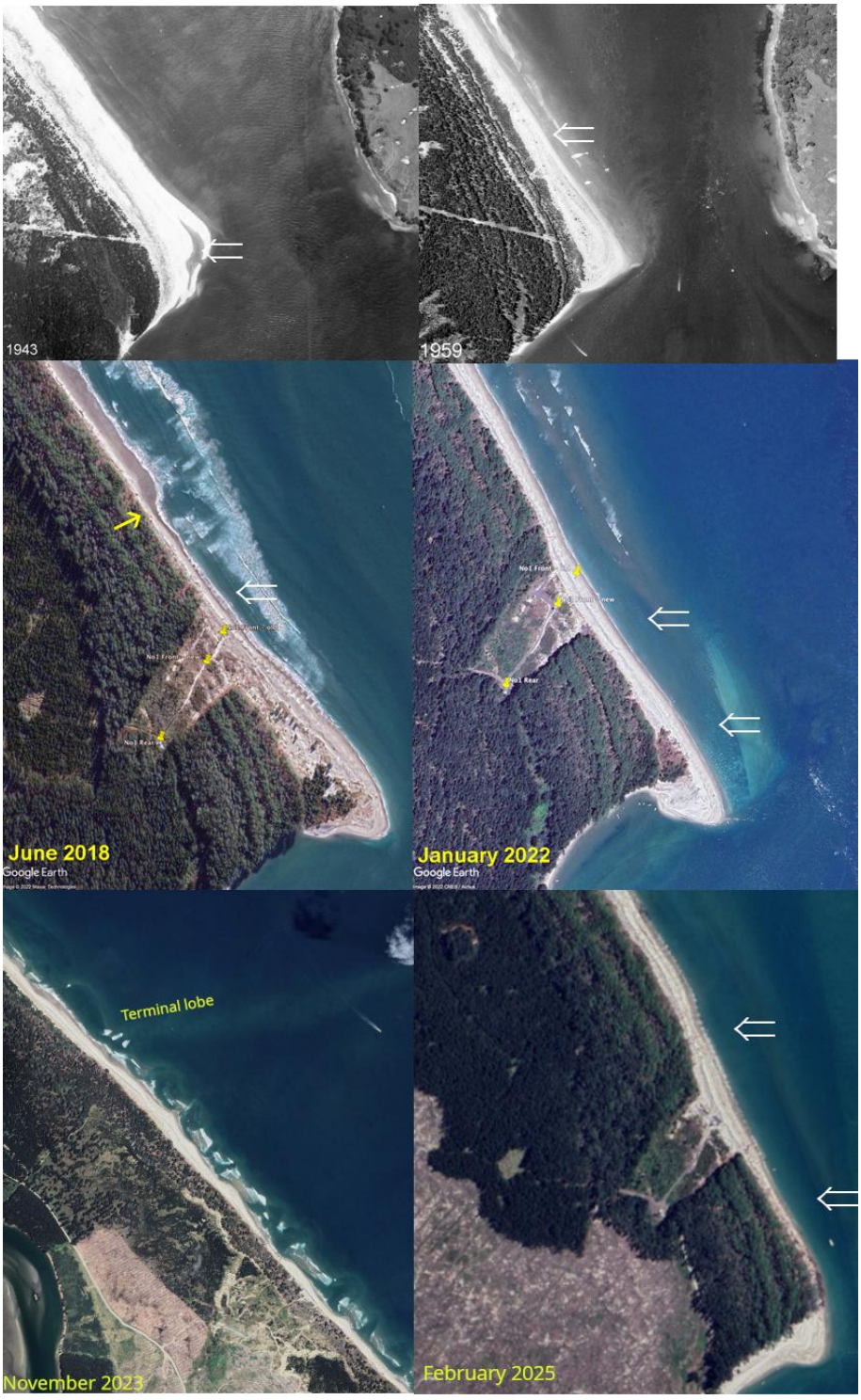



*Figure 49 - Aerial photographs for 1943 and 1969, and Google Earth images for June 2018, January 2022, February 2025 of the entrance to Tauranga Harbour showing changes to Panepane; and a Google Earth image for November 2023 for the shoreline adjacent to the western side of the ebb tidal delta. Open white arrows mark the positions of the marginal flood channel on the seaward side of the spit, and the yellow arrow on the June 2018 mars and arcuate embayment associated with swash bar focussing wave energy.*

Also subsequent to 2018, the enhanced shoreline flood flow led to the progressive development of a flood marginal channel along the shoreline (open white arrows for January 2022, and February 2025). While this channel does not directly erode the upper beach and dunes along the shoreline, it provides

additional longshore flow to remove sediment eroded by waves. This reduces the amount of sediment available for post-storm beach recovery, which results in more erosion in following storm events.

The formation of a flood marginal channel was also evident in the 1959 aerial photograph, while the 1943 aerial photograph shows the last stages of infilling of the flood marginal channel. Closure of this channel reduces the volume of longshore transport associated with wave disturbance of the beach sediments.

Based on the timing of periods of arcuate embayment and flood marginal channel appearance along the coast between Waihi Beach and Papamoa suggests that the ENSO climate variability affects the extent of beach/dune erosion and overall longshore transport along Matakana Island, which may explain why the Katikati and Tauranga ebb tidal deltas and associated spits undergo similar changes at the same time (de Lange, 2023).

Matthews (2024[87]) examined the historical changes for the Katikati flood tidal delta using aerial photographs and satellite imagery, combined with a shallow seismic survey. Her results suggest that there are similar changes occurring at Katikati that coincide with the changes in the Lower Western Channel at Tauranga. Unfortunately, there are limited historic hydrographic surveys for the Katikati Basin of Te Awanui, making it difficult to quantify the changes there.

de Lange (2025)[88] examined the factors contributing to erosion of the Matakana Island shoreline, and a significant increase in the maintenance dredging volumes within No.1 Reach and western Cutter Channel, near Panepane Point. This included an analysis of the tidal currents measured by an ADCP mounted at No.2 Tanea Bouy since 2003. A comparison of the tidal current constituents used to define the tidal hodographs (Figure 27) between the most recent available data (2024-2025) and earlier studies by Vennell (1999; 2012; 2017)[89,90,91] found that there was no significant change in the tidal current behaviour, consistent with the findings of the earlier studies. Figure 40 shows the annual distribution of 1%, 5% and 50% percentiles of the ebb (negative) and flood (positive) current velocities for 2003 to 2025.

The extreme (tail) percentiles are quite variable, but the median (50%) are very consistent, albeit with a slight trend for decreasing velocities following the capital dredging in 2015-2016. This decrease is consistent with the results of the numerical modelling discussed above. The variability for the extreme (peak) tidal current velocities was in response to weather events and tsunamis.

Figure 51 shows a high resolution (15 s sampling interval, ±0.05 mm water level) dataset collected by GeoNet from a tsunami monitoring gauge near Salisbury wharf (Station TAUT). The raw data collected were detided using the *tidem* routine in the R package OCE. Due to the short record the residual water levels retain short-period tidal oscillations associated with overtides present in Te Awanui. Mean sea level atmospheric pressure data from the Tauranga Airport AWS, was used to calculate the sea level

[87] Matthews, E, 2024. Seismic reflection characterization and geomorphology of the Katikati Basin, Te Awanui (Tauranga Harbour), Aotearoa New Zealand. MSc thesis, The University of Waikato, Hamilton. 90 p.
[88] de Lange, WP, 2025. Recent sediment accumulation at junction of Entrance Channel (No.2 Reach) and western Cutter Channel. Report to the Port of Tauranga Ltd, September 2025. 87 p
[89] Vennell, R, 1999. Prediction of tidal streams in the Entrance to Tauranga Harbour from ADCP measurements. University of Otago, Technical Report. Prepared for Port Tauranga Ltd. 48 pp.
[90] Vennell, R, 2012. Tidal current maps, Port of Tauranga. Acoustic Doppler Current Profiler Surveys 2007. Ocean Currents Ltd. Prepared for Port of Tauranga Ltd. 211 pp.
[91] Vennell, R, 2017. Tidal current maps, Port of Tauranga. Acoustic Doppler Current Profiler Surveys 2016. Ocean Currents Ltd. Prepared for Port of Tauranga Ltd. 266 pp.

response to changes in atmospheric pressure (referred to as the Inverse Barometric Effect - IBE), which is approximately half the storm surge response if the wind stress is directly onshore.

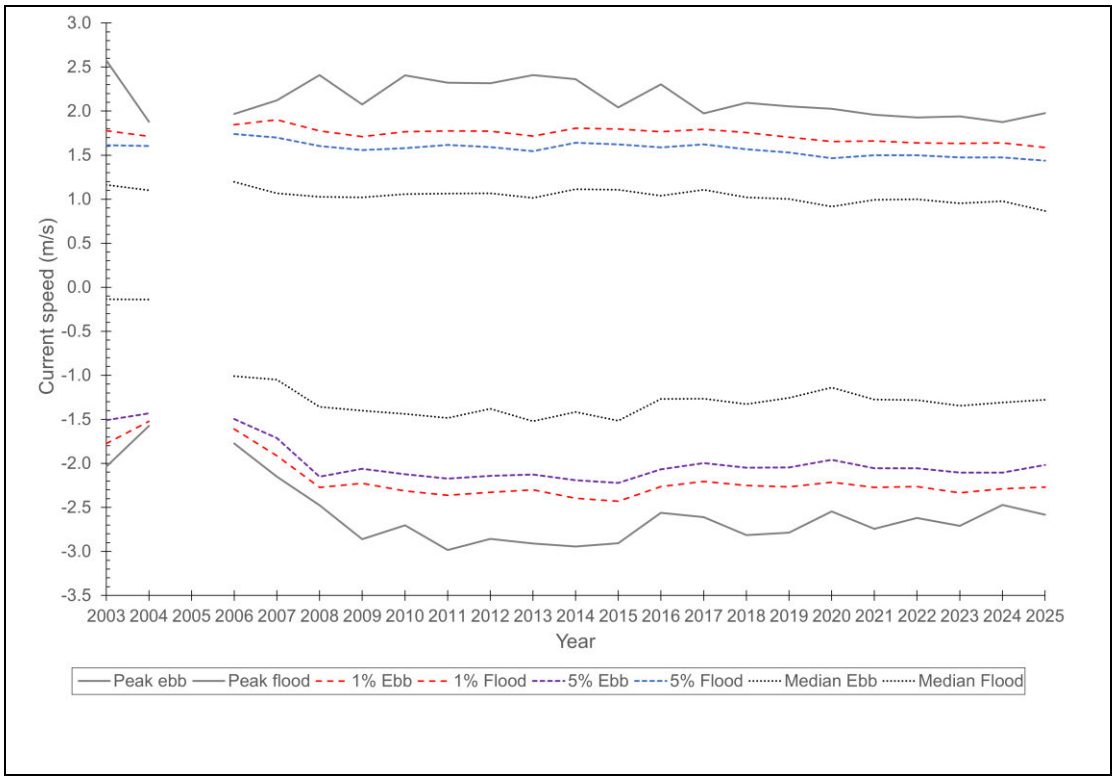



*Figure 50 - Summary time series of statistics for the flood (positive) and ebb (negative) speeds recorded by the Port of Tauranga ADCP. Before 2006, the ADCP was bottom mounted within the channel. From 2006 to 2025, a rotating series of ADCPs were buoy mounted at No.2 Tanea on the eastern side of the channel.*

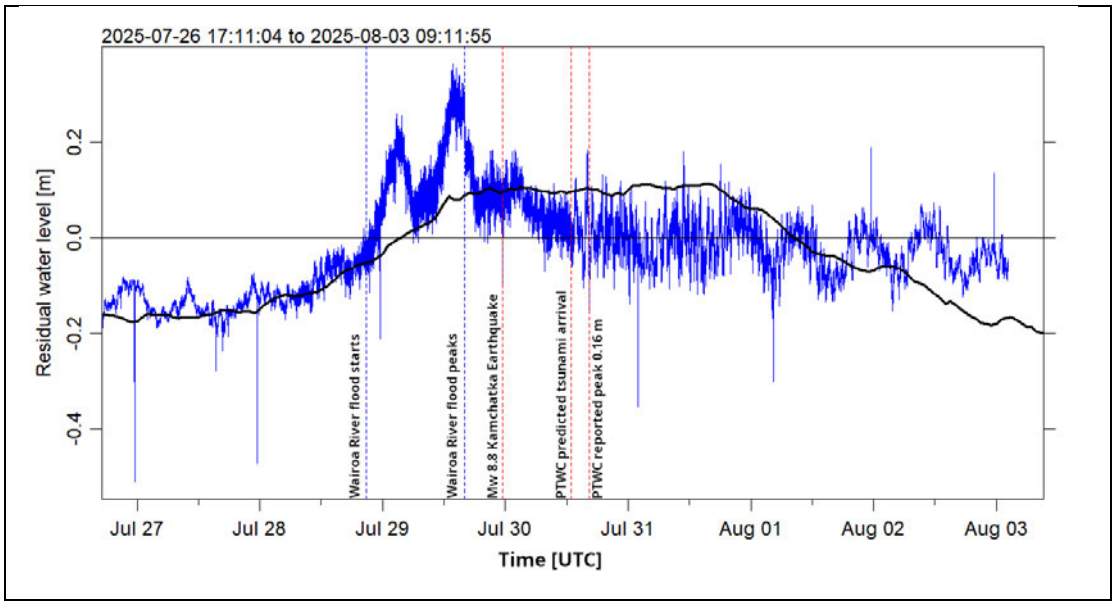



*Figure 51 - A time series of water elevations recorded by the GeoNet station TAUT near Salisbury Wharf, Mt Maunganui, showing the changes in mean water level due to the inverse barometric effect (IBE - black line), and the timing of the flooding in the Wairoa River and the 29 July 2025 Kamchatka Tsunami (see text for further explanation).*

The short record in Figure 51 includes the effect of a storm surge, freshwater flooding, and a tsunami. The Wairoa River above Ruahihi recorded 3 flood events peaking at 134 $m^3s^{-1}$ on 11 July NZST, and 790 $m^3s^{-1}$ on 30 July 2025 NZST. These 2 events correspond to the higher residual water levels on 11 and 30 July in Figure 51. The Pacific Tsunami Warning Centre (PTWC) predicted tsunami arrival times

(UTC) at Mt Maunganui and Port of Tauranga were 12:39 and 12:52 on 30 July. A peak tsunami amplitude of 0.16 m was reported by the PTWC for the Port of Tauranga at 16:22 UTC on that day.

The IBE (black line) accounts for most of the longer-term deviation from mean sea level. The timing of the onset and peak flood above Ruahihi are marked. During this period rainfall occurred directly into the harbour, as well as increasing freshwater discharge, increased water levels within the harbour during flood tides. The excess water largely drained from the harbour during ebb tides. This produced the two large peaks before the Kamchatka Earthquake occurred. Elevated discharge from the Wairoa River continued until 7 August 2025 UTC (not marked), producing smaller oscillations as the discharge decreased and no rainfall occurred. Flood water that didn't drain out of the harbour during ebb tides probably contributes to the deviations between residual sea level and the IBE sea level.

The Kamchatka Tsunami arrived 20-30 minutes after the arrival time predicted by PTWC modelling, but the peak tsunami height matches the 0.16 m reported by the PTWC. The tsunami decayed quite rapidly and becomes impossible to visually and numerically distinguish from the other oscillations in the record within 24 hours.

Figure 52 shows a tidal current analysis on the ADCP data corresponding the water elevation record in Figure 51, using the MATLAB package *Utide*. This analysis treats ebb currents as positive and flood currents as negative (the opposite of Figure 39). Note that the ADCP was replaced around noon on 1st August, as part of the normal maintenance schedule. Unfortunately, the 3 ADCPs used in rotation by the Port of Tauranga, do not measure exactly the same directions, which results in the apparent shift in the east velocities around noon on 1st August.

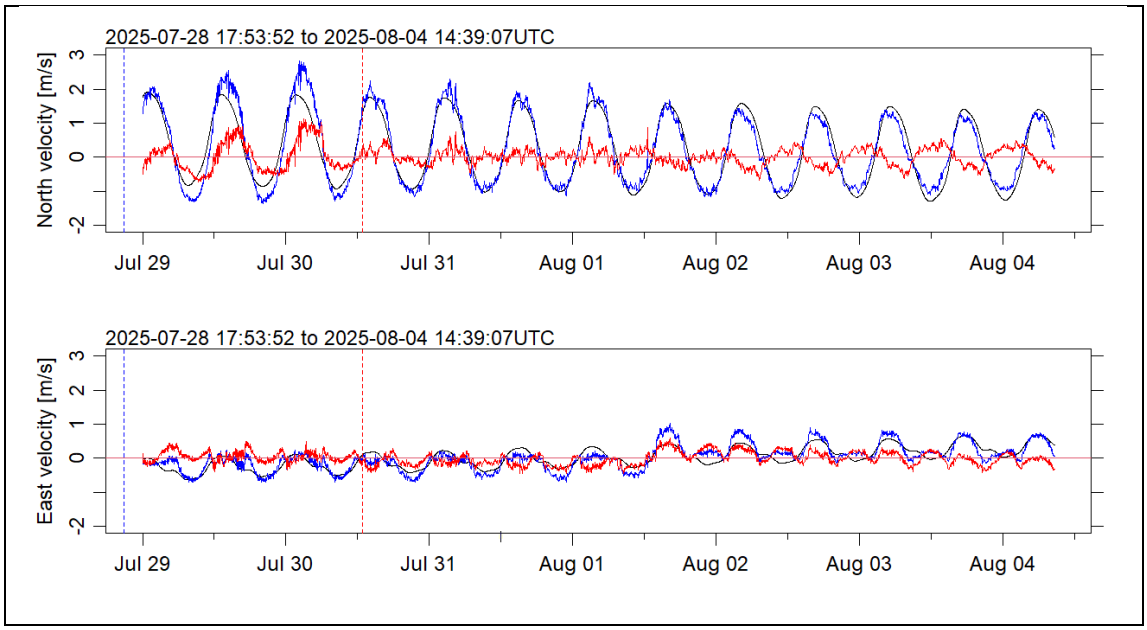



*Figure 52 - North and East current vectors for No.2 Tanea Buoy during the period 29 July to 4 August 2025: blue = ADCP measured; black = predicted; and red = residual. Vertical blue and red dashed lines mark the onset of flooding in the Wairoa River, and PTWC predicted Kamchatka Tsunami arrival time respectively.*

Due to the short record length only 7 tidal constituents could be extracted, and the residuals (red line in Figure 52) still contain a significant tidal component. The largest current residuals occur during the increasing freshwater discharge before the peak of the Wairoa River flooding (Figure 51). The highest velocities occur during the ebb tide, particularly after mid-tide causing the measured peak velocities (blue curve) being larger and later than predicted by the tidal constituents (black curve) for the N-S velocities (top panel, Figure 52). The smaller increase in flood velocities represents the influence of the storm surge elevating water levels on the ocean side of the inlet. The tsunami produced short

duration oscillations in the tidal velocities that had almost the same magnitude effects on the ebb and flood currents.

The small changes in tidal characteristics predominantly due to weather conditions (atmospheric pressure, wind and rainfall) indicate that other factors may be contributing to erosion/accretion of the Matakana Island shoreline and maintenance dredging volumes within the shipping channels.

de Lange (2025) examined the role of waves on the sediment transport of the Tauranga tidal delta system. He found that the system varied between tidally dominated and wave dominated predominantly in response to interannual and decadal scale changes in wave conditions. As discussed above in relation to the numerical modelling studies by MetOcean Solutions, the harbour and offshore hydrodynamics vary seasonally, and response to the ENSO. The longest record of directional wave data near the Tauranga Entrance is from the Bay of Plenty Regional Council wave buoy offshore from Pukehina (Figure 53). de Lange (2025) also shows seasonal and annual results for wave measurements at A Beacon, and the Pukehina and Bowentown wave buoys.

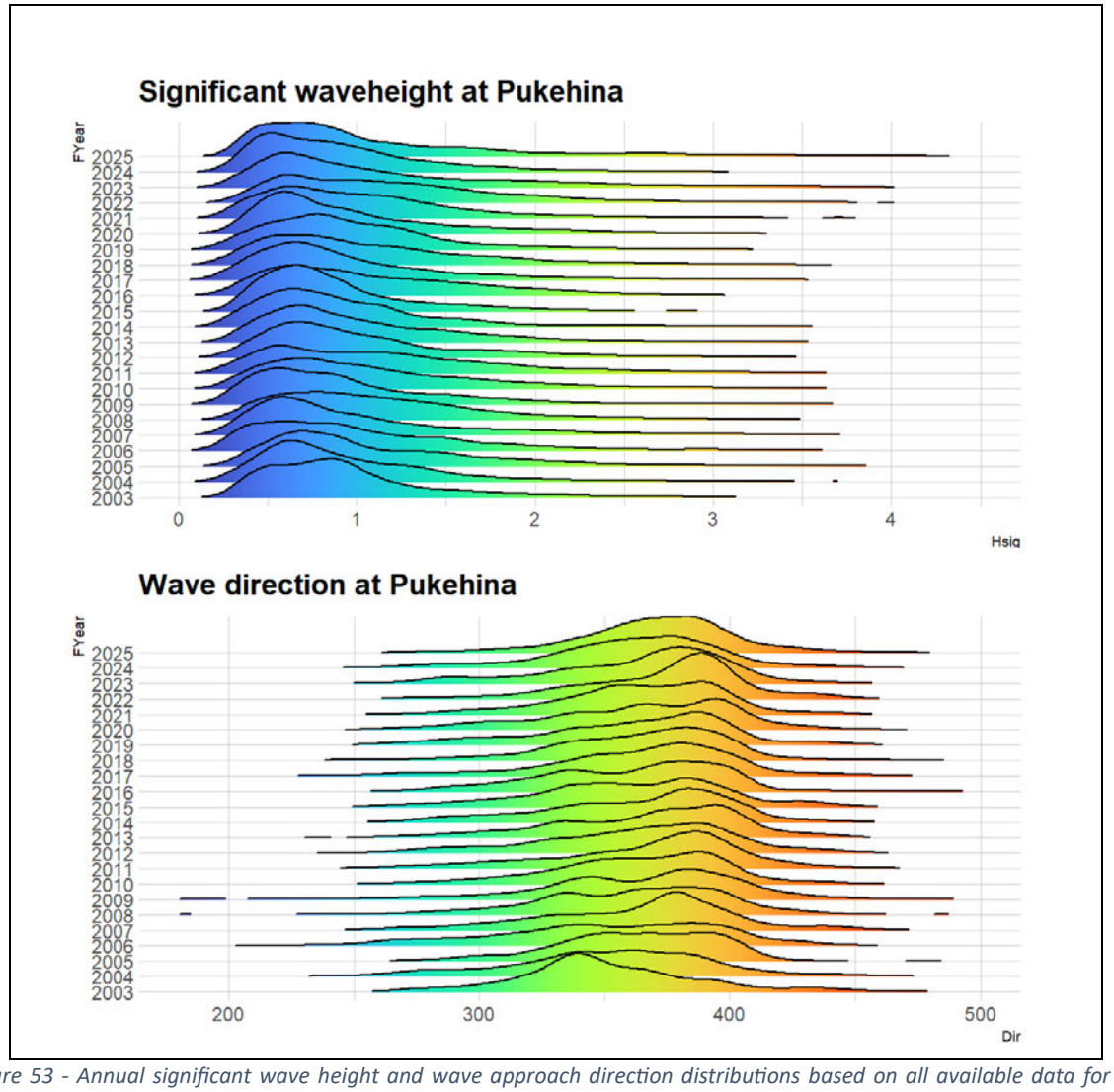



*Figure 53 - Annual significant wave height and wave approach direction distributions based on all available data for the Pukehina wave buoy. To make it easier to visualise the direction values have been adjusted by adding 360° to recorded directions less than 180°.*

There are seasonal changes evident in the western Bay of Plenty wave climate, with the largest waves tending to occur January to April, with a maximum usually in February. These are associated with

extratropical storms (cyclones) that have transitioned from tropical cyclones. However, there are also peaks in wave heights during winter and early spring with a maximum in July, which are associated with Tasman and mid-latitude depressions. However, the seasonal changes are much smaller than those experienced on the west coast of New Zealand, and smaller than those between East Cape and Steward Island on the east coast.

The interannual and decadal scale changes are larger, particularly with respect to wave approach direction (Figure 53). This reflects the variation in the frequency, magnitude, and track of tropical cyclones transitioning into the New Zealand region, and the changes in dominant wind directions in the Bay of Plenty associated with ENSO. Figure 54 shows the monthly Troup Southern Oscillation Index (SOI) between January 1970 and August 2025. This index indicates the ENSO state: El Niño SOI<-0.7; neutral -0.7<SOI<0.7; and La Niña SOI>0.70. Also shown in Figure 54 are periods when there was erosion of the ebb tidal delta involving the loss of swash bars and lowering of the swash platform, and erosion of the Matakana Island shoreline near Panepane Point.

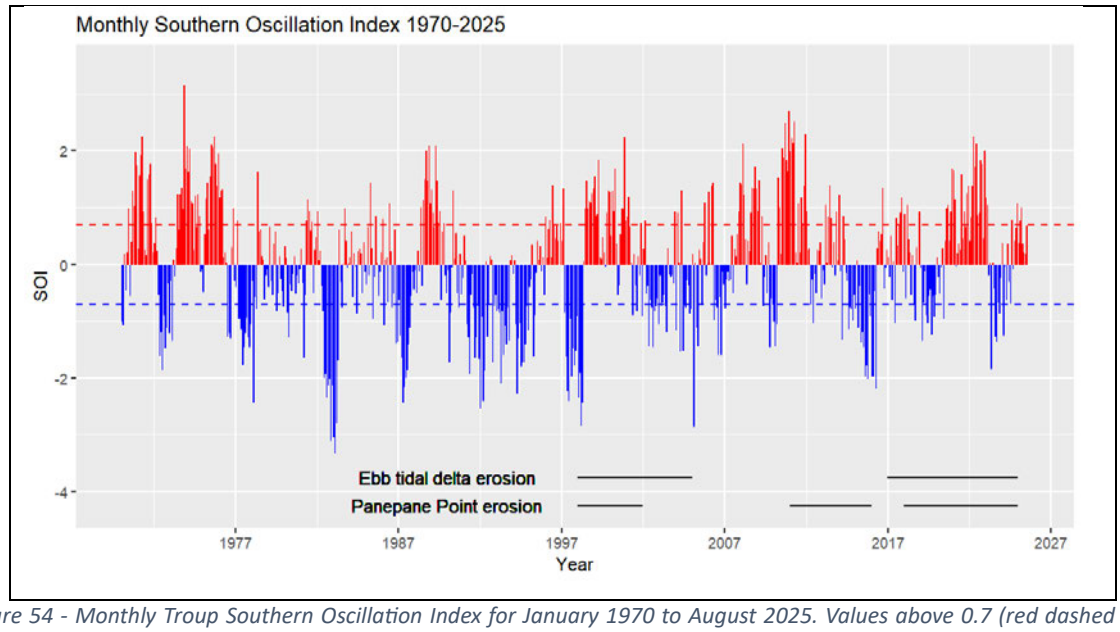



*Figure 54 - Monthly Troup Southern Oscillation Index for January 1970 to August 2025. Values above 0.7 (red dashed line) correspond to La Niña conditions; below -0.7 (blue dashed line) correspond to El Niño conditions; and between 0.7 and -0.7 correspond to neutral conditions. The calendar years with periods of erosion for the ebb tidal delta and Panepane Point shoreline are shown. SOI data from Australian Bureau of Meteorology[92].*

The historical erosion events are associated with periods of increased La Niña conditions in terms of duration, but not necessarily in terms of intensity (de Lange, 2025). Wang et al (2024)[93] investigated the relationship between tropical Pacific interannual to interdecadal variability and the duration of ENSO extremes. Due to the climatic impacts and teleconnections associated with multi-year La Niña ENSO extremes, they focussed on "super-long" La Niña extremes, where the 3-month running average Niño3.4 index shows La Niña conditions for more than 30 months and falls to more than -1 (Figure 55).

The Niño3.4 index represents the average equatorial sea surface temperatures across the Pacific from about the dateline to the South American coast, whereas the Troup SOI is based on pressure differences between Darwin and Tahiti. Therefore, these indices measure changes in different

[92] https://www.bom.gov.au/climate/enso/indices.shtml#aboutIndices

[93] Wang, R, Ren, H-L, & Liu, M, 2024. Roles of tropical-Pacific interannual–interdecadal variability in forming the super long La Niña events. Climate Dynamics, 62(9), 9117-9132.

parameters on opposite sides of the Pacific Ocean, which can result in different details in the patterns for ENSO phases. However, the overall patterns are similar.

A comparison of Figure 54 and Figure 55 indicates that the erosion events at the Tauranga entrance to Te Awanui are associated with super-long La Niña events. In part this reflects an increase in wave energy, associated with an increase in waves approaching from the NNW sector. The other critical components are the availability of sediment, and the sediment transport patterns over the ebb tidal delta (de Lange, 2025). Tidal inlets act as barriers to longshore sediment transport, commonly trapping sediment resulting in accretion of the tidal deltas, and then episodically releasing sediment for downdrift transport, resulting in erosion. The rates and timing of accretion and erosion depend on the rate of updrift longshore sediment transport, and the frequency and magnitude of episodic events, usually storms, triggering bypassing (de Lange, 2025).

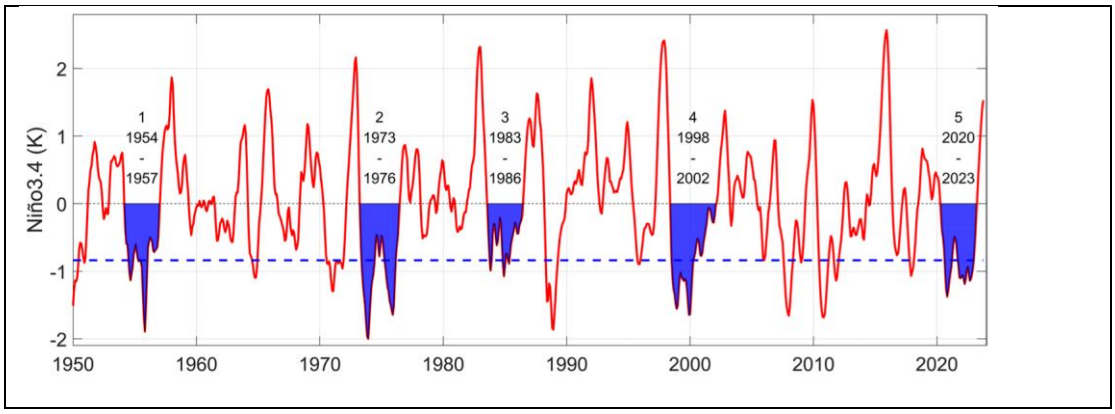



*Figure 55 - Time series of 3-month running average Niño3.4 index between 1950 and 2024. The blue dashed line corresponds to an index of -1 (1 standard deviation), and the blue shaded areas are super-long La Niña events. (Figure 1, Wang et al, 2024).*

Pullig et al (2025)[94] investigated the morphological changes at a headland-controlled tidal inlet in Babitonga Bay, Southern Brazil, which is similar to the Tauranga entrance without a dredged channel. They tracked the morphological changes over 160 years from 1862 to 2021, and developed a conceptual model for the behaviour of the ebb tidal delta (Figure 56). They demonstrated that the volume flux of longshore sediment transport was the main predictor for the behaviour of the inlet, particularly whether there was bar or tidal bypassing. Their model also predicts zones of enhanced accretion associated with different levels of longshore sediment transport.

Allowing for the presence of the Entrance Channel, the findings of Ramli (2016) and the MetOcean Solutions modelling discussed above are consistent with the model of Pullig et al (2025). de Lange (2025) combined all three models for the tidal inlet system, with additional survey data for the ebb tidal delta, and tidal current data from the Tanea No.2 ADCP, to produce a conceptual model for the decadal-scale evolution of the ebb tidal delta.

This model recognises that there is a relationship between the sediment characteristics - including texture (grain size), shape and density – and the mode of sediment transport, and the distance sediment grains are transported. Grains that are very coarse, dense, or have shapes that form imbricated surfaces, may not be transported very far, if at all. Coarse to medium sand grains will tend to move as bedforms, and may only move under more extreme conditions. Fine sands can remain in suspension sufficiently long, particularly in areas of high turbulence, to be carried up to a couple of kilometres. Finer sediments (silts and clays), can remain in suspension with low levels of turbulence, and will be transported the furthest.

[94] Pullig, MC, Klein, AHdF, Pool, L, Alves, DCL, & de Menezes, JT, 2025. Bypassing at a headland-controlled meso-scale tidal inlet. *Geomorphology*, *469*, 109512

This means that, given the tidal asymmetry resulting from the propagation of tidal waves into the harbour and the discharge of freshwater increasing ebb tidal volumes, the Tauranga tidal inlet will export fine sand, silt and clay. The fine sand is deposited on the ebb tidal delta by the ebb jet and associated tidal eddies, while the finer sediment is transported further offshore as a turbid plume. However, the medium and coarse sand tends to be imported into the harbour, primarily as bedload in the shallows close to Panepane Point by a combination of wave-induced entrainment and flood tidal flows. This sediment tends not to be re-entrained once it is deposited on the flood tidal delta (de Lange, 2025).

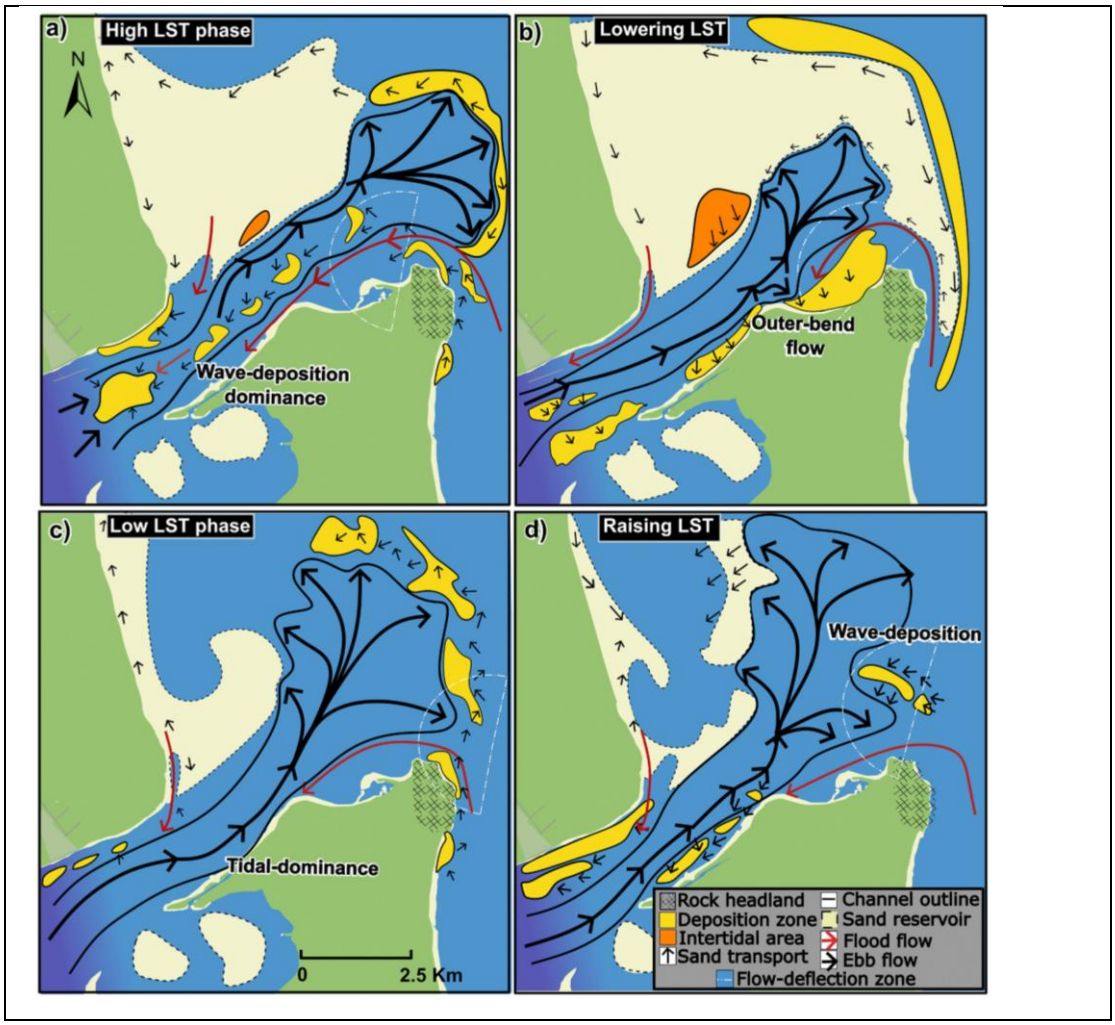



*Figure 56 - Conceptual model for tidal inlet bypassing in the vicinity of a headland in response to changing rates of wave-induced longshore transport (LST). Figure 11 from Pullig et al (2025).*

Over the ebb tidal delta there is a gradient in the available energy to drive sediment transport for both tidal and wind waves. On average, tidal energy is at a maximum at the tidal inlet gorge and a minimum at the terminal lobe, and the opposite for wind wave energy. However, these gradients change over time, resulting in wave-dominated and tidal-dominate extremes (Figure 56). In particular,

- The tidal gradient strengthens with increasing effective tidal range, including: from neap tide to spring tide; from apogean to perigean tides; and with increasing freshwater discharge into the harbour. It also changes spatially with changes to the orientation of the ebb jet;
- The wind wave energy gradient strengthens with increasing wave height, and changes spatially in response to the water depth over the ebb tidal delta (including the size and location of swash bars).

There may also be changes in response to the strength and orientation of winds, but wind-induced currents are generally weak close to shore, but increase further offshore on the inner shelf and probably have little influence on the tidal inlet system. Wind-induced currents do play a role in enhancing cross-shore sediment transport for the open coastline: onshore winds contribute to offshore sediment transport; and offshore winds contribute to onshore sediment transport (de Lange 2025).

The relative influence of the various factors affecting sediment transport within the Tauranga tidal inlet system vary with ENSO state, and the frequency and magnitude of storms. The main effects are as follows (Figure 57):

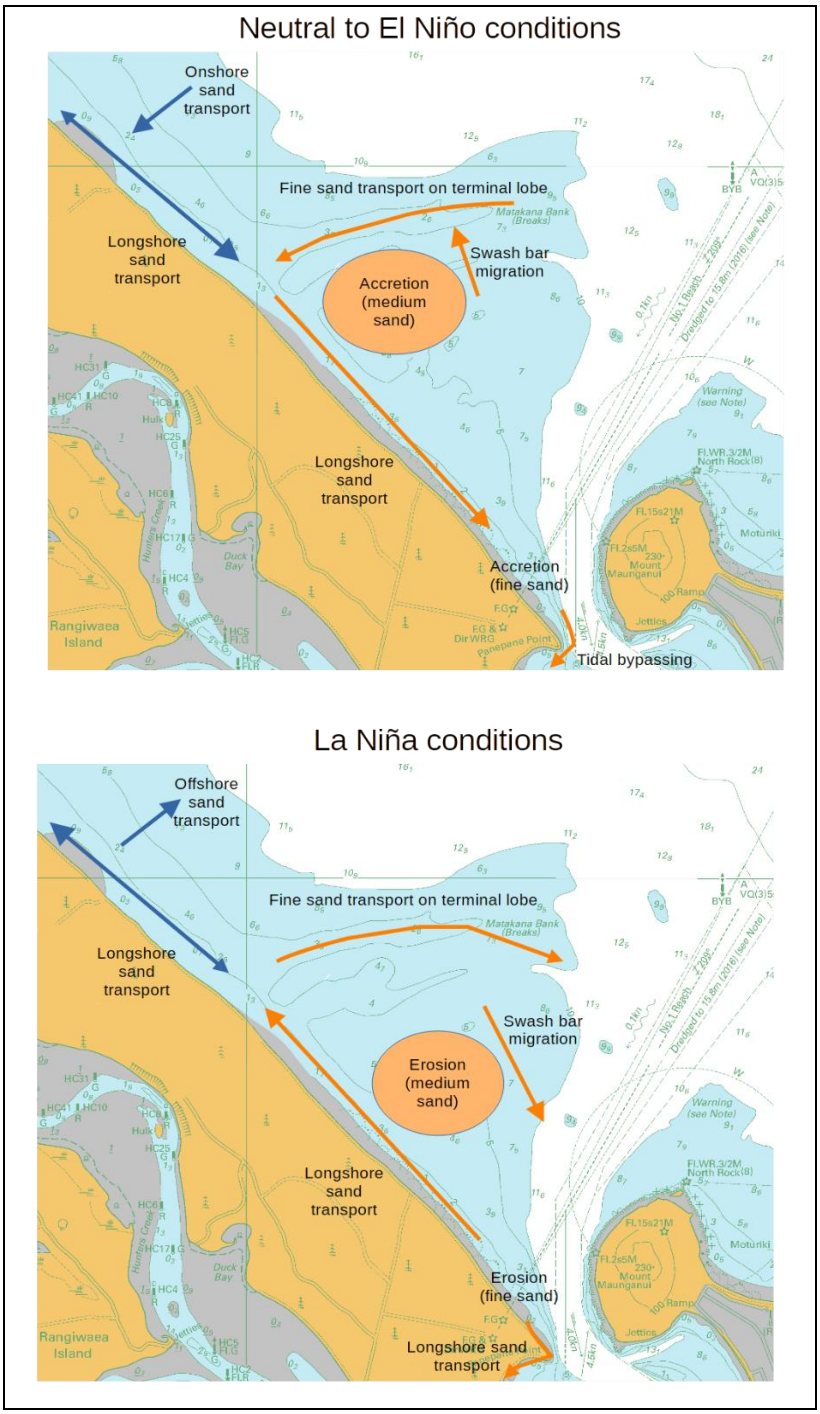



*Figure 57 – Schematic diagrams of the sediment transport patterns and associated areas of erosion and deposition associated with different ENSO patterns.*

## 5.1 Neutral to El Niño conditions

Neutral ENSO is the most common condition for the Tauranga tidal inlet system (SOI between -0.7 and 0.7 in Figure 54). Onshore sediment transport in the Western Bay of Plenty due to waves supplies sediment to the surf zone contributing to shoreline accretion, and providing extra sediment for longshore transport. This is enhanced by increased frequency of offshore winds during El Niño conditions. However, the wave approach directions are close to shore normal, so longshore transport is small and bi-directional. Any sediment that does reach the Matakana Banks ebb tidal delta contributes to accretion of the ebb tidal delta and Panepane Point shoreline.

The ebb tidal delta is tidally-dominated. Fine sands are predominantly transported anticlockwise over the swash platform, and accumulate on the western side of the delta. Some is added to the offshore bar, and transported along the shoreline contributing to accretion of the Panepane Point shoreline. Flood tidal currents transport fine sand into the harbour, to be returned via the ebb jet. A proportion is deposited within the Entrance Channel (No.1 Reach) by the ebb tidal eddies on the eastern side of the ebb jet. Medium to coarse sand is concentrated in swash bars, and the number and size of swash bars increases during a transition to an El Niño phase which enhances the onshore movement of sediment.

## 5.2 La Niña conditions

Onshore wind conditions are more prevalent, leading to shoreline erosion and offshore movement of beach sediment. More waves approaching from the NNW sector, increases longshore sediment transport, contributing to shoreline erosion including at Panepane Point.

The ebb tidal delta becomes increasingly wave dominated during a La Niña phase. Sediment movement is clockwise over the swash platforms, and swash bars shrink in size and number. Medium to coarse sand is deposited in the outer Entrance Channel (middle to southern No.1 Reach). Sediment is eroded from the swash platform, with fine sediment in suspension transported into the harbour (mostly onto the flood tide delta, Te Paritaha). Medium to coarse sediment is transported as bedload (sand waves) towards the harbour, mostly in or immediately seaward of the marginal flood channel along the Matakana Island foreshore.

If La Niña conditions are prolonged, or there was a low volume of accumulated sediment present before the La Niña event began, the overall depth of the swash platform increases by 1-3 m. Deeper water over the swash platform allows large waves to approach closer to the shore, and also appears to result in a more rapid dispersion of the ebb jet so that it does not extend as far offshore as during neutral or El Niño conditions. This enhances the clockwise sediment transport, and moves it closer to shore. Under these conditions sediment deposition within the Entrance channel moves southward. Under prolonged La Niña conditions medium to coarse sand is deposited in No.2 Reach near Panepane Point.

## 5.3 Episodic storm events

Storms can produce rapid changes in sediment transport rates. Significant storms can occur under all ENSO conditions, and depending on their behaviour can enhance either tidally- or wave-dominated conditions. Specifically:

- Storms associated with intense or prolonged rainfall (e.g. cyclones or atmospheric rivers), can increase the ebb tidal prism and strengthen the ebb jet. This favours anticlockwise transport over the swash platform, and increases export of sediment from the harbour.
- Storms tracking over land west of the Bay of Plenty tend to drive onshore sediment transport (offshore winds), and tend to be short duration.
- Storms tracking east of the Bay of Plenty tend to drive offshore sediment transport, and are more likely to stall and be of longer duration. Increased duration results in larger waves reaching the shore, and increased wave dominance for the ebb tidal delta.

It is very difficult to predict storm tracks more than a few hours to days in advance.

## 5.4 Implications for dredging

The available evidence indicates that capital dredging is not a controlling factor in the evolution of Panepane Point or the ebb tidal delta (Matakana Banks). For maintenance dredging, it is evident that the infill rates for the Tauranga Entrance to Te Awanui vary over time: both in terms of the total volume, and the locations where infill occurs. This obviously affects the timing and volumes of maintenance dredging, as some areas are more critical in terms of navigability than others. Timing is also affected by the availability of suitable dredges.

The conceptual model above does allow some forecasting of future maintenance dredging volumes for the Entrance Channel and No.2 Reach (de Lange), but not for shipping channels further from the tidal inlet as those areas are mostly affected by terrestrial sediment discharge from the harbour catchments. However, forecasting is dependent on being able to reliably forecast future ENSO states, and the magnitude and frequency of storms. This is not currently possible to do this reliably, although there is some evidence that it possible to infer the likely pattern for the next 20-30 years, based on historical patterns (de Lange, 2025). In summary, the frequency and duration of ENSO extremes appear to vary with the Interdecadal Pacific Oscillation (IPO). The key features of the historical patterns are:

- The IPO cycle varies from 40-60 years, with phase transitions occurring at intervals of 20-30 years.
- Transitions from the negative to positive phase appear to be preceded by an increased frequency, magnitude and duration of La Niña events, including the occurrence of super-long La Niña events (i.e. every 40-60 years).
- Although the relationships are unclear, the IPO involves teleconnections, and it appears that climate oscillations such as the Atlantic Meridional Oscillation (AMO) may interact with IPO (or ENSO) and trigger transitions. This suggests that forecasting the IPO will improve in the future.

Given that it is now 28 years since the last transition (positive to negative), and there have been 5 La Niña dominated years since 2019, it is likely that there will be a negative to positive IPO transition soon. This will result in El Niño events dominating ENSO for the next 20-30 years until the next transition to a negative IPO. Further, once a negative IPO phase reoccurs, it is likely that there will not be a super-long La Niña until the last half of the phase. Hence, once the IPO transition occurs there will be at least 25-30 years when, assuming sufficient longshore transport, sediment will accumulate over the western side of the ebb tidal delta, and the Matakana Island shoreline will accrete. This is likely to result in further shoaling of the Lower Western Channel and Te Paritaha.

Due to changes in infill patterns due to ENSO variability, it is not feasible to extract the same volume every maintenance dredging campaign. Further, as occurred recently, it is possible to have periods of up to 4 years when infill rates are increased due to the effects of multiple storms. This is most likely to occur during super-long La Niña events when the tidal inlet is wave dominated: sediment transport over the ebb tidal delta is clockwise, the swash bars move landward and towards the tidal inlet, and the swash platform is lowered. These events are infrequent (5 since 1950), and do not always result in increased infill.

Assuming a stable longshore sediment transport supply, and taking into account the historical patterns of maintenance dredging, a continuation of previous consented volumes would be appropriate, with an allowance for episodic extreme events. Hence, the limits could be:

- An average limit of 250,000 $m^3y^{-1}$ over the period of the consent.

- A cap of 350,000 $m^3y^{-1}$ to allow for doubling of infill for the outer channels (No.1 and No.2 Reaches) in response to a wave dominated tidal inlet. I expect that the extra volume will be balanced by reduced volumes in years when the inlet is tidally dominated.

# 6.0 Summary

Te Awanui consists of two basins that are only connected around high tide: the Katikati basin in the northwest; and the Tauranga Basin in the southeast. The Katikati basin occupies a depression, possibly a caldera, that represents the southern extent of the Coromandel Volcanic Arc, and is largely infilled by younger volcanic deposits. The Tauranga basin occupies a rift, and possibly another caldera, formed during the initial formation of the Taupo Volcanic Zone. It is infilled by younger deposits from the Taupo Volcanic Zone consisting of pyroclastic flows, tephra deposits and reworked volcaniclastic sediments forming alluvial fans with interbedded lake and swamp deposits, overlain by sequences of marine sediments derived from the continental shelf during interglacials. There is some evidence to suggest that parts of the Tauranga basin are still subsiding in response to the ongoing rifting of the Taupo Volcanic Zone.

Although the two basins are connected around high tide, numerical modeling and analysis of sediment transport pathways indicates that there is little exchange of water and sediment between the two basins. Modern sediments in both basins consist predominantly of marine sediment derived from offshore within the flood tidal delta systems close to the tidal inlets (Te Paritaha and surrounding channels in the Tauranga basin), and terrestrial sediment from local catchments for the rest of the basins.

The Port of Tauranga Ltd undertakes two types of dredging:

- Capital dredging to increase the depth and/or width of the sitting basins and/or channels to accommodate larger vessels in response to changing dimensions of international shipping fleets. This dredging predominantly involves extraction of older sediment that has not previously been affected by anthropic activities, and hence does not contain additional contaminants (volcaniclastic sediments naturally have elevated concentrations of some heavy metals that may exceed environmental standards).
- Maintenance dredging, to remove modern sediment accumulating within the channels and sitting basins and reducing the available clearance for vessels using the port. The modern sediment may be marine sediment, which is uncontaminated, and terrestrial sediment, which may be contaminated depending on land use within the source catchments (which include stormwater catchments in urban areas).

Dredging may result in adverse impacts during three phases of activity:

- During the excavation of the seabed by the dredge;
- During the disposal of the extracted sediment (which includes reclamation utilising the sediment); and
- During the post-dredging or recovery period.

The identified impacts for Te Awanui are summarised and discussed below.

The impacts during the excavation phase are dependent on the production rate of the dredge (larger volumes of sediment moved per unit time generally produce larger impacts), and the type of dredge. The Port of Tauranga Ltd proposes using a Trailer Suction Hopper Dredge (TSHD) for most of the dredging activities, and a Back-Hoe Dredge (BHD) for areas that are difficult to excavate with a TSHD. The BHD has a low production rate and is usually confined to a small area when excavating, while a TSHD has higher production rates and the dredge usually moves along a track so can potentially affect a larger area than a BHD.

During the excavation phase, the main potential impacts are excavation of benthic biota, and the release of potential contaminants into the water column including suspended sediment (turbidity) and dissolved or absorbed materials such as heavy metals, hydrocarbons and pesticides. This report focussed on the generation and dispersal of suspended sediment associated with capital dredging, which may involve the largest production rates, and does involve predominantly uncontaminated sediment.

Numerical modelling of sediment plumes assumed at TSHD with 15,000 $m^3$ capacity, which is much larger than the *Balder R* with a 6,000 $m^3$ hopper capacity used for the 2015-2016 capital dredging, and the *Albatros* with an 1,800 $m^3$ hopper capacity used for maintenance dredging. The generation of plumes scales with dredge capacity, and also varies with the dredging methodology used. If smaller capacity TSHDs are used, or methods employed that minimise or prevent sediment discharge, the impacts will be less than reported from the modelling results.

A TSHD generates suspended sediment that may form plumes from three sources:

- The cutter head disrupting the sediment in the seafloor to allow it to be pumped up into the dredge hopper;
- The overflow discharge of water pumped into the hopper along with the sediment; and
- In shallow conditions, the dredge propellor wash or jet can disturb sediment on the seafloor, and disrupt the settling process for the plumes produced by the other two sources.

The predominant source of suspended sediment is usually the overflow discharge. This forms a dynamic plume that is higher density than the surrounding seawater, so that it flows down towards the seabed. Most of the sediment within the dynamic plume is deposited rapidly when the plume reaches the seabed, but fine sediment may remain in suspension if it is absorbed onto air bubbles formed by the overflow process, or due to high turbulence from currents or propellor wash. Due to the higher density of the plume, the plume tends to be confined to deeper channels (especially the near-bed cutter head and dynamic overflow plumes).

Mitigation of the impacts of suspended sediment plumes involve reducing the production rate of fine sediment within the overflow discharge, and controlling the direction the plume can travel after leaving the source region by the dredge (mixing zone). The available options are:

- Reduce the entrainment of air bubbles into the overflow, such as using green-valve technology;
- Control the duration of overflow so some of, or all, the water and sediment pumped from the seafloor is retained in the hopper;
- Reduce the production rate by using a smaller TSHD or a BHD; and
- Only dredging when the tidal currents transport plumes away from areas of concern.

Numerical modelling was used to assess the formation and dispersal of suspended sediment plumes for a large TSHD and a BHD excavating within the Port shipping channels. The potential impact on areas of concern (Te Paritaha, Bridge Marina, and Whareroa Marae foreshore) was assessed, with a maximum suspended sediment concentration of 70 $mg.l^{-1}$ used as the threshold for adverse effects. Modelling showed that most suspended sediment generated by dredging was transported within near-bed plumes that were confined to the shipping channels, and most sediment was deposited with the 600 m mixing zone (predominantly within 200 m) for both the large TSHD and BHD. The modelling also predicted that turbulence associated with strong tidal currents could mix the TSHD near-bed plume into surface waters, causing increased surface turbidity well outside the mixing zone. This behaviour has not been observed during historical dredging for the Port.

Numerical modelling including assessment of mitigation approaches: dredging with no overflow; and dredging only during tidal flow conditions that transported the plume away from areas of concern. The modelling did not include ambient turbidity levels. The Port operates a network of turbidity sensors that can monitor the turbidity of water entering and leaving the port area. A potential mitigation approach is to modify dredging operations if average ambient levels exceed the 70 $mg.1^{-1}$ threshold, or a lower threshold to allow for the additional sediment associated with the dredge plumes. Numerical model results indicate that within the areas of concern, the dredge plume concentrations very rarely exceed 1 $mgl^{-1}$, and therefore will be difficult to detect in real time.

The modelling results indicate for all scenarios that the Bridge Marina and Whareroa Marae Foreshore would not be exposed to sediment plumes exceeding the threshold, and were unlikely to experience detectable plumes. Te Paritaha was subject to limited (1 or 2 over 62 days of simulation, depending on the weather conditions simulated) short-duration events exceeding threshold. These events involved dredging in the Entrance Channel during extreme peak spring flood tide currents, where turbulence re-entrained the near-bed plume into the surface waters with a large TSHD. This is unlikely to occur with a smaller TSHD. It should also be noted, that adverse ecological impacts required continual exceedance for days and this did not occur in the simulations.

During the disposal phase, the main potential impacts are burial of benthic biota, and the release of potential contaminants into the water column including suspended sediment (turbidity) and dissolved or absorbed materials such as heavy metals, hydrocarbons and pesticides.

Sediment disposal involves only one source of suspended sediment, the discharge from the hopper, forming a dynamic plume. Assessment of the impacts of previous dredging activities at the Port, show that the adverse impacts are confined within the boundaries of the disposal grounds, and that there is a rapid recovery post-dredging (dependent on the total burial depth). The surficial texture within the disposal sites post-dredging is very similar to the pre-dredging conditions, apart from the presence of biota that normally occur inside the harbour. The deepest H1 and H2 disposal sites appear to be non-dispersive as intended, with no sediment loss detected by post-disposal surveys.

Numerical modelling indicates that the disposal plumes will be confined within the disposal sites, provided the sediment is released sufficiently far from the boundaries. Numerical modelling indicates most sediment is deposited on the seafloor within 100 m radius of the release point.

During the post-dredging or recovery phase, the main potential impacts are: changes to the tidal circulation and sediment transport within and outside the harbour; changes to the behaviour of depth-dependent phenomena, such as waves and storm surges; changed patterns of erosion and accretion; and dispersal of sediment from the disposal site. Changes to tidal circulation primarily may occur within the harbour, but can affect the ebb-tidal delta, and manifest as changes to the shape of the tidal elevation curve (affecting tidal range, the timing of high and low tide, the duration of flood and ebb tidal flows, and tidal flushing). The post-dredging changes may be permanent, or persist for years before returning to pre-dredging conditions.

The impacts during the post-dredging phase are predominantly determined by the changes made to the morphology (mostly the tidal channels), and the subsequent morphodynamics response, which involves an interactive system of changing currents and morphology. Usually, areas subject to dredging are naturally changing in response to processes such as weather events and variations in sediment supply.

Depending on the scale of the changes produced by dredging, it can be difficult to identify the extent of adverse effects due dredging. Therefore, it has been standard practice to verify the model

predictions made for past capital dredging after the completion of dredging to assess if the models are reliable. For the ebb and flood tidal deltas, it is clear that it is also useful to evaluate the changes occurring at the Katikati Entrance to Te Awanui as it is evident that the two tidal inlets display similar responses to changing waves conditions in the Bay of Plenty. Unfortunately, the Katikati Entrance is not surveyed very frequently, making it difficult to correlate changes between the two tidal inlets of Te Awanui over the full 1852-present record available for the Tauranga Entrance.

Current velocities within an estuary depend on the slope of the water surface, and the cross-sectional area and wetted perimeter of the channels (and intertidal flats). Dredging can change:

- the tidal range by changing the friction and/or constrictions affecting the movement of the tide, which changes the water slope;
- the timing of high and low tide within the harbour, which is only important for current velocities if the timing changes differ between high and low tide, changing the asymmetry of the tidal wave;
- the duration of flood and ebb flow (which vary with tidal asymmetry), which also changes the water slope;
- the wetted cross-sectional area and wetted perimeter of the channels.

Theory, modelling and observations for historic capital dredging in Te Awanui has demonstrated that within the Port, dredging has had little impact on the tidal range, a small impact on the timing of the tide along the shipping channels, and significantly increased the channel cross-sectional areas (with an associated increased in wetted perimeter length). These changes have resulted in a reduction in tidal velocities. The largest change in velocities were associated with the initial capital dredging in the 1960s, particularly the excavation of the Cutter Channel that resulted in greatly reduced tidal currents in Pilot Bay Channel. Subsequent capital dredging programmes have had less impact, except for areas of significant deepening in Stella Passage. The changes at the southern end of Stella Passage are also the result of the constriction of flow by the Tauranga Harbour Crossing.

Numerical modelling of the originally proposed 2026 capital dredging predicted little change in the tidal characteristics, and hence, unsurprisingly, it predicted a reduction in tidal velocities for the dredged areas of the shipping channels proportional to the increased cross-sectional area. The modelling also showed, consistent with before and after observations of previous capital dredging, that there are no detectable changes to tidal characteristics and tidal velocities beyond the immediate area of the dredged channels. The smaller proposed reconsenting capital dredging will have correspondingly smaller impacts than modelled.

Modelling was also undertaken to assess the impact of the 2015/2016 capital dredging on tidal currents. This used the 2023 bathymetry, which was also being using as a baseline to assess the impact of proposed dredging. The modelling indicated that current velocities increased within part of the Lower Western Channel following the capital dredging. This was a consequence of shoaling decreasing the channel cross-sectional area. The shoaling appears to have been due to erosion of Panepane by changed storm wave conditions due to lowering of the ebb tidal delta swash platform during a higher incidence of La Niña conditions over the last decade, which increased the sediment transport into the harbour. This highlights the difficulty of identifying the impacts of dredging on sediment transport, since the changes in transport due to the impacts of dredging on currents are much smaller than the changes associated with variations in weather at decadal scales.

Monitoring of shoreline changes at Panepane are an ongoing requirement of the consent conditions for the 2015/2016 capital dredging. This recognised a short phase of erosion of the sub-tidal spit tip during and immediately after the capital dredging, which was consistent with the modelling

predictions. This erosion included the loss of the overlying subaerial beach sediments as the slope adjusted in response to scouring. Starting in 2018 arcuate embayments formed adjacent to the western ebb tidal delta in response to wave erosion caused by wave focussing of storm waves by swash bars. This subsequently resulted in the formation of a marginal flood channel along the Panepane shoreline, which has contributed to shoreline erosion by transported sediment eroded by waves into the harbour.

This pattern of behaviour appears to be linked to changes in wave conditions in response to the La Niña extreme of ENSO. It is a pattern of behaviour that has occurred in the past, including before any dredging occurred, and affects the whole coastline between Waihi Beach and Papamoa. There is no link to dredging-induced changes in tidal flow within the shipping channels and the tidal-delta system.

Overall, the post-dredging impacts are concentrated in the immediate area of the dredging excavation and disposal. Further away, there are no identified unintended impacts due to the discharge of sediment into the water during excavation and disposal, or changes to tidal wave propagation and associated currents. Not that the replenishment of beaches by direct or indirect deposition of suitable dredge spoil is considered an intentional impact.

# 7.0 Appendices